MINISTRY OF HIGHER EDUCATION AND SCIENTIFIC RESEARCH
UNIVERSITY OF BABYLON
COLLAGE OF ENGINEERING
DEPARTMENT OF CIVIL ENGINEERING

NONLINEAR ANALYSIS OF STEEL FIBER REINFORCED CONCRETE MEMBERS UNDER CYCLIC LOADING

A

THESIS

SUBMITTED TO THE COLLEGE OF ENGINEERING OF THE UNIVERSITY OF BABYLON IN PARTIAL FULFILLMENT OF THE REQUIREMENTS FOR THE DEGREE OF MASTER OF SCIENCE IN STRUCTURAL ENGINEERING

By

Ayoub Abbas Ibrahim

B. Sc. ٢٠٠٢

September ٢٠٠٥

التحليل اللاخطي للأعضاء الخرسانية المسلحة بالألياف الحديدية تحت الأحمال الدورية

أطروحة

مقدمة إلى جامعة بابل - كلية الهندسة
وهي جزء من متطلبات نيل درجة
ماجستير علوم في الهندسة
المدنيـــــــة

من قبل

أيوب عباس إبراهيم

أيلول

٢٠٠٥

بِسْمِ اللَّهِ الرَّحْمَنِ الرَّحِيمِ

يُؤْتِي الْحِكْمَةَ مَنْ يَشَاءُ وَمَنْ يُؤْتَ الْحِكْمَةَ فَقَدْ أُوتِيَ

خَيْرًا كَثِيرًا وَمَا يَذَّكَّرُ إِلَّا أُولُو الْأَلْبَابِ

صدق الله العظيم

سورة البقرة. أية(٢٦٩)

التحليل اللاخطي للأعضاء الخرسانية المسلحة بالألياف الحديدية تحت الأحمال الدورية

الخلاصة

في هذه الدراسة تم تقديم طريقة التحليل اللاخطي الطبقي بالاعتماد على أسلوب العنصر المحدد مع الصلابة المماسية لدراسة تصرف الهياكل الخرسانية المعززة بالألياف الحديدية تحت تأثير الأحمال المتغيرة دوريا.تم استخدام أسلوب الطبقات (Layered Approach) للاخذ بنظر الاعتبار التغير في خواص المادة خلال المقطع.

عوامل مختلفة أخذت بنظر الاعتبار في هذه الطريقة وهي:- لا خطية التصرف للمادة ،اللاخطية الهندسية للمنشأ وتداخل التأثير بين العزم ، قوة القص والقوة المحورية.

كذلك تم الأخذ بنظر الاعتبار قاعدة الصلابة (Hardening rule)، قاعدة الجريان (Flow rule) وتقوية الشد(Tension stiffening) للخرسانة .آلية الانهيار في هذا البحث تتم بالسحق الموقعي للخرسانة خلال طبقة معينة.

تم استخدام نموذج التصرف اللاخطي للخرسانة ونموذج التصرف ثنائي الخط (Bilinear)للحديد مع افتراض الترابط التام بين الخرسانة المسلحة بالالياف الفولاذية والحديد.

لقد تم حل بعض الامثلة وقورنت النتائج مع نتائج مختبرية منشورة سابقا لغرض التحقق من صحة النتائج المستحصلة. وأخيرا تم دراسة العوامل التي تتائثر بوجود الألياف الحديدية، النسبة الحجمية للألياف (نسبة حجم الألياف إلى حجم الخرسانة)، النسبة الباعية (نسبة طول أليف إلى قطرة المكافيء)، و التسليح جزئيا بالألياف، وتغير المقطع الخرساني مع الطول وتوزيع الأحمال وتبين (كما هو معلوم عمليا) بان الألياف لها دور كبير في تحسين سلوك ومقاومة الخرسانة المسلحة للأحمال الدورية.

ABSTRACT

Concrete containing steel fibers have been use at the beginning of the last century. It is only in the last ٢٠ years that extensive researches for predicting the behavior of steel fiber concrete have been started. Some examples of structural and non-structural uses of steel fiber concrete may be mentioned as, hydraulic structures, airport and highway paving and overlays, industrial floors, bridge decks, in shotcrete linings, in shortcrete coverings and concrete beams.

The behavior of reinforced concrete members under the effect of monotonic and cyclic loads through the addition of steel fibers was investigated. The main parameters studied were: the ratio of the longitudinal steel reinforcement, the volume fraction and aspect ratio of steel fibers, partial-depth steel fiber, and loading distribution.

The fiber reinforced concrete members are represented by layered modeling. In the layered modeling, fibrous concrete is divided into a set of layers, while the reinforcing steel is smeared between fibrous concrete layers. In this study, a layered non-linear procedure based on finite element method with tangent stiffness approach is presented to study the behavior of reinforced concrete plane frames subjected to monotonic and cyclic loads.

Different parameters are included in the present method, which are: material nonlinearity, geometric nonlinearity and effects of coupling between bending moment, shear and axial forces. The hardening rule, flow rule and tension-stiffening rule for fibrous concrete are taken into account. Failure can be predicted by crushing of concrete at a certain layer.

Many examples are analyzed to approve the validity of the proposed model presented in this study. These examples show reasonable accuracy in comparison with previous studies. The study of main parameters indicated that, with an increase of ١٪ volume fraction of steel fibers could replace about ٠.١٥٪ of flexural steel reinforcement. Also the deflection is a decreased about ٤٠٪ with increasing steel fiber content from ٠.٥٪ to ٢٪. However, when the aspect ratio an increased from ٦٠ to ١٠٠ for fiber diameter ٠.٥ mm, the deflection decrease about ١٨٪. Steel FRC subjected to reversible cyclic load and continuous members is more acceptable than the partial-depth steel FRC members.

The present investigation was implemented by a computer program prepared by Kadim [٢٩] and coded in Fortran ٧٧ language. The computer program is capable to analyze fiber reinforced concrete plane frames under different load conditions including monotonically increasing load, cyclically varying load.

TABLE OF CONTENTS

NOTATIONS

SYMBOL DESCRIPTION

{a}	**Flow vector.**
As_i	**Area of steel layer (j).**
b	**Width of element.**
[B]	**The strain-displacement matrix.**
$[D]_c$	**Elastic constitutive matrix for concrete.**
$[D]_s$	**Elastic constitutive matrix of steel.**
{d}	**Displacement vector.**
D_f	**Diameter of fiber.**
D λ	**Plastic Multiplier.**
Ec	**Concrete modulus of elasticity.**
Ec_f	**Modulus of elasticity of fibrous concrete.**
Ec_i	**Modulus of elasticity of fibrous concrete layer (i).**
Ec.	**Initial modulus of elasticity of concrete.**
Es_j	**Modulus of elasticity of steel layer (i).**
Es.	**Initial tangent modulus of elasticity of steel.**
F_{be}	**Bond efficiency factor of fiber.**
f'_C	**Compressive strength of concrete.**
f'_{Cf}	**Compressive strength of steel fiber reinforced concrete.**
f_t	**Tensile strength of concrete.**
f_{tf}	**Tensile strength of steel fiber reinforced concrete.**

SYMBOL DESCRIPTION

f_{uc}	**Unloading compressive stress.**
f_{rc}	**Reloading compressive stress.**
{F}	**Force vector.**
f_0	**Residual compressive stress.**
G_{Cf}	**Shear modulus of elasticity of concrete.**
$\overline{G}$	**Shear modulus of elasticity of cracked concrete.**
RI	**Reinforcing index** ($V_f \times L_f / D_f$)
H′	**Plasticity hardening modulus for fibrous concrete.**
h	**Overall depth of member.**
Δh_i	**Thickness of fibrous concrete layer (i).**
Δh_j	**Thickness of steel layer (j).**
I₁	**First stress invariant.**
I'₁	**First strain invariant.**
J₂	**Second deviotoric stress invariant.**
J'₂	**Second deviotoric strain invariant.**
[K$_e$]	**Stiffness matrix of element.**
[K]$_c$	**Stiffness matrix of concrete.**
[K]$_s$	**Stiffness matrix of steel.**
k$_r$, K$_u$	**Unloading and reloading parameters.**
L	**Total length of element.**

L_f **Fiber length.**

L_C **Critical fiber length.**

M١ Moment at node (١) in an element.

SYMBOL DESCRIPTION

N١ Axial force at node (١).

N_f **Effective number of fibers per unit cross section area.**

n_u **, P Unloading curve parameters.**

Nc Total number of concrete layers.

Ns Total number of steel layers.

u١ Axial displacement at node (١) in an element.

u(x,z) Total axial displacement at any point (x,z).

u.(x) Axial displacement due to axial effect at a section at a distance (x).

V١ Shear force at node (١) in an element.

V_m **Volume fraction of matrix.**

V_f **Volume fraction of fiber.**

w١ Shear force at node (١) in an element.

W(x,z) Lateral displacement at any point (x,z).

W.(x) Lateral displacement at the centerline of the element at a distance (x) from the first end of the element.

dn Neutral axis.

z Slope of the descending portion of the compressive stress-strain.

Zi Displacement from the top of the element to the centerline of i^{th} concrete layer.

Zj Displacement from the top of the element to the centerline of

	i^{th} steel layer.
ε_c	**Concrete strain.**
ε_{CP}	**Strain at ultimate fibrous concrete strength.**
ε_{PC}	**Residual strain.**

SYMBOL DESCRIPTION

ε_{Cuf}	**Concrete ultimate total strain.**
ε_X	**Concrete strain in local direction (x).**
ε_{SX}	**Steel strain in local direction (x).**
ε_P	**Concrete plastic strain.**
ε_e	**Concrete elastic strain.**
ε_{uc}	**Unloading compressive strain.**
ε_{rc}	**Reloading compressive strain.**
ε_0	**Strain at ultimate fibrous concrete strength.**
ε_n	**Fibrous concrete strain in local direction (x).**
σ_n	**Fibrous concrete stress in local direction (x).**
σ_S	**Steel stress.**
σ_{S0}	**Yield strength of steel.**
τ_{xz}	**Concrete shear stress- in xz plane.**
τ_{sxz}	**Steel shear stress- in xz plane.**
γ_{xz}	**Concrete shear strain- in xz plane in layer (i).**
γ_{sxz}	**Steel shear strain- in xz plane.**
α_f, β_f	**Stress function parameter.**
β_i	**Rotation at node (i) in an element.**
$\beta(x)$	**Rotation of the normal to the centroidal axis due to flexural**

effect at a section at a distance (x) from the first end of the element.

μ **Partial-depth factor.**

SYMBOL DESCRIPTION

η_l **Length correction factor.**

η_0 **Orientation factor.**

η_b **Bond efficiency factor.**

τ_u **Average bond strength between fiber and matrix.**

Note: any other notation may be explained where it appears in the thesis.

AKNOWLEDGMENTS

I wish to express my deep appreciation to my supervisors ***Dr. Mustafa B. Dawood*** and ***Dr. Haitham AL-daamy*** for suggesting the problem, their valuable assistance and continuous guidance.

I would like to express my thank to my **family** and my friends **Moslem** and **Mohamed**, for their encouragement and support during the course of this thesis.

Ayoub A. Ibrahim

٢٠٠٥

CERTIFICATE

We certify as an examining committee that we have read this thesis entitled **"Nonlinear Analysis of Steel Fiber Reinforced Concrete Members under Cyclic Loading ",** and examined the student **Ayoub A. Ibrahim** in its content and what related to it, and found it meets the standard of thesis for the degree of Master of Science in Civil Engineering.

Signature:
Name: Asst. Prof. Dr. **Nameer A. Alwash**
(Member)
Date: / / ٢٠٠٥

Signature:
Name: Asst. Prof. Dr. **Ammar Y. Ali**
(Member)
Date: / / ٢٠٠٥

Signature:
Name: Asst. Prof. Dr. **Ihsan A. S. Al-Shaarbaf**
(Chairman)
Date: / / ٢٠٠٥

Signature:
Name: Asst. Prof. Dr**. Mustafa B. Dawood**
(Supervisor)
Date: / / ٢٠٠٥

Signature:
Name: Asst. Prof. Dr. **Haitham Al-daamy**
(Supervisor)
Date: / / ٢٠٠٥

Approval of the Civil Engineering Department

Signature:

Name: Asst. Prof. Dr. **Ammar Y. Ali**

Head of the Civil Engineering Department

Date: / / ٢٠٠٥

Approval of the College of Engineering

Signature:

Name: Prof. Dr. **Haroun AK. Shahad**

Dean of the College of Engineering

Date: / / ٢٠٠٥

CHAPTER ONE
INTRODUCTION

١.١ General

Reinforced concrete (RC) has become one of the most important construction materials and is widely used in many types of engineering structures. The economy, efficiency, strength and the stiffness of reinforced concrete make it an attractive material for a wide range of structural applications. For its use as a structural material, concrete must satisfy the following conditions [٢٨]:

١. The structure must be strong and safe. The proper application of the fundamental principles of analysis, the laws of equilibrium and the consideration of the mechanical properties of the component materials should result in a sufficient margin of safety against collapse under accidental overloads.
٢. The structures must be stiff and appear unblemished. Care must be taken to control deflections under service loads and to limit the crack width to an acceptable level.
٣. The structures must be economical. Materials must be used efficiently, since the difference in unit cost between concrete and steel is relatively large.

Reinforced concrete structures are commonly designed to satisfy criteria of serviceability and safety. In order to ensure the serviceability requirements, it is necessary to predict the cracking and the deflections of RC structures under service loads. In order to assess the margin of safety of RC structures against failure, an accurate estimation of the ultimate load is essential and the prediction of the load-deformation behavior of

the structure throughout the range of elastic and inelastic response is desirable.

The development of analytical models of the response of RC structures is complicated by the following factors [٢٨]:

- Reinforced concrete is a composite material made up of concrete and steel, two materials with very different physical and mechanical behavior.
- Concrete exhibits nonlinear behavior even under low level of loading due to nonlinear material behavior, environmental effects, cracking, biaxial stiffening and strain softening.
- Reinforcing steel and concrete interact in a complex way through bond-slip and aggregate interlock.

The present study is a part of this continuous effort and concerns the analysis of fiber reinforced concrete member under cyclic load reversals.

١.٢ Fiber Reinforced Concrete

Fiber reinforced concrete is a concrete mix that contains short discrete fibers that are uniformly distributed and randomly oriented. Fiber material can be steel, cellulose, carbon, polypropylene, glass, nylon, and polyester [٢٠]. The amount of fibers added to a concrete mix is measured as a percentage of the total volume of the composite (concrete and fibers) termed volume fraction (Vf). Vf typically ranges from ٠.١ to ٣٪ [٢٠]. Aspect ratio (L_f/D_f) is calculated by dividing fiber length (L_f) by its diameter (D_f). For fibers with a non-circular cross section, an equivalent diameter for the calculation of aspect ratio is usually used.

This research focuses on steel fibers. Steel fiber length ranges from ١.٥ to ٧٥ mm and aspect ratio ranges from ٣٠ to ١٠٠ [٢٠]. Fiber shapes are illustrated in Fig. (١.١).

The typical applications for steel fibers include [٦٣]:

- Explosive and impact resistant structures.
- Shotcrete in mining/tunneling.
- Slabs and pavements on ground.
- Refactory shotcrete and castables.
- Dam and water course lining.
- Pipline coatings.
- Airport taxiways.
- Chemical containment requirements.
- Highways and roadways.
- Seismic resistant structures.
- Precast elements.
- Bored piers.
- Spillways.

Fibers work with concrete utilizing two mechanisms [٢٠]: the spacing mechanism and the crack bridging mechanism. The spacing mechanism requires a large number of fibers which are well distributed within the concrete matrix to arrest any existing micro-crack that could potentially expand and create a sound crack. For typical volume fractions of fibers, utilizing small diameter fibers or micro fibers can ensure the required number of fibers for micro crack arrest.

The second mechanism term crack bridging requires larger straight fibers with adequate bond to concrete. Steel fibers are considered a prime example of this fiber type that is commonly referred to as large diameter fibers or macro fibers. Benefits of using discrete steel fibers, Fig. (١.٢),

includes impact resistance, flexural and tensile strengths, ductility, and fracture toughness.

The shortcoming of using steel fibers in concrete is reduction in workability. Workability of steel FRC is affected by fiber aspect ratio and volume fraction as well as the workability of plain concrete. As fiber content increases, workability decreases. Most researchers limit Vf to ٢.٠٪ and L_f/D_f to ١٠٠ to avoid unworkable mixes [٢٠]. In addition, some researchers have limited the fiber reinforcement index [$V_f \times (L_f/D_f)$] to ١.٥ for the same reason. To overcome the workability problems associated with SFRC, modification of concrete mix design is recommended. Such modifications can include the use of additives.

The steel fibers can be used on their own, or combined with other reinforcement to improve the energy absorbing capabilities and significantly increase spalling and impact resistance. The properties of steel fibers are listed in Table (١.١).

Table (١-١): Physical Property of Steel fibers [٦٣]

Physical Property	Beneficial Effect
Modulus of Rupture	١ to ٢ × plain concrete
Shear Strength	١.٢٥ to ٢ × plain concrete
Torsional Strength	١.٢٥ to ٢ × plain concrete
Impact Energy Absorption	٢ to ١٥ × plain concrete
Fatigue Resistance	١.٢ to ٢ × plain concrete
Cavitation and Erosion	١ to ١.٤ × plain concrete
Resistance Restrained Shrinkage Cracks	Reduced Crack widths

١.٣ Objective of Research

The objective of this research is directed to study analytically the effect of many parameters on the ratio of longitudinal main steel reinforcement. These parameters are; the content and the aspect ratio of steel fibers, partial-depth steel fiber reinforced concrete, element type, loading distribution, cyclic and repeated loading.

The analytical investigation was performed to model the stress-strain relationship of SFRC members. By using, a computer program developed for the nonlinear analysis of reinforced concrete plane stress members under monotonic and cyclic loads, with the inclusion of the effect of steel fibers.

The fibrous concrete is represented by layered modeling with two-node for each layer with three degrees of freedom at each node. A smeared fixed crack approach will be used to model the cracked fibrous concrete.

Many examples are analyzed to prove the validity of the adopted constitutive materials relationship and the solution algorithm and the results are compared with published experimental results.

١.٤ Layout of the Thesis

The thesis is consists of six chapters. The first chapter gives an introduction to the general subject of research and objectivity of the presented. Chapter two introduces a literature review to the related previous studies. Material properties-modeling of fiber reinforced concrete in brief description are outlined in chapter three. The stiffness matrix including effect of shear deformation for reinforced concrete plane frame element is presented in chapter four. Chapter five contains numerical applications of some SFRC members and parametric study on SFRC members using nonlinear approach layered modeling, and is

compared with published experimental results. Chapter six contains the conclusions and the need for further studies.

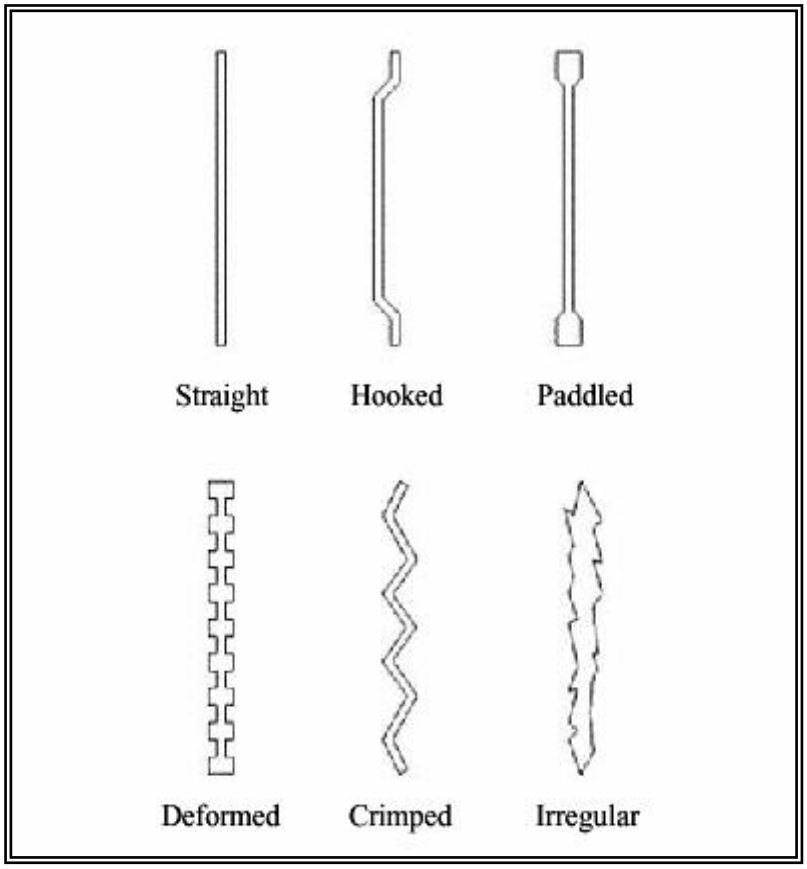

Fig. (١.١). Shapes of steel fibers

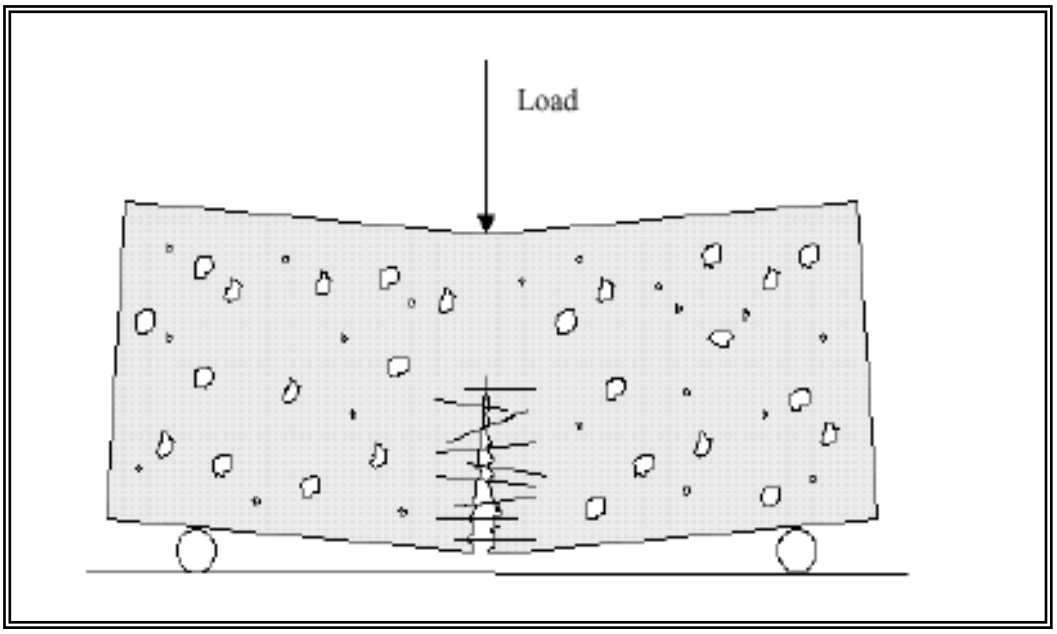

Fig. (١.٢) Bridging action of steel fibers

CHAPTER TWO
REVIEW OF LITERATURE

٢.١ Introduction

The concrete is considered as a brittle material. This is primarily due to its low tensile strength and low tensile strain capacity prior to fracture. In most applications, poor tensile performance of concrete is compensated by the inclusion of steel reinforcing bars in the tensile zones of accurate structure.

The overall behavior of any reinforced concrete member can be roughly divided into three stages: the un-cracked elastic stage, crack propagation, and plastic stage. Concrete can be modified to perform in a more ductile manner by adding discrete of steel fibers through the concrete. This results in a composite of brittle concrete and ductile steel fibers to form an elastic-plastic system. The primary advantage of this system is the development of pre-crack and post-crack load carrying capacity in concrete elements rather than a catastrophic failure at the first fracture.

Experimental trials and patents involve the use of discontinuous steel reinforcing elements-such as nails, and metal chips-to improve the properties of concrete dated from ١٩١٠. During the early ١٩٦٠$_s$ in US, the first major investigation was made to evaluate the potential of steel fibers as reinforcement for concrete. With NATO pacts development of hangar protection, the military research in fiber reinforced concrete began. Falling concrete pieces damaged planes after bomb strikes on hangars, so there was a need to find a way to minimize the distance between the reinforcing elements to avoid this. The FRC had the properties to improve the situation and planes were less damaged after FRC application.

The civilian industries of the NATO countries have overtaken then the military experience and developed methods for shotcrete, industry floors, and later even for concrete elements.

Since then, a substantial amount of research, development, experimentation, and industrial application of steel fiber reinforced concrete have occurred all over the world [٢٤].

٢.٢ RC Members under Cyclic Loading

The behavior of reinforced concrete members and structural systems under cyclic loads has been the subject of intensive investigations since the ١٩٦٠s. Because of the complexities associated with the development of rational analytical procedures, present day design methods continue in many respects to be based on empirical formula, using the results obtaining from the available experimental data.

Mikkola and Sinisalo, in ١٩٨٢, adopted elastic-plastic model for concrete [٤٤], bilinear elastic- plastic model for reinforcement, smeared cracks, maximum stress criterion, and different direct integration schemes, in nonlinear finite element analysis. They analyzed beams and slabs subjected to static, cyclic and dynamic loads. The numerically computed values were compared with the corresponding experimental results. The theoretical prediction were somewhat satisfactory, but not in desirable accuracy.

In ١٩٨٧, Yankelevesky and Reinhardt developed a one-dimensional model for random cyclic behavior of concrete in compression [٧٧]. The model determines a set of focal points that govern the pieced linear branches of the unloading and reloading curves, Fig. (٢.١). The complete unloading and reloading curves, for the developed model, were reproduced graphically for any starting point on the envelope curve. The model laws were also mathematically formulated

providing equations of various characteristics. Three different procedures were considered: the linear incremented method. The nonlinear incremented method and the direct method.

Bahn and Hsu, in ١٩٩٨, tested experimentally the behavior of concrete under cyclic compressive unaxial loading [٥]. The sizes of specimens were (٧٦ mm) in diameter by (١٥٢.٤ mm) in height cylinders of normal concrete, using four different loading patterns; monotonic loading; cycles to envelope curve; cycles to common point and cycles with random.

D'Ambrisi, and Filippou, in ١٩٩٩, improved analytical methods for simulating the nonlinear static and dynamic response of reinforced concrete frames [١٠]. The model used the nonlinear static response of concrete columns and beam-column subassemlages subjected to cyclic lateral loads. They found good agreement between analytical and experimental results.

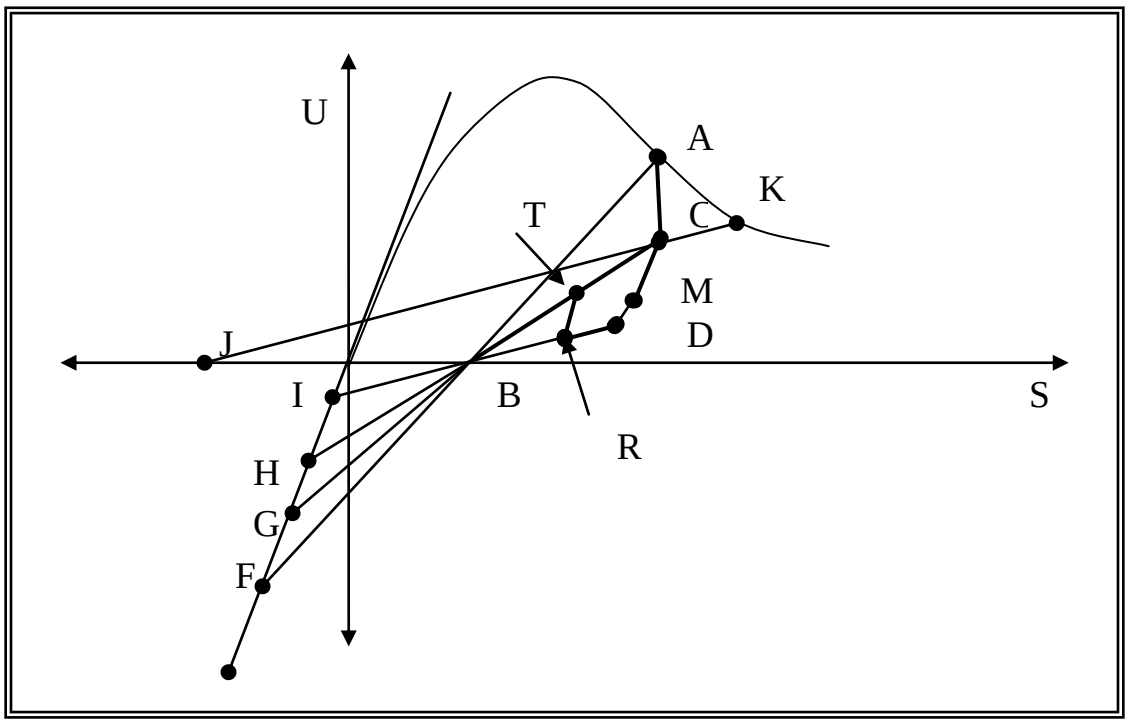

Fig. (٢.١) Scheme of focal points in compression

(Yankelevesky and Reinhardt ١٩٨٧)

In ١٩٩٩, Lan and Guo, investigated the behavior of concrete subjected to repeated biaxial compressive loading [٤٠]. The concrete specimens tested were ١٠٠×١٠٠×٤٠ mm (flat plate). The repeated loading included two different unloading schemes (complete unloading to zero and partial unloading to ٠.٢f_c stress level). The main results can be summarized as follows:

١. In proportional biaxial compression, the envelope of stress-strain curves, strength, strain at failure, and failure mode of concrete specimens subjected to repeated loading had no significant difference from those subjected to monotonic loading.

٢. The magnitude of the normalized residual strain (plastic strain) depended on the unloading strain on the envelope curve Fig. (٢.٢).

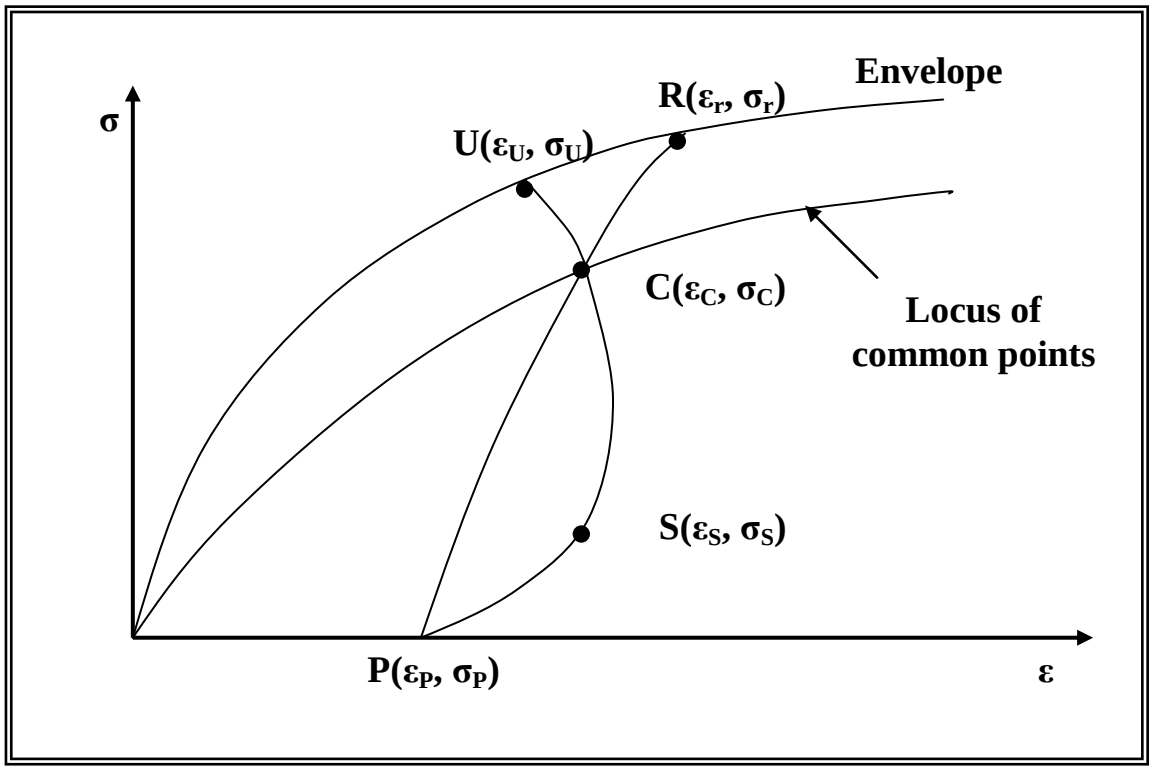

Fig. (٢.٢) Designated points on stress-strain curve

[Lan and Guo ١٩٩٩]

Mansour, et. al ٢٠٠١ described the shear behavior of reinforced concrete membrane elements [٤٧]. The three characteristics of the cyclic stress-strain curves of concrete are as follows:

١. The backbone envelope curve of concrete in compression can be expressed by the monotonic stress-strain curve for compression.
٢. The backbone envelope curve of concrete in tension can be expressed by the monotonic stress-strain curves for tension.
٣. Unloading and reloading stress-strain curves of concrete are expressed analytically by a set of points connected by straight lines

٢.٣ Steel Fibers Reinforced Concrete

Concrete is the most frequently used construction material in the world. However, it has low tensile strength, low ductility, and low energy absorption. An intrinsic cause of the poor tensile behavior of concrete is its low toughness and the presence of defects. Therefore, improving concrete toughness and reducing the size and amount of defects in concrete would lead to better concrete performance. An effective way to improve the toughness of concrete is by adding a small fraction (usually ٠.٥ – ٢ % by volume) of short steel fibers to the concrete mix during mixing [٢٤].

According to ***Shah, and Rangan, in 1971,*** the analysis of results of tensile tests done on concretes with glass, polypropylene and steel fibers, indicated that with such large volume of aligned fibers in concrete, there was substantial enhancement of the tensile load carrying capacity of the matrix[٦٤]. This might be attributed to the fact that fibers suppress the localization of micro-cracks into macro-cracks and consequently the apparent tensile strength of the matrix increases.

In ١٩٧٤, ***Swamy, et al.*** predicted the first crack and ultimate flexural strength of randomly oriented steel fibrous concrete, using

equations developed by crack control-composite mechanics approach [٧٠]. The various factors which influence the fiber reinforcement of cement matrices are briefly discussed. The equations showed an excellent correlation with available test result from various studies.

These equations are:

(a) First crack composite strength;

$$f_{cf} = 0.843\, f_m V_m + 2.93 V_f \frac{L_f}{D_f} \quad \text{[MPa]} \qquad (٢\text{-}١)$$

(b) The ultimate composite flexural strength;

$$f_{cu} = 0.976 V_m + 3.41 V_f \frac{L_f}{D_f} \quad \text{[MPa]} \qquad (٢\text{-}٢)$$

where

V_m, V_f The volume fraction of the matrix and fiber respectively.

L_f, D_f The length and diameter of the fiber respectively [mm].

f_m The tensile strength of the matrix [MPa].

Hughes and Fattuhi, in ١٩٧٧, studied experimentally the effect of the addition of various fibers, including fibrillated and polypropylene, as well as round straight, Duoform, crimped and hooked steel [٢٢]. The specimen of concrete ١٠٢×١٥٢×٢١٣٥ mm beams was reinforced with ٢.٠% by volume. All beams were loaded at the third-points. The addition of polypropylene fibers decreased the flexural and splitting strengths, whereas the addition of steel fibers resulted in significant increases, in the flexural and splitting strengths of the beams. It was shown that the fracture toughness of reinforced beams was increased considerably for all the fibers.

In ١٩٨٠, Mindess investigated torsion tests of steel fiber reinforced concrete [٤٢]. Fiber contents ranged from ٠ to ٢.٠ % by volume and two

different fiber lengths. It was shown that neither fiber concentration nor fiber length have any particular effect on the torsional behavior of small steel fiber reinforced concrete specimens. The fiber reinforced specimens did not break completely into two pieces at the maximum load, while the unreinforced specimens did; the fiber tended to hold the two halves together, thus providing certain a mount of post-cracking ductility. Most of the specimens failure was due to the diagonal tensile stresses occurring at about ٤٥° to the axis of the specimen and few specimens failed in shear. This probably Due to the occurrence of localized regions of low fiber content in these specimens.

Delvasto, et. al, in 1986, explained the effects of applying pressure after casting on the flexural response of high strength fiber reinforced mortar in which up to ٥% fibers were premixed [٩]. Several types of fibers were used in the form of randomly distributed discontinuous reinforcement, including polypropylene fibers, carbon fibers in two lengths, steel fibers, glass fibers, and asbestos fibers. Predicted increase in both strength and toughness were observed when the direction of casting the tensile face of the flexural specimen was changed from horizontal to vertical.

Gray and Johnston, in 1987, tested experimentally the influence of the shear strength of the fiber-matrix interfacial bond on the mechanical properties of steel fiber reinforced cementitious mortars under uniaxial tensile and flexural loading [١٩]. Two types are selected of fibers, plain and Duoform with aspect ratios for the fiber diameter of ٠.٤١ mm are ٩٤ and ٤٧.The fiber concentrations of ٠.٦ and ١.٧% by volume showed that the fiber-matrix interfacial bond strength interacts in a significant manner with two factors, the aspect ratio and concentration of the reinforcing fibers.

Lim, et al., in1987, studied the effect of shear and moment capacity of reinforced steel fiber-concrete beams [٣٧]. It was predicted that the addition of short discrete steel fibers to a conventional reinforced concrete member increases its strengths stiffness and ductility. Steel fibers may therefore wholly or partially replace stirrups in reinforced members.

In ١٩٩٠, Saied presented a comprehensive study on the behavior of (SFRC) beams subjected to monotonic loading [٧١]. The test results showed that increasing the volume fraction and aspect ratio of fibers resulted in an increase in the bending capacity of the beams. The increase in the bending capacity was more prominent when using hooked-end fibers than when using straight smooth fibers.

In 1991, Ezeldin and Lowe, studied the compressive strength properties of rapid-set materials reinforced with steel fibers[١١]. The primary variables were (a) rapid-set cementing materials, (b) fiber type, and (c) fiber content. Four fiber types made of low-carbon steel were incorporated in this study. Two were hooked and one was crimped at the ends, the other was crimped throughout the length. Steel fibers were added in the quantities of ٥٠, ٧٥ and ١٠٠ lb/yd^{٣} (٣٠, ٤٥, and ٦٠ kg/m^{٣}). The results indicated that steel fibers could be successfully mixed with rapid-set materials up to a quantity of ٧٥ lb/yd^{٣} (٤٥ kg/m^{٣}). An increase in the compressive strength in the range of ٥ to ٢٥٪ within ٢٤ hours was observed. The magnitude of the increase was dependent on the fiber shape and the content.

In 1991, Johnston and Zemp examined the performance of steel fiber reinforced concrete under flexural fatigue loading in terms of fiber content from ٠.٥ to ١.٥ percent by volume, fiber aspect ratio from ٤٧ to ١٠٠, with four different types of steel fiber [٢٦]. The results showed that both fiber content and aspect ratio were important when the fiber contents

in excess of ١.٠ percent were associated with better performance, as were fiber aspect ratios above ٧٠ compared with those around ٥٠, and the best performance was obtained with ١.٥ percent volume of ٧٥ aspect ratio.

Soroushian,and Bayasi, in ١٩٩١, reported the results of an experimental study on the relative effectiveness of different types of steel fiber in concrete[٦٥]. A constant fiber volume fraction of ٢ % was used throughout this investigation. The fresh fibrous mixes were characterized by their slump, inverted slump-cone time, subjective workability, and the hardened materials by their compressive and flexural load-deformation relationships. The overall workability of fresh fibrous mixes was found to be largely independent of the fiber type, with crimped fibers producing only slightly higher slumps. Hooked fibers were found to be more effective than straight and crimped ones in enhancing the flexural and compressive behavior of concrete. Under flexural loads, crimped fibers were slightly less effective than straight ones in improving the strength and energy absorption of concrete.

In ١٩٩١, Kwak, et al. [٣٢] reported that the use of steel fibers had been increased the flexural members and columns of such concrete structures subjected to cyclic loadings such as bridge decks, highway roads, runways of airport, and buildings. However, few experimental tests has been carried out under fatigue loading. In the this study, reinforced concrete beams with fiber volume fractions of ١ and ٢ percent, with and without stirrups were investigated. In fatigue tests, it was found that the failure of the beam was usually due to breaking of fibers rather than fiber pullout.

AL-Ta'an, in ١٩٩٢, described a method for nonlinear flexural analysis of concrete beams, reinforced both longitudinal steel bars and steel fibers [١]. The method took into account the nonlinear response of the fiber concrete in compression and the stiffening effect of steel fibers

in the tension zone in the pre and post peak stages . The analysis was performed under monotonic increasing loads and capable of tracing the behavior of members in the post peak stages . The analytical results obtained such as deflection, curvature, strains, neutral axis position, maximum crack width, and ultimate loads showed good agreement with the published test results (mentioned in [٣]) .

In ١٩٨٢, Mansur [٤٥], made an experimental investigation on steel-reinforced concrete beams under combined bending and torsion force. It was used ten groups of beams, each consisting of three specimens. On the basis of the observed skew-bending mechanism of torsional failure, equations were derived for ultimate torque. The main conclusions drawn from the work were:

١. Uncracked torsional stiffness of a beam was dependent on torsion to moment ratio.
٢. Failure of a fiber-reinforced concrete beam in tension or in combined bending and torsion occured by bending about a skew axis.
٣. The increase in torsional strength with increasing beam depth was approximately linear.
٤. A small increase in bending moment significantly reduces the torsional capacity.

In ١٩٩٢, Ezeldin and Balaguru, conducted tests to obtain the complete stress-strain curves of steel fiber-reinforced concrete with compressive strengths ranging from ٣٥ MPa to ٨٤ MPa (٥,٠٠٠ to ١٢,٠٠٠ psi) [١٢]. The matrix consisted of concrete rather than mortar. Three volume fibers fractions of ٣٠ kg/m^{٣}, ٤٥ kg/ m^{٣} and ٦٠ kg/ m^{٣} and three aspect ratios of ٦٠,٧٥ and ١٠٠ were investigated. It was reported that the addition of hooked-end steel fibers to concrete, with or without silica

fume, increased marginally the compressive strength and the strain corresponding to peak stress.

Chern, et al., in ١٩٩٢, studied experimentally the strength and deformation behavior of steel fiber reinforced concrete subjected to multiaxial stresses[٨]. The tested results showed that steel fiber reinforced concrete performed better than plain concrete, particulary when tensile stresses were involved. Adding steel fibers to cementitious materials improved many engineering properties by providing a different deformation and failure mechanism than that of a plain cementitious matrix, the fibers could provide a crack arrest mechanism and thus greatly improved the toughness of concrete. The effect of fiber was more obvious under tensile loading than compressive loading.

In ١٩٩٢, Hsu, et al. presented a computer algorithm that analyzes the complete moment-curvature and load-deflection behavior of steel fiber reinforced concrete (SFRC) beams [٢٣]. An empirical investigation suggested expressions for a complete stress-strain curve for normal concrete with steel fibers. The use of computer program just mentioned had been designed to carry out the theoretical analysis of complete load-deformation behavior of simply supported beams under two-point loading. The theoretical results of the load-deformation relationship carried out by the presented computer program had been compared with actual test, and showed a good correlation between each other.

Siah, et al., in ١٩٩٢, conducted the micromechanical model which was used to the stress-strain relationship for a typical region in a steel fiber reinforced material [٦٦]. The result showed that the tensile strength, toughness, and fracture toughness of cementitious were increased by the addition of small percentages by volumes of fibers. The mechanical properties of the resulting composite material were dependent on the properties of its constituent materials (matrix material, fibers, and fiber-

matrix interface) and the geometry of the composite (fiber volume, geometry, and spacing).

Kovács, et. al , in ١٩٩٨, presented a new composite material model, suitable for modeling fiber reinforced concrete under static loading [٣٣]. The model considered three phases in the composite material, an elastic one, a brittle fracture (concrete), and composite fiber yielding. Two permanent variables were introduced, the first related to matrix cracked, and the other to plastic fiber deformation.

Wu, in ١٩٩٩, predicted that when fiber reinforcement was used, the composite could become tougher and stronger, resulting from the additional increase in fracture toughness due to the toughening effect of the fibers in front of the crack tip and the bridging effect of the fibers behind the crack tip [٧٦]. For randomly oriented short fibers and complete fiber pullout, the ultimate tensile strength of the composites was found proportional to the fiber content and interfacial bond. The critical fiber volume fraction had been defined as the minimum fiber quantity required ($Vf_{critical}$) for achieving multiple cracking. The exact magnitude of this quantity depended on all relevant materials parameters, including fracture toughness of matrix, fiber properties, and interfacial bonds.

Maalej, in 1999, predicted the moment-curvature relationship for steel fiber reinforced (SFR) concrete [٤٦]. The prediction was based on a tensile stress-strain model where the softening branch was modeled by a bilinear stress-strain relationship. Model-predicted moment curvature relationships were found in an overall good agreement with published experimental data.

Hartmann, in 1999, investigated experimentally the flexural behavior in statically indeterminate steel fiber reinforced concrete beams [٢٤]. They tested beam specimens ١٠٠ mm (height) × ٢٥٠ mm (width) and a length of ١٨٦٠ mm. using two fiber contents ٦٠ kg/m^3 and ١٠٠

kg/m³, with an aspect ratio (L_f/D_f) of ٦٥. The main conclusions drawn from the work were:

١. Steel fiber significantly increased ductility of concrete.
٢. Evaluated the influenced of different fiber content on the load capacity of the statically indeterminate beams, the specimens contained ٦٠ kg/m³ showed higher strengths than that contained ١٠٠ kg/m³.
٣. The fiber distributed played a significant role in the failure of the crack-prepared.
٤. Peak load was generally reached at approximately ٢٠ mm deflection in the main crack section for all beams.

In ٢٠٠٠, Noghabai investigated shear and bending on beams of fibrous concrete [٥٢]. The tests were conducted on ٣٢ beams with four different depths: ٢٥٠, ٣٠٠, ٥٠٠, and ٧٠٠ mm. Various types of fibers (metallic and nonmetallic) were added to the concrete matrix. Contrast to the nonmetallic fibers, steel fibers were more able to redistribute the strains amoung the arisen cracks. It was found that the failure may also occur in the tension zone as a bond failure, which manifests in longitudinal splitting cracks.

Wang, et al., in 2000, predicted that the fiber reinforcement could effectively improve the toughness, shrinkage, and durability characteristics of concrete [٧٥]. They reported that using of recycled fibers from industrial or postconsumer waste could additional advantages of waste reduction and resources conservation. Many shown fibers have been used for concrete reinforcement, and they included steel, glass, natural cellulose, carbon, nylon, and polypropylene, among others.

In 2001, the improvement of fatigue properties of RSFC over RC beam had been investigated by ***Suthiwarapirak, et al.*** [٦٩]. From the analysis, the addition of fibers led to the improvement in fatigue life of

reinforced concrete beams, particularly the improvement in shear fatigue resistance. Shear fatigue life increased significantly, and thus, the failure mode of RC beams with fibers could be changed from shear which was brittle to flexure which was ductile. This also revealed that fiber-concrete could be used for the repair and improvement of structures subjected to fatigue load, such as bridge decks.

The behavior of steel fiber reinforced concrete prisms subjected to centric or eccentric compressive loading were researched by ***Schumacher, et al.*** [٧٢] ***2001***. The goal was to describe the softening behavior of the prisms and to make the Compression Damage Zone model applicable for fiber reinforced concrete. It was used ٤٠ kg per m^3 hooked ends steel fiber, and ٣٠ mm fiber length with ٤٥ aspect ratio.

Gustafsson and Noghabai, investigated experimentally if steel fibers could replace stirrups as shear reinforcement in high strength concrete beams [١٥]. It was used twenty beams which were fabricated with various types and amounts of fibers. They concluded that by addition steel fibers in relatively small concentrations, ١٪ volume or less, it was possible to reach shear capacities of the same order as in the case of conventional shear reinforcement, at least for small beams with an effective depth of about ٢٠٠ mm. In addition, a mix of short, straight fibers, ٦/٠.١٥, and longer fibers, ٣٠/٠.٦, that were hooked in the ends, providing the best contribution to the shear resistance of the beams. A possible explanation was that the small fibers started to act at an early stage, arresting and could not contribute at the same degree anymore. Instead, the longer fibers that bridges were used.

In ٢٠٠٢, Padmarajaiand and Ramaswamy had an experimental and analytical comparison of the flexural behavior of high – strength concrete specimen(No conventional reinforcement) with an average plain concrete cube strength of nearly ٦٥ MPa containing rough shape steel fibers [٥٨]

with a volume fraction ranging from ٠ to ١.٥ % and having a constant aspect ratio of ٨٠. Increased toughness and a more ductile stress-strain response were observed with an increase in fiber content, when the fibers were distributed over the full/partial depth of the beam cross section.it was showed the toughness index was greater for full-depth FRC beams. Predicted full-depth FRC would be needed in concrete elements subjected to high strain rates, repeated loading and stress reversal.

In ٢٠٠٢ , Gencoglu, et al., studied several methods which had been developed to predict the flexural strength of beams reinforced with both bars and fibers [١٨]. Fig. (٢.٣) shows that one of these methods was developed by Ezeldin and Shiah and presented as follows, [١٨].

$$f_{tu} = 0.00772 \times F_{be} \times (L_f \times D_f) V_f \text{ [MPa]} \qquad (٢\text{-}٣)$$

where

F_{be} is the bond efficiency factor of fibers, which varies from ١.٠ to ١.٢ depending upon fiber characteristics.

V_f is the percent of fibers by volume.

After the cross-section is cracked, by using the compressive stress strain and tensile stress–strain relationship of SFRC, the moment equilibrium equation can be written with respect to the location of CC and is given in expression (٢-٤).

$$M = A_s f_{St}(d - \lambda_c) + A_s' f_{Sc}(\lambda_c - d') + C_T(\lambda_T - \lambda_C) \qquad (٢\text{-}٤)$$

where

S_T the tensile force of As,

S_C the compressive force of A’s,

C_C the compressive force of SFRC,

C_T the tensile force of SFRC,

f_{St} the steel tensile stress of As,

f_{sc} the steel compressive stress of A′s,

y_c the neutral axis depth,

λ_C, λ_T are the location of CC and CT force, respectively.

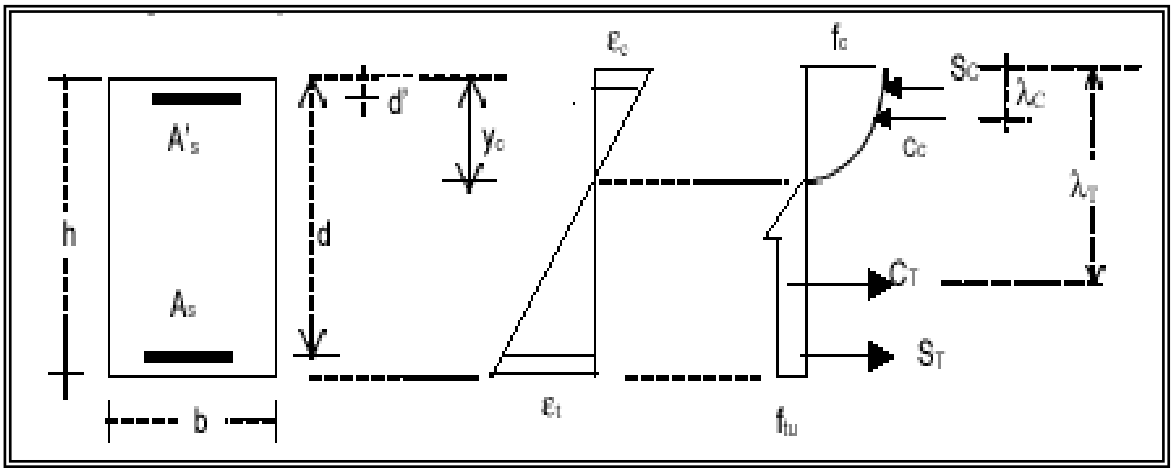

Fig. (٢.٣) bending behavior of SFRC beams [Gencoglu ٢٠٠٢]

In 2002, Harajli, et al. studied experimentally the characteristics of the local bond strength and slip behavior of reinforcing bars embedded in plain and fiber reinforced concrete (FRC) [٢٥]. The influence of two main parameters on the bond-slip response was evaluated namely, the ratio of concrete cover to bar diameter and the volume fraction of steel fibers. It was found that the adding fibers in ١ and ٢% by volume fraction increased the splitting bond strength, on average, by ٢٦ and ٣٣%, respectively, and resulted in asignificant improvement in the ductility of bond failure.

Lee et al., in 2002, proposed empirical equation and studied the effects of steel fibers and/or steel hoops in fly ash concrete [٣٦]. The proposed equation fitted well in various concrete mixtures including steel fibers and/or hoops, and can be found useful in studying the behavior of fly ash concrete structures reinforced with steel fibers in addition to the standard steel reinforcing bars and stirrups. It was found that the addition

of steel fibers improves the post peak behavior. This proves that addition of steel fiber is good for ductility improvement. As indicated in Fig. (٢.٤), the ductility of concrete can be significantly improved by adding steel fibers and/or hoops in concrete.

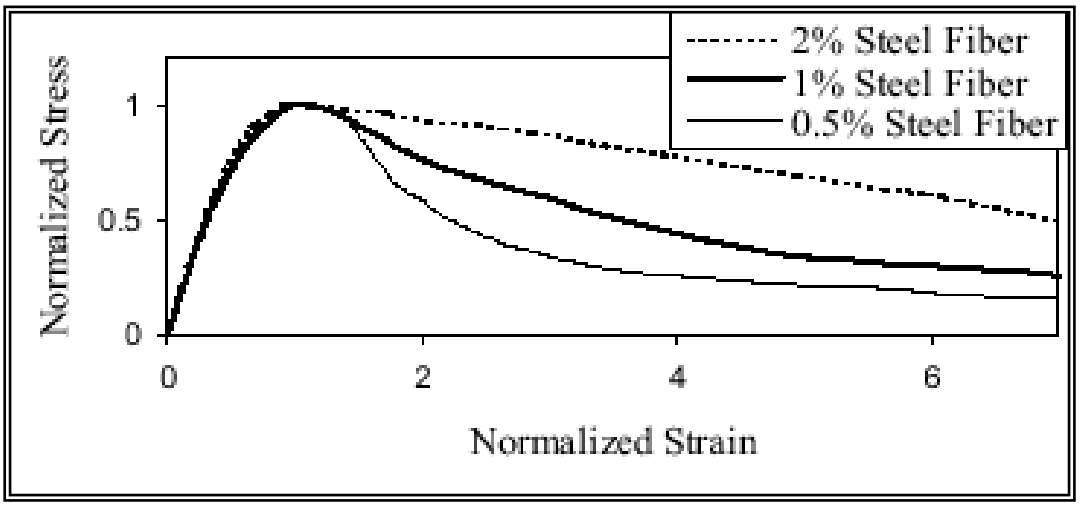

Fig. (٢.٤) Normalized Stress-Strain Curve for Steel Fiber Concrete, ٢٠٪ Fly Ash Replacement, (Lee and Punurai ٢٠٠٢)

Kholmyansky, in 2002, studied experimentally the influence of steel fiber reinforced concrete (SFRC) load resistance model [٣٠]. Four stages were considered: the elastic stage, the stage of closed isolated crack development, and the stages of through-crack development in the absence of fiber ruptures. The main results of these experiments were as follows:

١. Longitudinal resistance of fibers to crack growth reaches a maximum, after which it decreases to zero.
٢. Transverse resistance increases monotonically.
٣. The total resistance increases if the crack opening is small and decreases if it is larger.
٤. Increase in the SFRC strength was larger when the bond was better.

In 2002, Şener, et al. investigated experimentally the failure of notched concrete beams with or without steel fiber reinforcement subjected to four-point bending [٦٧]. The bending failure in the steel fiber-reinforced beams exhibited a greater size effect and higher brittleness than beams without steel fibers.

In 2003, Löfgren, and Betong discussed the flexural behavior and crack propagation in FRC members, and was also compared with conventional reinforced concrete members [٤١]. Special attention was given to how the combined effect of fiber bridging and reinforcement bars influence the structural behavior the serviceability- and ultimate limit state. The effects of the fiber bridging were investigated by means of analytical models and finite element analyses, both based on non-linear fracture mechanics and uniaxial material properties.

Kan et al, in 2003, studied experimentally the toughness of heavy concrete based on ASTM C١٠١٨ [٣٤]. It was used mixture including ٠%, ٠.٥%, ١% and ١.٥٪ of steel fiber content by volume fraction. Test results revealed that tensile strength, rupture modulus and strengths appeared increasing with the increase of steel fiber content. It was showed that the toughness of heavy concrete grew with the steel fiber fraction.

Farhang and Silfwerbrand, tested the combined mechanical and thermal loading on plain and steel fiber reinforced concrete beams [١٣]. Ten beams were conducted on plain concrete beams (PCB) and ١٤ beams of steel fiber reinforced concrete with ٠.٧٥ percent by volume of Dramix steel fibers (٦٠ kg/m^{٣}) with a fiber length of ٣٠ mm and fiber diameter of ٠.٥ mm. The test included heating the top surface of the test beams provided thermal load, whereas mechanical load was introduced by applied a point load at mid-span of the tested beams. It was found in both

mechanically and thermally loaded tests, the failure occurred as a result of flexural bending at the mid-span of the beams.

In 2003, Ouaar, et al. studied experimentally the mechanical behavior of Steel Fiber Reinforced Concrete (SFRC) [٥٦]. The several specimens of concrete and fiber-reinforced concrete were with different volume fractions of fibers. The specimens tested under four point bending. It was showed an energy-based damage model that the damage in the material was linked to the history of elastic plastic state variables.

There are a number of factors that influence the behavior and strength of FRC in flexure. These are summarized by ***zia, et al.*** [٧٩]. These include: type of fiber, fiber length (L), aspect ratio (L/d_f) where df is the diameter of the fiber, the volume fraction of the fiber (V_f), fiber orientation and fiber shape, fiber bond characteristics (fiber deformation). Also, the factors that influence the workability of FRC such as W/C ratio, density, air content and the like could also influence its strength. The ultimate strength in flexure could vary considerably depending upon the volume fraction of fibers, length and bond characteristics of the fibers and the ultimate strength of the fibers. Depending upon the contribution of these influencing factors, the ultimate strength of FRC could be either smaller or larger than its first cracking strength.

Generally, there are three stages of the load-deflection response of FRC specimens tested in flexure and schematically they are shown in Fig. (٢.٥). The three stages are:

١. A more or less linear response up to point A. The strengthening mechanism in this portion of the behavior involves a transfer of stress from the matrix to the fibers by interfacial shear. The imposed stress is shared between the matrix and fibers until the matrix cracks at what is termed as "first cracking strength" or "proportional limit".

٢. A transition nonlinear portion between point A and the maximum load capacity at point B (assuming the load at B is larger than the load at A). In this portion, and after cracking, the stress in the matrix is progressively transferred to the fibers. With increasing load, the fibers tend to gradually pull out from the matrix leading to a nonlinear load–deflection response until the ultimate flexural load capacity at point B is reached. This point is termed as "peak" strength.

٣. A post peak descending portion following the peak strength until complete failure of the composite. The load–deflection response in this portion of behavior and the degree at which loss in strength is encountered with increasing deformation is an important indication of the ability of the fiber composite to absorb large amounts of energy before failure and is a characteristic that distinguishes fiber-reinforced concrete from plain concrete. This characteristic is referred to as toughness.

The nonlinear portion between A and B exists, only if a sufficient volume fraction of fibers is present. For low volume fraction of fibers (V_f < ٠.٥٪), the ultimate flexural strength coincides with the first cracking strength and the load–deflection curve descends immediately after the cracking load, Fig. (٢.٦). Typical load–deflection curves of FRC beams observed experimentally for different types of fibers are shown in Fig. (٢.٧).

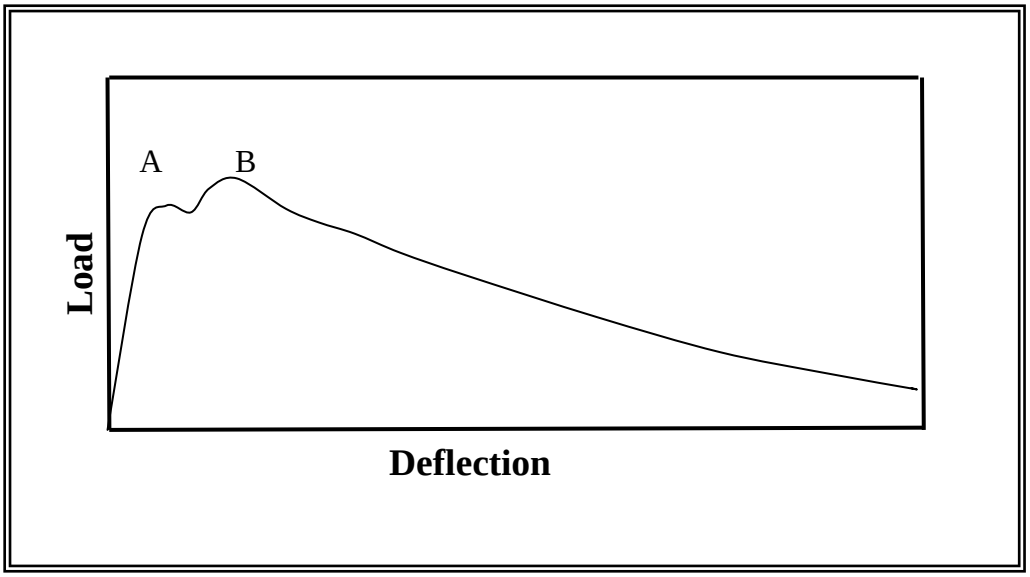

Fig. (٢.٥) Schematic load-deflection diagrams

(*zia, et al.* [٧٩]

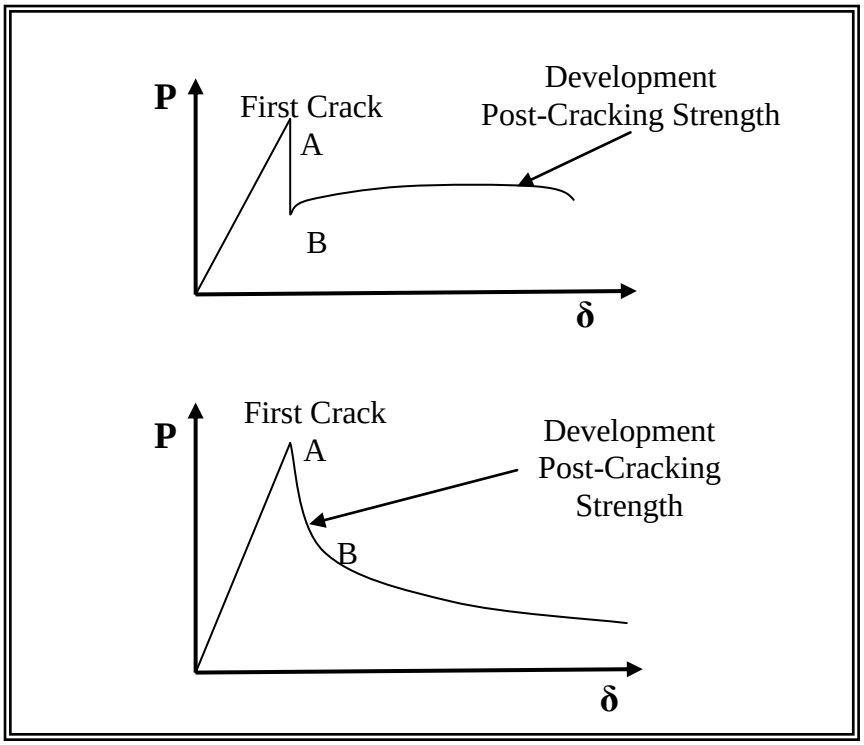

Fig. (٢.٦) Typical load-deflection curves of FRC beams with low volume fraction of fibers (*zia, et al.* [٧٩])

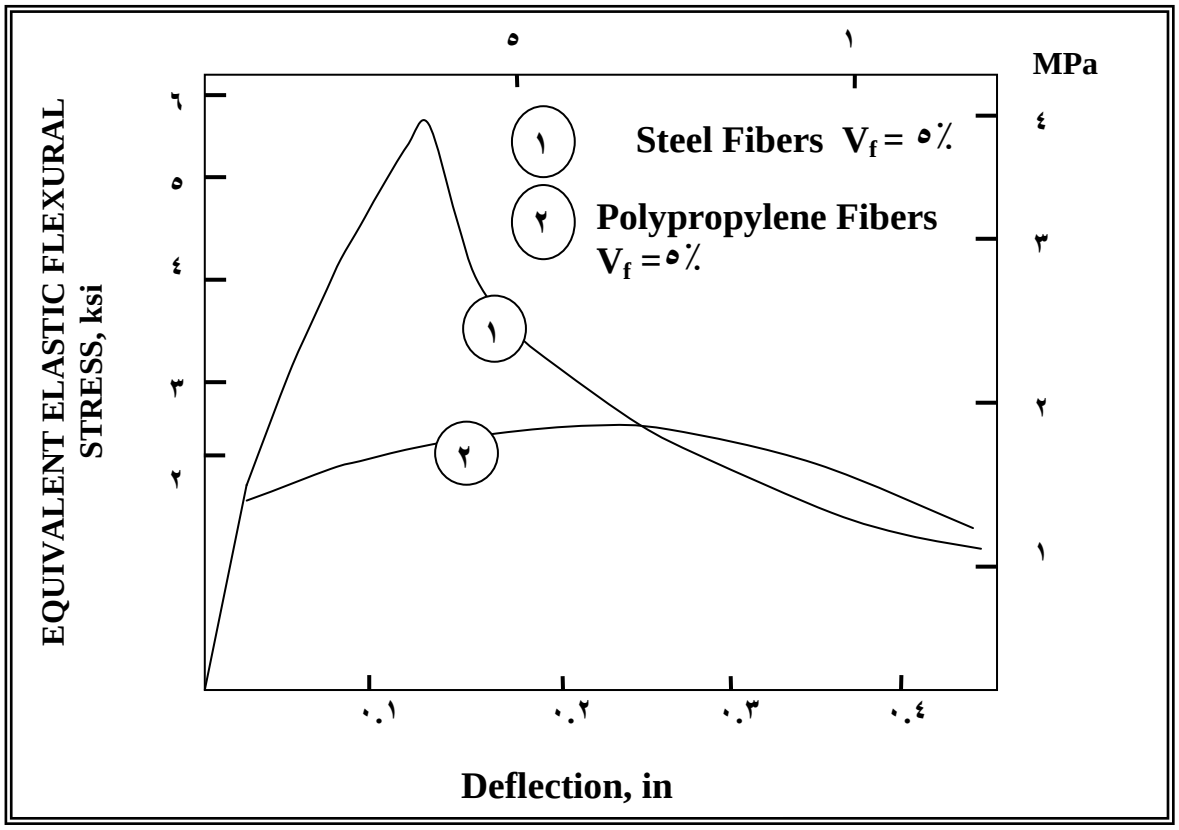

Fig. (٢.٧) Experimentally observed load-deflection curves of steel and polypropylene fiber reinforced concrete beams (***zia, et al.*** [٧٩])

٢.٤ (SFRC) Members under Cyclic Loading

The addition of fibers to concrete has been shown to be significantly increase the toughness and to promote more ductile material behavior additives. For these reasons, fiber reinforced concrete had been proposed for using in structures that must withstand extreme loading condition such as these induced by earthquakes.

Morris and Garrett, in ١٩٨١, studied the effects of steel fiber addition on the comparative static and fatigue properties of cement mortar, tested in both tension and compression [٤٣]. The compressive specimens ٦٠×٦٠×١٨٠ and tensile specimens ٧٦×٧٦ ×٣٢٥ mm. Typical volume fraction (٢٪) of fixed dimension (Duoform) was used. The post-

failure resistance to cracking was substantially improved by the addition of steel fiber. It was found the compressive strength a small (٧٪) increase but only the Duoform-type fibers. The fatigue strength at ١ million cycles (ran out) was increased from approximately ٥٥٪ to bout ٦٠-٦٥٪ of the maximum static stress with the addition of steel fibers.

In ١٩٨٦, Gopalaratnam and Shah, [١٧] showed that linear unloading and reloading curves with a slope equal to the initial modulus of elasticity of the matrix may well simulate the response of (SFRC) material under the effect of cyclic loads, Fig. (٢.٨).

Otter and Naaman, in ١٩٨٨, conducted an experimental investigation in an attempt to describe the behavior of steel fiber reinforced concrete when it was subjected to cyclic compressive loading [٥٣]. The main result concluded that:

١. The envelope curve was shown to govern cyclic response.
٢. Toughness under cyclic loading was found to be at least as great as that under monotonic loading.

Soroushian and Lee, in ١٩٨٩, [٦٨] presented a constitutive model to represent the compressive stress-strain relationship of SFRC as a function of the matrix strength f'_c and the fiber reinforcement index $\left(\frac{V_f L_f}{D_f}\right)$, as shown in Fig. (٢.٩), the model consists of a curvilinear ascending portion

$$f = f'_{cf}\left(\frac{2\varepsilon}{\varepsilon_{cp}} - \left(\frac{\varepsilon}{\varepsilon_{cp}}\right)^2\right) \text{ [MPa]} \qquad \varepsilon \leq \varepsilon_{cp} \qquad (٢\text{-}٥)$$

and a bilinear descending portion

$$f = z\left(\varepsilon - \varepsilon_{cp}\right) + f'_{cf} \geq f_o \text{ [MPa]} \qquad \varepsilon > \varepsilon_{CP} \qquad (٢\text{-}٦)$$

where

f , ε compressive stress and the corresponding strain, respectively.

f'_{cf} , ε_{cp} compressive strength and the corresponding strain of SFRC, respectively.

z slope of the descending portion of the compressive stress-strain curve.

One of the significant discrete fibers is their ability to arrest and slow down the progress of tensile cracking. Addition of steel fibers increases concrete tensile strength by (٤٠-٣٠) percentage. ***Sorourshian and Lee*** [٦٨] suggested the following formula to estimate the tensile stress of fibrous reinforced concrete;

$$f_{tf} = f_t\left(1 + 0.16\, N_f^{1/3} + 0.5\pi\, D_f\, L_f\, N_f\right)[\text{MPa}] \qquad (٢\text{-}٧)$$

where:

f_{tf} The tensile strength of steel fiber reinforced concrete in MPa.

f_t The tensile strength of plain concrete also in MPa.

N_f The number of fibers per unit cross section area and is given by

$$\cdot\ N_f = \eta_o \frac{4V_f}{\pi\, D_f^2} \qquad (٢\text{-}٨)$$

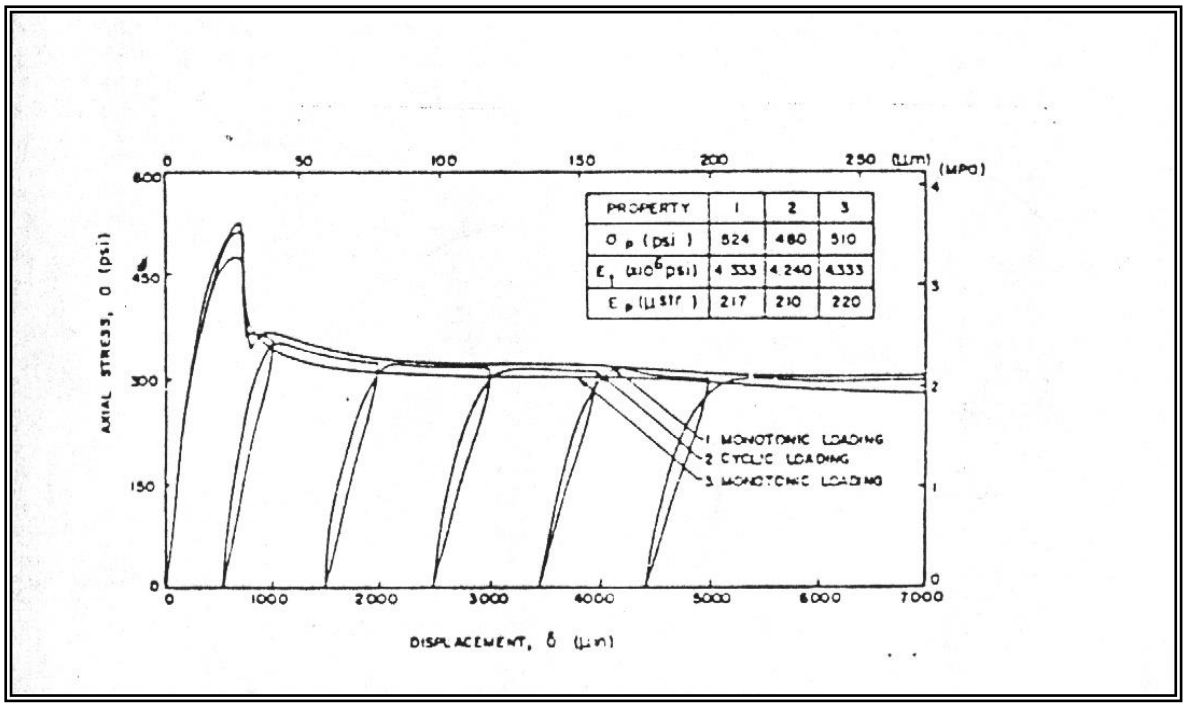

Fig. (٢-٨) Experimental stress-displacement relationship for SFRC in tension (Gopalaratnam and Shah ١٩٨٦)

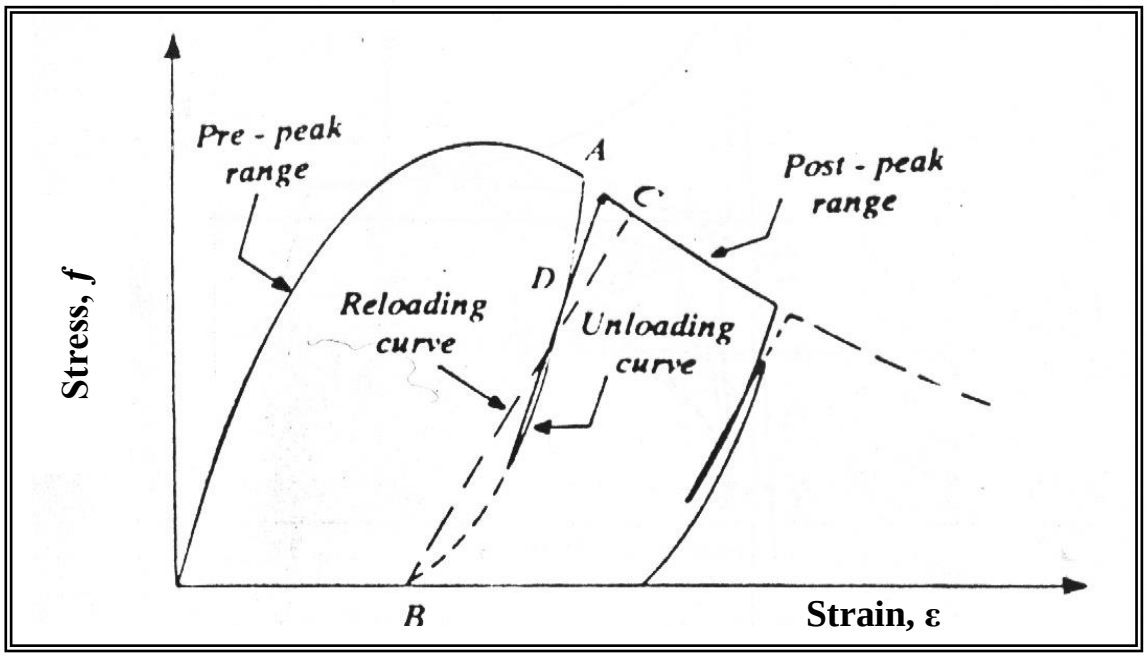

Fig. (٢.٩) Compressive stress-strain relationship of SFRC material (Soroushian and Lee ١٩٨٩)

Otter and Naaman, in ١٩٨٩, developed a model to predict the stress-strain behavior of concrete composite under random cyclic compressive loadings [٥٤]. The model used the envelope unloading strain as an index of load history. The plastic and the reloading strain were predicted as functions of the envelop unloading and reloading stages of behavior. The proposed model was shown in Fig. (٢-١٠). Expressions for the plastic and the reloading strains were.

$$\frac{\varepsilon_{pc}}{\varepsilon_{cp}} = \frac{\varepsilon_{uc}}{\varepsilon_{cp}} - k_u\left(1 - e^{\frac{\varepsilon_{UC}}{k_u \varepsilon_{cP}}}\right) \qquad (٢\text{-}٩)$$

and

$$\frac{\varepsilon_{rc}}{\varepsilon_{cp}} = \frac{\varepsilon_{uc}}{\varepsilon_{cp}} + k_r \qquad (٢\text{-}١٠)$$

Expression for the unloading and the reloading curves were

$$\frac{f}{f_{uc}} = \left(1 - p\right)\frac{\varepsilon_c - \varepsilon_{pc}}{\varepsilon_{uc} - \varepsilon_{pc}} + p\left(\frac{\varepsilon_c - \varepsilon_{pc}}{\varepsilon_{uc} - \varepsilon_{pc}}\right)^{nuc} \qquad (٢\text{-}١١)$$

and

$$\frac{f}{f_{rc}} = \frac{\varepsilon_c - \varepsilon_{pc}}{\varepsilon_{rc} - \varepsilon_{pc}} \qquad (٢\text{-}١٢)$$

where:

f_{uc}, ε_{uc} unloading compressive stress and strain , respectively

f_{rc}, ε_{rc} reloading compressive stress and strain respectively.

k_u, k_r unloading and reloading constant.

p , n_{uc} unloading curve parameters.

Zhang, Stang, and Li, in ١٩٩٩, investigated a semi-analytical method to predict fatigue behavior in flexure of fiber reinforced concrete (FRC) based on the equilibrium of force in the critical cracked section [٨٠]. The predicted optimum fatigue behavior of (FRC) structures in bending can be a chivied by optimizing the bond properties of aggregate-matrix and fiber-matrix interfaces. Good correlation between experiments and the model predictions was found.

In ٢٠٠٠, Zhang, et al. studied experimentally the crack bridging in steel-fiber-reinforced concrete (SFRC) materials under deformation-controlled uniaxial fatigue tension [٨١]. Two types of steel fibers, straight steel fiber and hooked end steel fiber. It was shown that the hooked fiber can efficiently improve the monotonic crack bridging performance compared to straight fibers in (FRC) materials under cyclic loading.

Michael Gebman, in ٢٠٠١, investigated experimentally beam-column subjected to seismic loading [٢٠]. The concrete mix with a ٢٪ volume fraction of hooked end steel fibers and had a length (٣١ mm) and a diameter (٠.٥ mm) resulting in aspect ratio of about ٦٠. The effects of steel fibers on mechanical properties of concrete are depicted in Fig. (٢.١١). As shown in the Fig. (٢.١١) the addition of steel fibers increases the tensile toughness and ductility. It also increases the ability to withstand stresses after significant cracking (damage tolerance) and shear resistance.

In ٢٠٠٢, Gençoglu and Eren showed that ductility and strength capacity could be increased by using SFRC and confinement regions of the beam and confinement regions of the beam and column [١٦]. The specimens tested under reversed cyclic loading. The test results showed that ductile behavior and the strength capacity of beam-column connections depended on the volume content, aspect ratio of the fibers, and fiber type.

Summary:

It is clear from the preceding review that there is no detailed study that deals with the inelastic non-linear behavior of partial-depth steel fibers reinforced concrete members under cyclic loading. This problem is treated in this study, by using the layering technique to treatment of the variation in material properties though the thickness. The hardening rule, flow rule, tension stiffening and crushing state are taken into account. Material non-linearity, geometric non-linearity and coupling between bending moment, shear and axial forces are taken into account.

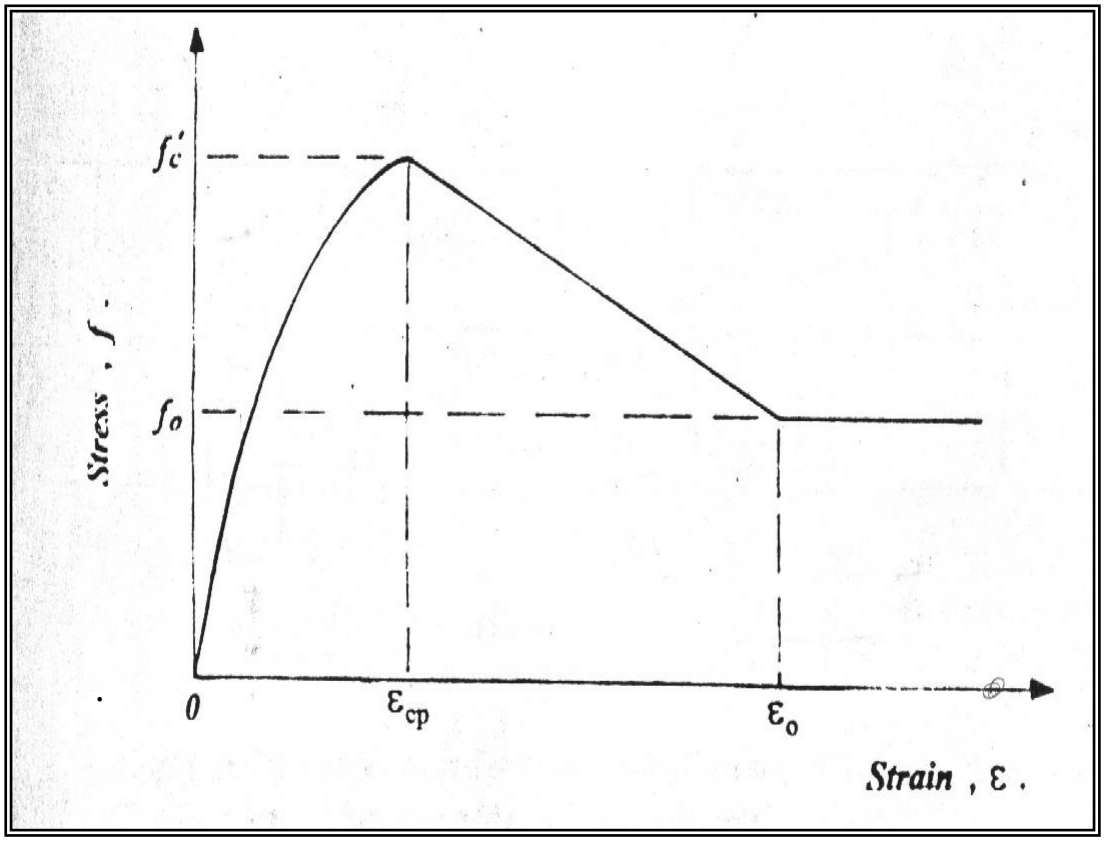

Fig. (٢.١٠) Compressive stress-strain model for FRC material under cyclic loading (Otter and Naaman ١٩٨٩)

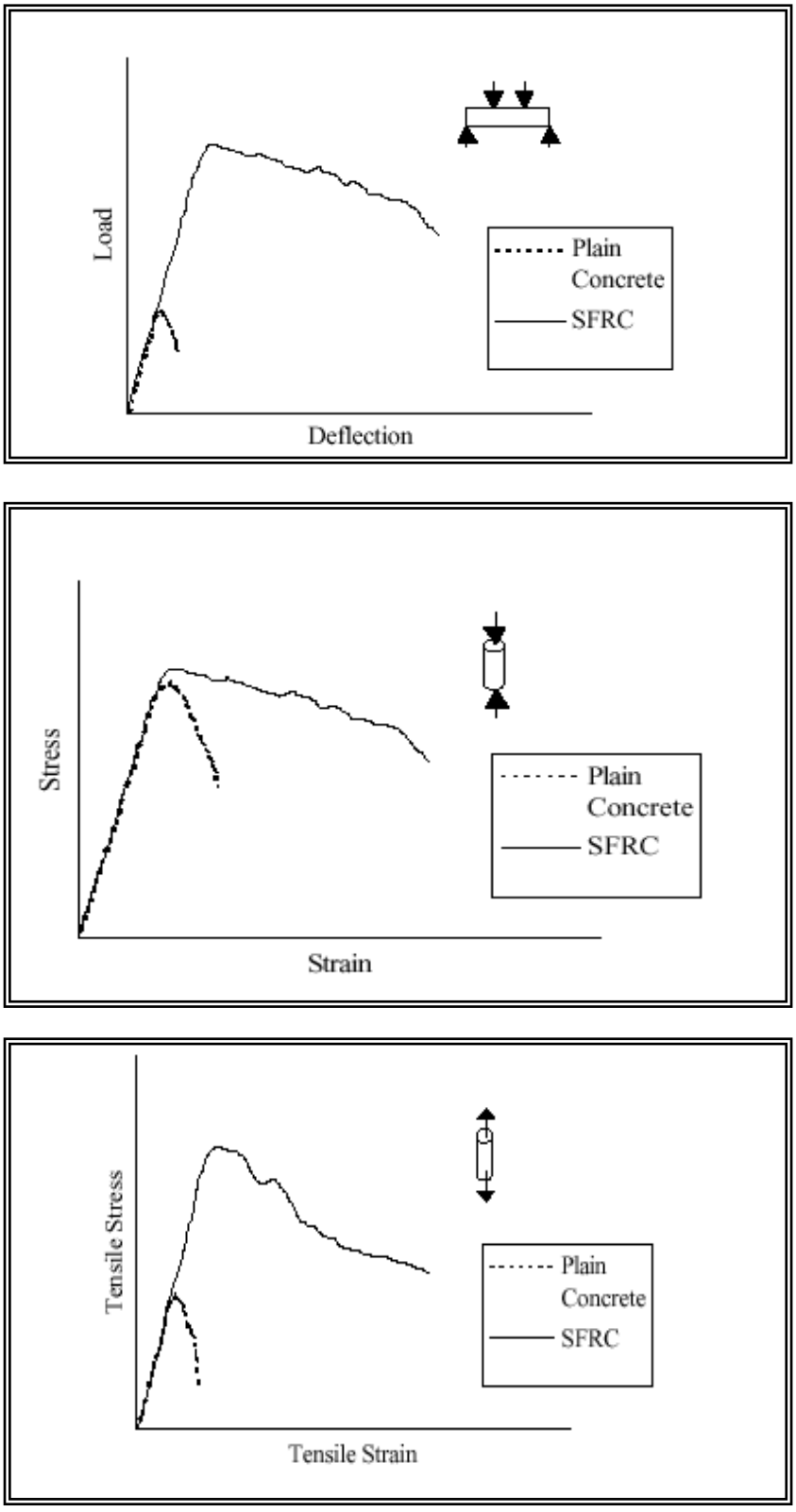

Fig. (٢.١١) Stress-strain curves of SFRC [٢٠]

CHAPTER THREE
MODELING OF MATERIAL PROPERTIES

٣.١ General

Plain concrete is a brittle material which has low tensile strength with low resistance to crack propagation. It is necessary to improve tensile resistance of member made of concrete. This has been done by the use of steel bars, but without increasing tensile strength of concrete itself. The presence of fibers in fibrous concrete matrix enhances the tensile strength properties and the stiffness of the resulting composite by controlling tensile cracking of the material. Steel fibers are added to concrete mixture for improving its ductility, fracture toughness, tensile, flexural and shear strength. For these aims, the use of fibers in concrete mixture started in the early١٩٦٠s, [١٨]. In the beginning, only straight steel fibers were used. The major problems encountered in early stages were the difficulty in mixing and workability. This process, called balling, was found to occur frequently for longer fibers.

The advent of deformed fibers and high-range water-reducing ad-mixtures a big boost to the fiber reinforced concrete use in the field. ***Ramarkishnan et al*** [٦٠] mentioned in [١٨] stated that obtained successful results from the point of ductility and toughness were by using the fibers with hooked ends and glued together at the edges with water-soluble glue, [٦٠,٦١] mentioned in [١٨].The use of these fibers and the water reducing admixtures eliminated the problem associated with reduction in workability have been reasoned homogenous mixtures. Steel fiber reinforced concrete, had been used in hydraulic structures, airports, highways, industrial floors.

In numerous investigations, it has been displayed that the flexure, shear, torsion, punching, dynamic impact behaviors of structural elements improved by the use of SFRC. Although SFRC improves the element behavior, it is not widely used in columns, beams or slabs since a non-empirical calculation model based on experimental results is not developed yet. One reason of the lack of a proper calculation model can be stated as the various parameters affecting the SFRC behavior. These primary factors are fiber volume fraction, the properties of fibers, length/diameter (aspect ratio), water reducing admixtures, fibers orientations in mixtures and concrete performances. However, the positive effects of SFRC on the flexure behavior of the structural elements are given as follows by ***Craig*** [٧] mentioned in [١٨].

i. increases moment capacity and cracking moment,

ii. increases the ductility,

iii. tensile strength increases,

iv. improves crack control,

v. increases rigidity,

vi. preserves the structural integrity after beam exceed the ultimate load.

٣.٢ Uniaxial behavior of Fibrous Concrete in Monotonic and Cyclic Loads.

٣.٢.١ Uniaxial Compressive Stress-Strain Relationship

An empirical model suggested by Soroushian and Lee [٦٨] is adopted in this study, Fig (٣.١). This model represents the stress – strain relationship of SFRC in compression as a function of the matrix strength, f'_c, and the

fiber reinforcement index $\left(\frac{V_f L_f}{D_f}\right)$ .The model consists of a curvilinear ascending branch given by

$$f = f'_{cf}\left(\frac{2\varepsilon}{\varepsilon_{cp}} - \left(\frac{\varepsilon}{\varepsilon_{cp}}\right)^2\right) \text{ [MPa]} \quad \text{for} \quad \varepsilon \leq \varepsilon_{cp} \qquad (٣\text{-}١)$$

and abilinear descending branch as

$$f = z\left(\varepsilon - \varepsilon_{cp}\right) + f'_{cf} \text{ [MPa]} \quad \geq f_o \quad \text{for} \quad \varepsilon > \varepsilon_{CP} \qquad (٣\text{-}٢)$$

$$f'_{cf} = f'_c + 3.6\frac{V_f L_f}{D_f} \quad \text{[MPa]} \qquad (٣\text{-}٣)$$

$$f_o = 0.12\, f'_{cf} + 14.8\frac{V_f L_f}{D_f} \quad \text{[MPa]} \qquad (٣\text{-}٤)$$

$$z = -343\, f'_c\left(1 - 0.66\left(\frac{V_f L_f}{D_f}\right)^{1/2}\right) \text{ [MPa]} \qquad (٣\text{-}٥)$$

$$\varepsilon_{cp} = 0.0007\frac{V_f L_f}{D_f} + 0.0021 \qquad (٣\text{-}٦)$$

where:

f , ε compressive stress and the corresponding strain, respectively.

f'_{cf} , ε_{cp} compressive strength and compression strain at peak stress level stress of SFRC, respectively.

f_o is the residual compressive stress.

V_f is the volume fraction of fibers.

z is the slope of the descending portion of the stress-strain compressive curve.

L_f, D_f are the length and diameter of the fiber, respectively.

The model recently developed by Otter and Naaman [٥٤] to predict the stress-strain behavior of concrete under cyclic loadings has been chosen to represent the cyclic behavior of SFRC in direct compression. Some of the key points to describe the response to cyclic loading are shown in Fig. (٣.١). Point A is the start of the unloading stage. Point C is the point at which the reloading parts of the curve meet the stress-strain envelop.

Expression for the plastic strain at zero stress and the stress-strain curve during unloading are given by:

$$\varepsilon_{pc} = \varepsilon_{uc} - \varepsilon_{cp} k_u \left(1 - e^{\frac{\varepsilon_{UC}}{k_U \varepsilon_{CP}}}\right) \qquad (٣\text{-}٧)$$

and:

$$f = f_{uc} \left[(1-p) \frac{\varepsilon - \varepsilon_{pc}}{\varepsilon_{uc} - \varepsilon_{pc}} + \left(\frac{\varepsilon - \varepsilon_{pc}}{\varepsilon_{uc} - \varepsilon_{pc}} \right)^{n_{uc}} \right] \text{ [MPa]} \qquad (٣\text{-}٨)$$

where:

$\varepsilon_{pc}, \varepsilon_{uc}$ are the plastic and unloading strains in compression, respectively.

f_{uc} is the compressive unloading stress.

k_u is the unloading constant (values of ٠.٨ are used).

p , n_{uc} are the unloading curve parameters (values of o.٩ and ٣ are used for P and n_{uc} respectively).

Expression for the reloading strain and the reloading part of the stress-strain curve are given by:

$$\varepsilon_{rc} = \varepsilon_{uc} + \varepsilon_{cp} k_r \qquad (٣\text{-}٩)$$

and:

$$f = f_{rc} \frac{\varepsilon - \varepsilon_{pc}}{\varepsilon_{rc} - \varepsilon_{pc}} \quad \text{(MPa)} \qquad (٣\text{-}١٠)$$

The unloading and reloading stress-strain curves of concrete are analytically expressed by a set of points connected by straight lines. The mean value for the strain between ε_{uc} and ε_{rc} is used:

$$\varepsilon_{ur} = \frac{\varepsilon_{uc} + \varepsilon_{rc}}{2} \qquad (٣\text{-}١١)$$

$$\varepsilon_{ur} = \frac{2\varepsilon_{uc} + \varepsilon_{cp} k_r}{2} \qquad (٣\text{-}١٢)$$

The unloading and reloading path are represented by the line connecting the two points $B(\varepsilon_{pc}, 0), H(\varepsilon_{ur}, f_{ur})$

where:

f_{uc}, ε_{uc} are the unloading stress and strain in compression, respectively.

f_{rc}, ε_{rc} are the reloading stress and strain in compression, respectively.

k_r is the reloading constant (a value of ٠.١ is used)

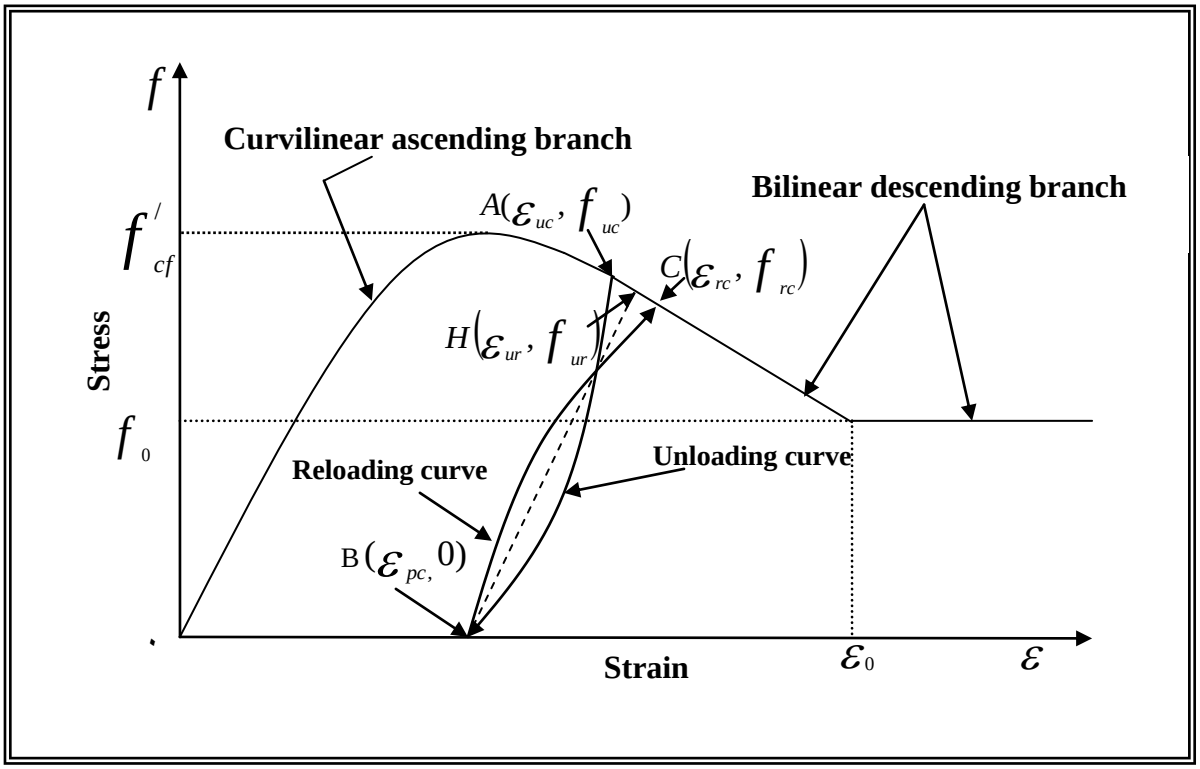

Fig. (٣.١) SFRC cyclic stress-strain curve in compression

Otter and Naaman [٥٤]

٣.٢.١.١ Crushing Strain

Results of previous study have shown that the compressive strain in fibrous concrete is greater than that of plain concrete with (ε_{cuf}) ranging between ٠.٠٠٣ to ٠.٠٠٦.

When the effective stress exceeds the compressive strength, the material is assumed to become perfectly plastic until crushing occurs. The crushing is assumed to occur, when the effective compressive strain (ε_P) exceeds the maximum compressive strain (ε_{cuf}), at which the material is assumed to lose all its strength and rigidity. Based on experimental results from reference [٦٤], the maximum strain for fibrous reinforced concrete (ε_{cuf}) was derived and adopted in reference [٣], which is given as:

$$\varepsilon_{cuf} = 3011 + 2295 V_f \qquad (٣\text{-}١٣)$$

where:

ε_{cuf} The maximum strain in microstrain.

٣.٢.٢ Uniaxial Tensile Stress-Strain Relationship

The addition of fibers to such matrices, whether in continuous or discontinuous form, leads to a substantial improvement in the tensile properties of the FRC in comparison with the properties of the unreinforced matrix. The stress-strain response of fiber composite in tension depends mainly on the volume fraction of fibers (V_f). Typical stress-strain curve for conventional SFRC composite is shown in Fig.(٣.٢). In general, the response can be divided into two distinct stages: the pre-cracking stage (where the matrix is uncracked) and post-cracking stage (where the matrix is cracked).

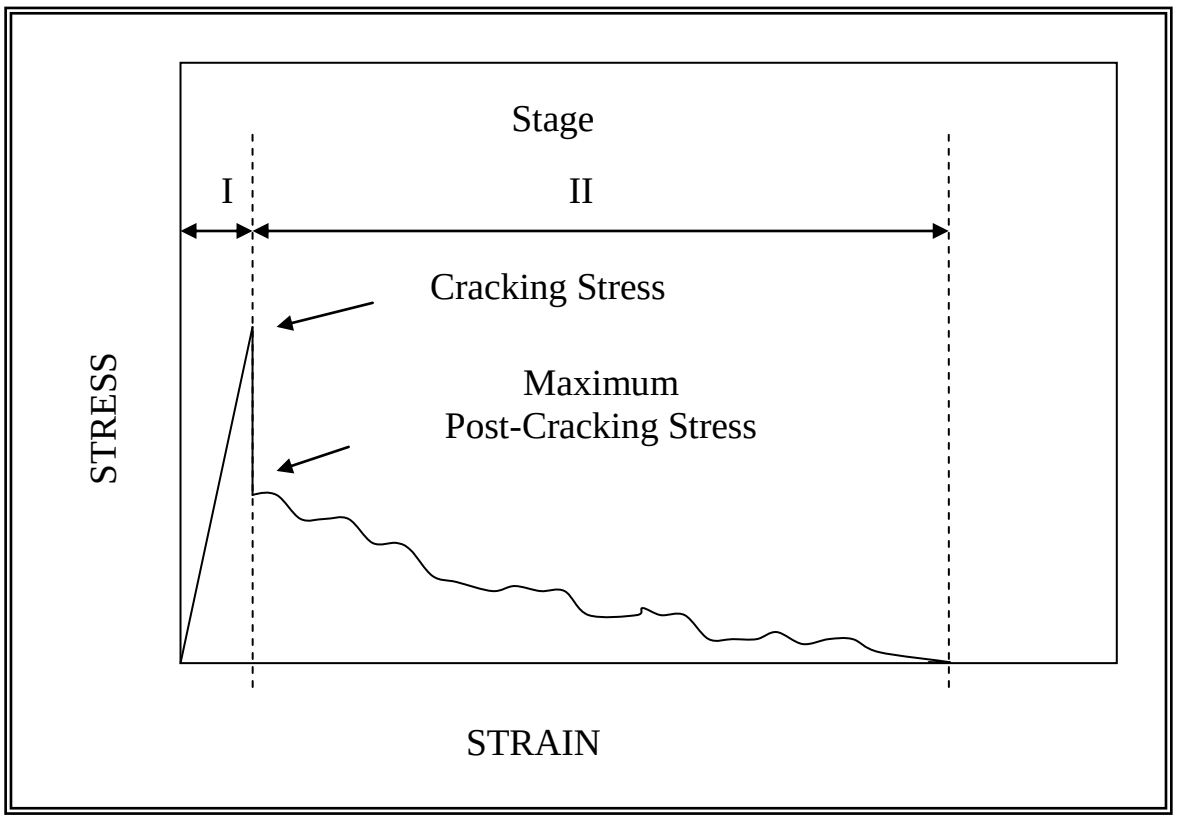

Fig. (٣.٢) Typical stress-stiran curve in tension of steel fiber reinforced concrete [٧٩]

In the pre-cracking stage before cracking, the composite (SFRC) can be described as an elastic material with a stress-strain response very similar to the un-reinforced matrix, where the influnce of matrix cracking in the composite is neglected. It is assumed that the steel fiber perfectly bounds with concrete matrix and that no slippage occurs at the fiber-matrix interface. The modulus of elasticity of concrete in tension E_{tf} , is asummed to be equal to the modulus of elasticity of concrete in compression.

Beyond the peak point, a post-cracking stage of behavior exists and is characterized by failure and/or pullout of the fibers about a single critical crack. The corresponding descending branch of the stress–strain curve can be steep or of moderate slope depending on the fiber reinforcing parameters and whether a brittle or ductile failure occurs. The following relationship which was proposed by Naji [٥١] and adopted by Jassim[٢٧] has been used in this study. This model describes the behavior of SFRC after cracking by exponential function ,Fig.(٣.٣), as follows:-

$$\sigma_n = \sigma_{Cr} \exp\left(-(\varepsilon_n - \varepsilon_0)/(\eta_O \eta_l \eta_b V_f + 0.001)\right) \quad \text{[MPa]} \qquad (٣\text{-}١٤)$$

$$\varepsilon_0 = \sigma_{Cr} / E_{Cf} \qquad (٣\text{-}١٥)$$

where

σ_{Cr} is the tensile stress at onest of cracking,

η_0 is the orintation factor,

η_l is the length factor,

η_b is the bond factor.

In this study a crack is assumed to be formed whenever a principal stress reaches the tensile strength of SFRC given by[١٤,٦٨]:

$$f_{tf} = f_t\left[1+0.016N_f^{1/3}+0.05\pi D_f L_f N_f\right] \quad \text{[MPa]} \qquad (٣\text{-}١٦)$$

$$\varepsilon_{tf} = \varepsilon_t(1+0.35 N_f \cdot D_f \cdot L_f) \qquad (٣\text{-}١٧)$$

f_{tf} The tensile strength of steel fiber reinforced concrete.

f_t The tensile strength of plain concrete.

N_f The number of fibers per unit cross-section area.

$$N_f = \eta_0 \frac{4V_f}{\pi D_f^2} \qquad (٣\text{-}١٨)$$

The residual tensile strength f_{tr} was related to the average ultimate pullout bond strength τ_u of the fiber:

$$f_{tr} = 2\eta_l \eta_0 \tau_u \cdot V_f \frac{L_f}{D_f} \text{ [MPa]} \qquad (٣\text{-}١٩)$$

The empirical expression for τ_u is adopted in Galli and Rinald (٢٠٠٣) [١٤]:

$$\tau_u = 2.26 - 0.0036 N_f \text{ [MPa]} \qquad (٣\text{-}٢٠)$$

ε_{tf} Composite tensile strain at peak tensile stress.

ε_t Matrix cracking strain.

The value of η_0 is between (٠.٣٣-٠.٥)[٣٩]. η_l is defined as the ratio of average fiber stress to the maximum stress,and

$$\eta_l = \begin{cases} 0.5 & for\ L_f \le L_C \\ 1 - L_C / 2L_f & for\ L_f > L_C \end{cases} \qquad (٣\text{-}٢١)$$

where:

L_f the actual length of fiber,

L_c the critical length of fiber ; ($L_c=f_{fu} .D_f /٢\tau_u$)

where: f_{fu} is the ultimate tensile strength of fiber.

In this study the value of η_l is between (٠.٥ - ١)[٢٧], η_b describes the bond state between the fibers and matrix, mainly depends on the shape of fiber, in this study the value of η_b is between (٠.٥ -١)[٢٧].

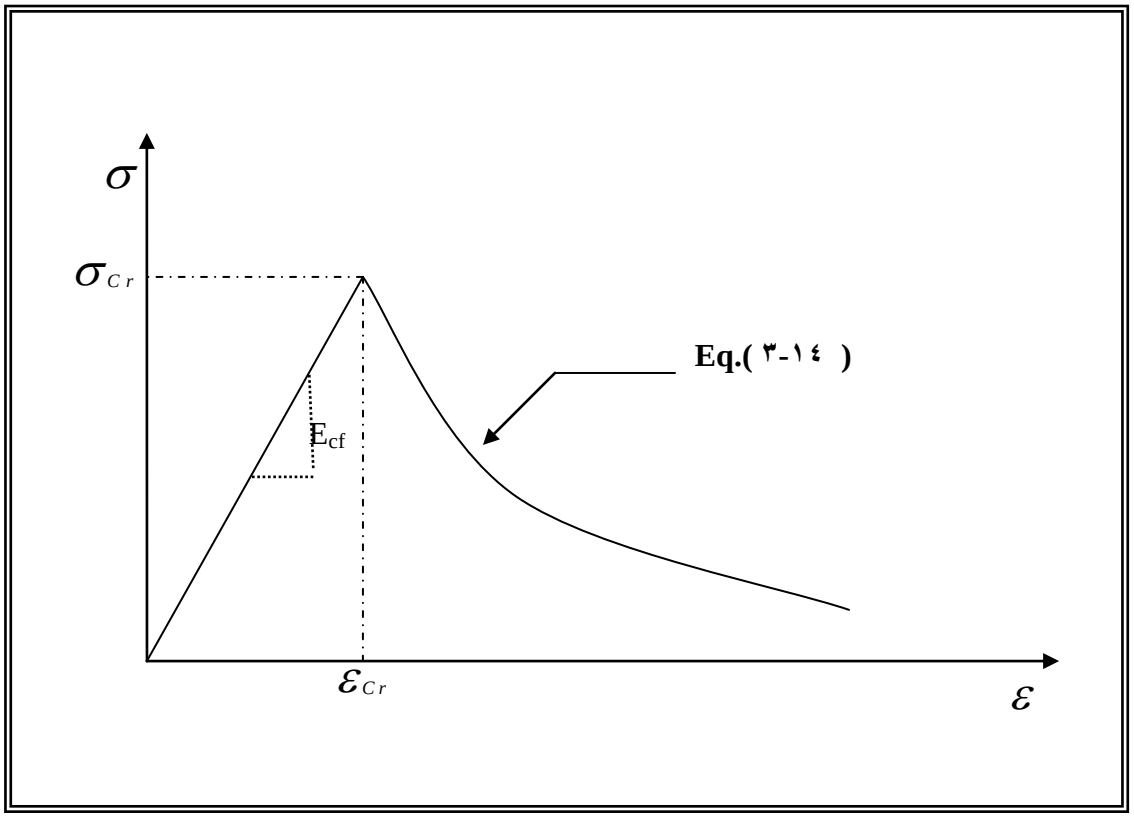

Fig. (٣.٣) Pre-cracking and post-cracking behavior of SFRC[٥١]

٣.٢.٢.١ Concrete in Tension (Behavior and Cracked Modeling)

The tension failure of concrete is characterized by a gradual growth of cracks which are joined together and eventually disconnect larger parts of the structure. It is a usual assumption that forming cracks is a brittle process and that the strength in tension-loading direction abruptly goes to zero after such cracks have formed. The concrete in tension is modeled linear-elastic strain softening material and the maximum tensile stress

criterion will be employed. In the finite element context, two main approaches have been used for crack representation: discrete crack model and smeared crack model. In the present study the researcher used the smeared crack model. A smeared representation for cracks is assumed, which implies that the cracks are distributed a cross the region of the finite element.

In the smeared crack simulation, two different models are used for defining the crack direction: fixed crack model and rotating crack model. In the present study, the fixed smeared approach will be adopted. In this model, the crack direction is fixed. Also concrete is initially isotropic, but cracking induces anisotropy. After cracking, the concrete is assumed to become orthotropic. Material properties therefore vary depending on the state of strain and stress. The Young's modulus is reduced in the direction perpendicular to the crack plan, and Poisson's ratio is usually neglected.

٣.٣ Modulus of Elasticity

The initial modulus of elasticity in plain concrete is taken to be the function of the compressive strength of concrete. Several empirical formulae were proposed to predict the modulus of elasticity, the following formula is recommended by ACI committee ٣١٨ [٢] and is given by:-

$$E_C = 4730\sqrt{f'_C} \qquad (٣-٢٢)$$

and:

$$E_C = \left(3320\sqrt{f'_C} + 6895\right)(wc/2300)^{1.5} \qquad (٣-٢٣)$$

As for fibrous concrete, the modulus of elasticity can be calculated from equation in references [٣]. The modulus of elasticity of fibrous concrete was found to be increased up to ٥٪ [٤٤]. The following formula used in the present study.

$$E_{Cf} = \left(1 + \alpha_E V_f \frac{L_f}{D_f}\right) E_C \qquad (٣\text{-}٢٤)$$

where:

E_C Modulus of elasticity of plain concrete in (MPa).

E_{Cf} Modulus of elasticity of steel fiber reinforced concrete in (MPa).

α_E Factor having the following values.

Table (٣-١) α_E values

α_E	Aspect Ratio
0.0476	$0 < L_f/D_f \leq 30$
0.0426	$30 < L_f/D_f \leq 75$
0.0333	$75 < L_f/D_f \leq 100$

٣.٤ Fibrous Concrete in Compression

The following three conditions have to consider in establishing the nonlinear relationships based on flow theory of Plasticity [٣]:

١. The yield criterion.

٢. The flow and hardening rules.

٣. Crushing condition.

(١) The Yield Criterion:

The strength of concrete under multiaxial state of stress functions as the state of stress and cannot be predicted by limitation of simple tensile, compressive, and shearing stress independently on each other. Therefore a proper evolution of plain and fibrous concrete strength can be achieved by considering the interaction of various component of state of stress. This can be accomplished by using yield criterion or yield Condition. This yield criterion determines the stress level at which plastic deformation begins. The yield criterion can be written in a general form as:

$$f = F(\sigma) - K(k) \qquad (٣\text{-}٢٥)$$

Where F is some function that represent the yield function, it can be represented by a surface called yield surface or loading surface and K is a material parameter. The term K may be a function of hardening parameter which will be discussed later. In Eq. (٣-٢٥) if f = ٠ this indicate that plastic state begins, and for f < ٠ this indicates elastic stage.

Many yield function were proposed to define the plastic stage [٦,٣]. In the present study the following yield function is used, which is adopted in many nonlinear analysis [٣].

$$f(I_1, J_2) = \left[\beta_f (3J_2) + \alpha_f I_1\right]^{0.5} = \sigma_0 \qquad (٣\text{-}٢٦)$$

Where α_f and β_f are material parameter and σ_0 is the compressive strength from uniaxial test ($f\acute{c}_f$).The stress components in the principal stress problem can be written as:

$$\beta_f\left[\left(\sigma_1^2+\sigma_2^2+\sigma_3^2\right)-\left(\sigma_1\sigma_2+\sigma_1\sigma_3+\sigma_3\sigma_2\right)\right]+\alpha_f\left(\sigma_1+\sigma_2+\sigma_3\right)=\sigma_0 \quad (٣\text{-}٢٧)$$

The material parameters have been obtained by Adul – Razzak (adopted in [٣]) by fitting biaxial test results of references [٣, ٣٨, ٧٨], as follows for uniaxial compression test:

$$\sigma_1 = f_{cf} \qquad \sigma_2 = \sigma_3 = 0 \quad (٣\text{-}٢٨)$$

for biaxial compression test:

$$\sigma_1 = \sigma_2 = \omega f_{cf} \quad (٣\text{-}٢٩)$$

using the experimental results of references [٣,٣٨,٧٨] then

$$\omega = e^X \quad (٣\text{-}٣٠)$$

where:

$$X = \frac{1}{3.339 - 0.9772 \ln \dfrac{V_f L_f}{D_f}} \quad (٣\text{-}٣١)$$

The use of Eq.(٣-٢٨) and Eq.(٣-٢٩) in Eq.(٣.٢٧) gives:

$$\beta_f = \frac{1-2\omega}{\omega^2-2\omega} \quad (٣\text{-}٣٢)$$

$$\alpha_f = \frac{1-\omega^2}{\omega^2-2\omega} \quad (٣\text{-}٣٣)$$

Equation (٣-٢٦) can be written in term of stress components in plane stress problem as:

$$f\left(\sigma\right)=\left[\beta_f\left\langle\left(\sigma_X^2+\sigma_Z^2+\sigma_X\sigma_Z\right)+3\tau_{XZ}^2\right\rangle+\alpha_f\left(\sigma_X+\sigma_Z\right)\right]^{1/2}=\sigma_0 \quad (٣\text{-}٣٤)$$

In the present study σ_Z will be neglected, and then Equation (٣-٣٤) can be rewritten as follow:

$$f\left(\sigma\right)=\left[\beta_f\left(\sigma_X^2+3\tau_{XZ}^2\right)+\alpha_f\sigma_X\right]^{1/2}=\sigma_0 \quad (٣\text{-}٣٥)$$

(٢) The Flow Rule

To construct the stress-strain relationship in the plastic stage, the normal plastic deformation rate vector to yield surface or the second flow rule is commonly assumed. The plastic strain increment then is defined as [٢٠]:

$$d_{\varepsilon p} = d\lambda \frac{\partial f}{\partial \sigma} \qquad (٣-٣٦)$$

where: $d\lambda$ is a constant proportionality, which determines the magnitude of the plastic strain increment. The current stress function $f(\sigma)$ is the yield condition or the subsequent loading function in strain hardening model.

The yield function derivative, which defines the flow vector [a] takes the following expression for the present yield surface:

$$a^T = \left[\frac{\partial f}{\partial \sigma_X}, \frac{\partial f}{\partial \sigma_Z}, \frac{\partial f}{\tau_{XZ}}\right] \qquad (٣-٣٧)$$

$$a_1 = \frac{\partial f}{\partial \sigma_X} = c + \left[2\left(c^2 + \beta_f\right)\sigma_X\right] / const. \qquad (٣-٣٨)$$

$$a_2 = \frac{\partial f}{\partial \tau_{XY}} = 6\beta_f \tau_{XZ} / const. \qquad (٣-٣٩)$$

where:

$$c = \frac{\alpha_f}{2\sigma_0}$$

$$const. = \left[\left(c^2 + \beta_f\right)\sigma_x^2 + 3\beta_f \tau_{xz}^2\right]^{0.5}$$

The constant dλ can be obtained as follow [٥٥]

$$d\lambda = \frac{\{a\}^T [D] \{a\}}{H' + \{a\}^T [D] \{a\}} d\varepsilon \qquad (٣\text{-}٤٠)$$

where: [D] is elasticity matrix for elastic fibrous concrete and H' is the hardening parameter which can be expressed as:-

$$H' = \frac{d\sigma}{d_{\varepsilon p}} \qquad (٣\text{-}٤١)$$

The total strain increment {dε} is the sum of elastic and plastic components, so that

$$d_\varepsilon = d_{\varepsilon e} + d_{\varepsilon p}$$

$$= [D] \{d\sigma\} + d\lambda \frac{df}{d\sigma} \qquad (٣\text{-}٤٢)$$

Substitute Eq. (٣-٤٠) into Eq. (٣-٤٢) to obtain the complete elastic-plastic incremental stress-strain to be:

$$d\sigma = Dep^{d\varepsilon} \qquad (٣\text{-}٤٣)$$

$$Dep = D - \frac{[D]\{a\}\{a\}^T [D]}{H' + \{a\}^T [D] \{a\}}$$

(٣) The Hardening Rule

The hardening rule defines the motion of the subsequent yield surface during plastic deformation, when a material is stressed beyond its initial yielding surface. In the present study, an isotropic hardening rule is adopted. At first, when a material is stressed beyond its initial yielding

surface, the yielding surface will expand until the effective stress reaches the ultimate stress f'_{cf}, after that the yielding surface will contract due to the softening effect until the failure occurs.

To calculate the uniaxial hardening parameter (H'), the tangential modulus of elasticity E_{cft} must be found at first, which will be calculated according to stress – strain model for concrete which was illustrated previously in this chapter and as shown below:

١. For the compression envelop curve, E_{cf} equals to the derivative of equation (٣-١) with respect to ε_c and has the form:

If $\varepsilon \leq \varepsilon_{cp}$

$$E_{cf} = f'_{cf}\left(\frac{2}{\varepsilon} - (\frac{\varepsilon}{\varepsilon_{cp}^{\ 2}})\right) \quad \text{[GPa]} \qquad (٣\text{-}٤٤)$$

If $\varepsilon > \varepsilon_{cp}$

$$E_{cf} = -343\, f'_{C}(1 - 0.66\left(\frac{V_f L_f}{D_f}\right)^{1/2}) \text{ [GPa]} \qquad (٣\text{-}٤٥)$$

٢. For the unloading and reloading paths in compression, E_{cf} equals to:

$$E_{cf} = \frac{f_{ur}}{\varepsilon_{ur} - \varepsilon_{pc}} \quad \text{[GPa]} \qquad (٣\text{-}٤٦)$$

٣. In the state of the unloading and reloading for the uncracked fibrous concrete in tension, the value of E_{cf} equals to E_{co}.

٤. The value of E_{cf} for the cracked fibrous concrete under tension will be calculated according to tension stiffening rule that will be illustrated later.

The hardening parameter is defined as:

$$H' = \frac{d\sigma}{d\varepsilon_P} \qquad (٣\text{-}٤٧)$$

where:

ε_P is the concrete plastic stain.

$$d\varepsilon_P = d\varepsilon_c - d\varepsilon_e \qquad (٣\text{-}٤٨)$$

where:

ε_e is the concrete elastic strain.

By substitution from equation (٣-٤٨) into equation (٣-٤٧) then:

$$H' = \frac{d\sigma}{d\varepsilon_c - d\varepsilon_e}$$

$$= \frac{E_{cf}\, d\varepsilon_c}{d\varepsilon_c - d\varepsilon_e}$$

$$= \frac{E_{cf}}{1 - \frac{d\varepsilon_e}{d\varepsilon_c}}$$

$$= \frac{E_{cf}}{1 - \frac{d\sigma}{E_{co}} \cdot \frac{E_{cf}}{d\sigma}}$$

$$H' = \frac{E_{cf}}{1 - \frac{E_{cf}}{E_{co}}} \qquad (٣\text{-}٤٩)$$

When H' equals to zero then the material is stressed to be perfectly plastic and when H' equals to infinity the material is still within elastic rang.

(٤) The Crushing Condition of Fibrous Reinforced Concrete

After the compression stress reaches the compressive strength of plain or fibrous concrete, a perfect plastic state is assumed until crushing will occur. Then the material is assumed to lose all its characteristics strength, and rigidity. The crushing type of such material is controlled by strain phenomenon. A simple way is to convert the yield criterion (describe in term as stresses) into strains [٣, ٥٥]. Thus;

$$\beta\left(3j_2'\right)+\alpha\, I_1'=\varepsilon_{cuf}^2 \qquad (٣\text{-}٥٠)$$

where: I١' is the first strain invariant. j'٢ is the second deviatoric strain, and ε_{cuf}^2 is the ultimate total strain extrapolated from the uniaxial compression test result.

The crushing condition can be expressed in terms of strain component as:

$$\left[\beta_f\left\{\left(\varepsilon_x^2+\varepsilon_z^2+\varepsilon_x\varepsilon_z\right)0.75\gamma_{xz}^2\right\}+\alpha_f\left(\varepsilon_x+\varepsilon_z\right)\right]^{0.5}=\varepsilon_{cuf} \qquad (٣\text{-}٥١)$$

When the strain reach the crushing surface the material is assumed to lose its characteristics of strength and rigidity.

In the present study ε_z will be neglected, and then Equation (٣-٥١) can be rewritten as follows:

$$\left[\beta_f\left(\varepsilon_x^2+0.75\gamma_{xy}^2\right)+\alpha_f\varepsilon_x\right]^{0.5}=\varepsilon_{cuf} \qquad (٣\text{-}٥٢)$$

٣.٥ Fibrous Concrete in Tension

In the finite element analysis plain or fibrous concrete is initially considered to be as isotropic material. In plane stress condition, the stress-strain relation take a simple form:

$$\begin{Bmatrix}\sigma_X\\ \sigma_Z\\ \tau_{XZ}\end{Bmatrix}=\frac{E_{cf}}{1-\nu^2}\begin{bmatrix}1 & \nu & 0\\ \nu & 1 & 0\\ 0 & 0 & \frac{1-\nu}{2}\end{bmatrix}\begin{Bmatrix}\varepsilon_X\\ \varepsilon_Z\\ \gamma_{XZ}\end{Bmatrix} \qquad (٣\text{-}٥٣)$$

When the maximum tensile stress exceeds the tensile strength. A crack is assumed to occur perpendicular to the direction of tensile stress. After cracking has occurred the cracked concrete becomes an orthotropic material and new stress-strain relationship must be derived. This is accomplished by modifying the stiffness in the direction perpendicular to crack direction.

$$\begin{Bmatrix}\sigma_X\\ \tau_{XZ}\end{Bmatrix}=\begin{bmatrix}E_{ts} & 0\\ 0 & \beta G\end{bmatrix}\begin{Bmatrix}\varepsilon_X\\ \gamma_{XZ}\end{Bmatrix} \qquad (٣\text{-}٥٤)$$

In plain concrete it was assumed that the modulus of elasticity is reduced to zero when a crack forms. But in fiber reinforced concrete after cracking has occurred a certain amount of tension stress is transferred to the fiber bridging the crack. The tension stiffening can be considered by evaluating the secant modulus to incorporate to over all stiffness which is given by [٥١]

$$E_{ts}=\frac{\sigma_{Cr}\exp\left(-(\varepsilon_n-\varepsilon_0)/(\eta_O\eta_l\eta_b V_f+0.001)\right)}{\varepsilon_n} \quad \text{for } \varepsilon_n \rangle \varepsilon_0 \qquad (٣\text{-}٥٥)$$

where β is a reducing factor of cracked concrete and the calculation of it is shown later on in this chapter.

٣.٥.١ Tension Stiffening Model

The tension stiffening of concrete after cracking is represented by providing the stress-strain curve with descending branch. The cracked concrete carries between cracks a certain amount of tensile force normal to the cracked plane. The concrete adheres to the reinforcing bars and contributes to the over all stiffness of the structure. The assumed shape of the stress-strain hystersis loops for cyclic loading in tension range is shown in Fig. (٣.٤); this behavior is illustrated through the following points:

١. At first, for uncracked concrete a linear path (O-A) will be adopted for the stress-strain behavior of concrete under tension with the modulus of elasticity equal to the nominal modulus of elasticity in compression E_{co} . This will be valid up to cracking strength σ_{Cr} beyond which a gradual release of the concrete stress component normal to the cracked plane occurs after the peak tensile strength point (A) as shown in Fig. (٣.٤). An exponential function, in the present study, is used and has the following expression [٥١]:

$$\sigma_n = \sigma_{Cr} \exp\left(-\left(\varepsilon_n - \varepsilon_0\right)/\left(\eta_O \eta_l \eta_b V_f + 0.001\right)\right) \quad \text{[MPa]} \qquad (٣\text{-}٥٦)$$

٢. Assign the point where unloading occurs B (ε_n , σ_n).

٣. For $\varepsilon_n < \varepsilon_o$ the unloading and reloading path follow a linear path (O-A) with a slope equal to the nominal modulus of elasticity in compression. Where ε_{cr} is the strain value at the ultimate concrete tensile strength (σ_{Cr}).

٤. For $\varepsilon_n > \varepsilon_o$ unloading occurs along a linear path (O-B) with a slope equal to the fictitious elasticity modulus E_{cf} given by:

$$E_{cf} = \frac{\sigma_n}{\varepsilon_n} \qquad (٣\text{-}٥٧)$$

The stress σ_n can be calculated from the following expression:

$$\sigma_n = \frac{\sigma_{Cr}}{\varepsilon_0} \cdot \varepsilon_n \qquad (٣\text{-}٥٨)$$

٥. If the strain component normal to the crack plane becomes negative (i.e. compressive), this implies that the crack is closed and the concrete is treated again as an uncracked material in the corresponding direction but the crack direction and maximum tensile strain continue to be stored.

٦. For $\varepsilon_n > \varepsilon_o$ reloading occurs along the linear path (O-B) with slope equals to the fictitious modulus of elasticity E_{cf} given by the equation (٣-٥٧).

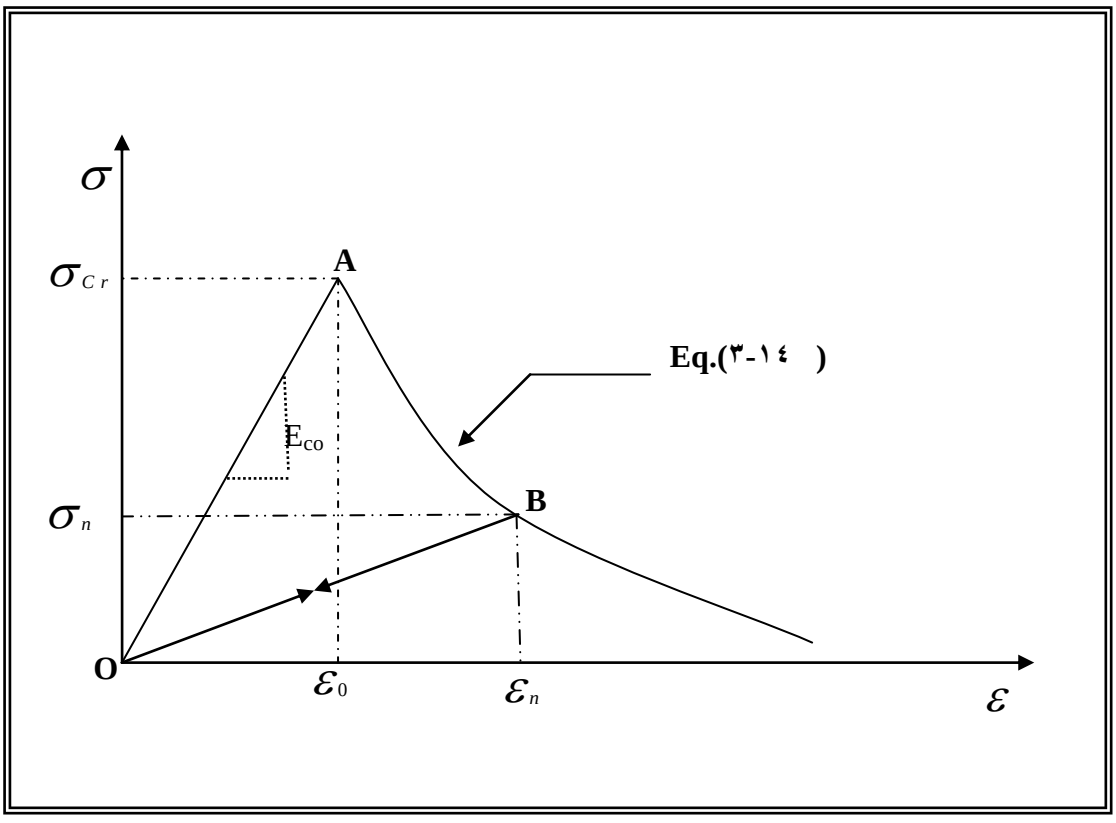

Fig.(٣.٤) Tension stiffening model of SFRC

٣.٥.٢ Shear Modulus of Cracked Concrete

Experimental results indicated that a considerable a mount of shear stress can be transferred across rough surface of cracked concrete. The shear transfer capacity is being reduced as the width of the crack increases.

These mechanisms are included in the smeared crack model by reducing the value of the shear modulus corresponding to the crack plane to a value $\overline{G}$ defined as:

$$\overline{G} = \beta G \qquad (٣-٥٩)$$

where:

G the shear modulus of uncracked concrete

β reducing factor ranging from (٠ to ١)

The following value for β is used in this study:

$$\beta = 1 - \left(\frac{\varepsilon_n}{0.005} \right)^{K_1} \qquad (٣-٦٠)$$

where:

ε_n The fictitious strain normal to the crack plane.

K_1 Parameter in the range (٠.٣-١).

٣.٦ Partial Steel Fiber Reinforced Concrete (PSFRC)

Steel fibers are known to act as crack arrestors in concrete [٥٩] and are most effective when aligned in the direction of maximum tensile stress. Since the length of the fibers and the thickness of the layer containing them play important roles in the orientation of the fibers.

٣.٦.١ Failure in Partially Steel – Fibers Reinforced Concrete

Three possible modes of failure in partially fiber–reinforced concrete flexural members are explained as follows [٥٩]:

١. For small thicknesses of the fiber–reinforced layer, the unreinforced concrete will reach its failure strength at the interface;

before the fiber – reinforced concrete yields; this type of failure is undesirable because it occurs suddenly, and without warning.

٢. For large thicknesses of the fiber – reinforced layer, the fiber – reinforced concrete will reach its yield strength at the tensile extremity before the un-reinforced concrete fails at the interface. This type of failure is preceded by cracking and are ductile.

٣. For a particular thickness of the fiber – reinforced layer, the fiber-reinforced concrete will reach its yield strength at the tensile extremity at the same time as the un-reinforced concrete reaches its limiting strain at the interface; this type of failure is preceded by cracking and are ductile. The beams that had fiber reinforcement in only the lower half (tension region) were found to possess ٢٥% higher flexural load values and a higher initial stiffness than the corresponding beam with fibers throughout the section.

٣.٦.٢ Determination of Partial – Depth Factor

The analysis that follows is based on the simplified assumption that [٥٨]:

١. The strain distribution across the section is linear.

٢. The fibers are assumed to be uniformly distributed and randomly oriented throughout the matrix up to the specified depth.

٣. The flexural tensile stress at which the ductile stress block build up is taken equal to the modulus of rupture of plain concrete i. e., $\sigma_t = \sigma_m$.

Let μD be the depth of fibers in the tensile zone required to a chive a balanced failure, Fiq. (٣.٦) shows the details of a cross section. Then from the equilibrium condition, (C=T), referring to Fig. (٣.٥c).

$$2/3\sigma_c\, kDb = \mu D\, \sigma_m bD + 1/2\,(1-k-\mu)Db\sigma_m \quad (٣-٦١)$$

From the strain diagram Fig. (٣.٥b).

$$\frac{\varepsilon_m}{\varepsilon_t} = (1-k-\mu)/(1-k) \quad (٣-٦٢)$$

$$\mu = (t-1)(1-k)/t \quad (٣-٦٣)$$

Substituting Eq. (٣-٦٣) for μ and $\gamma = \sigma_c/\sigma_m$, Eq. (٣-٦١) is reduced to

$$k = \frac{3(3t-1)}{6t-4\gamma t-3} \quad (٣-٦٤)$$

Assuming that the modulus of elasticity of concrete, E, is to be the same in the both tension and compression at the time of failure, we can get the following equations: (٣-٦٣) and (٣-٦٤).

$$\mu = \frac{(t-1)}{(t+\gamma)} \quad (٣-٦٥)$$

Substituting γ and μ from Eqs. (٣-٦٤) and (٣-٦٥) in Eq. (٣-٦١).

$$\gamma = \sqrt{3(2t-1)}/2 \quad (٣-٦٦)$$

The values of the tensile strain enhancement factor t are obtained from the tests. The regression analysis performed to get the relationship between an increase of t with different RI_S can be represented through a relation as:

$$t = 1.725(RI) + 1 \quad (٣-٦٧)$$

ε_m Ultimate compressive strain for plain concrete.

ε_t Ultimate tensile strain in FRC.

σ_t Flexural tensile stress.

σ_m Modulus of rupture of plain concrete.

t Tensile strain enhancement factor.

μ Provided partial depth factor in test specimens

RI ($V_f.L_f/D_f$) reinforcing index.

k Neutral axis coefficient.

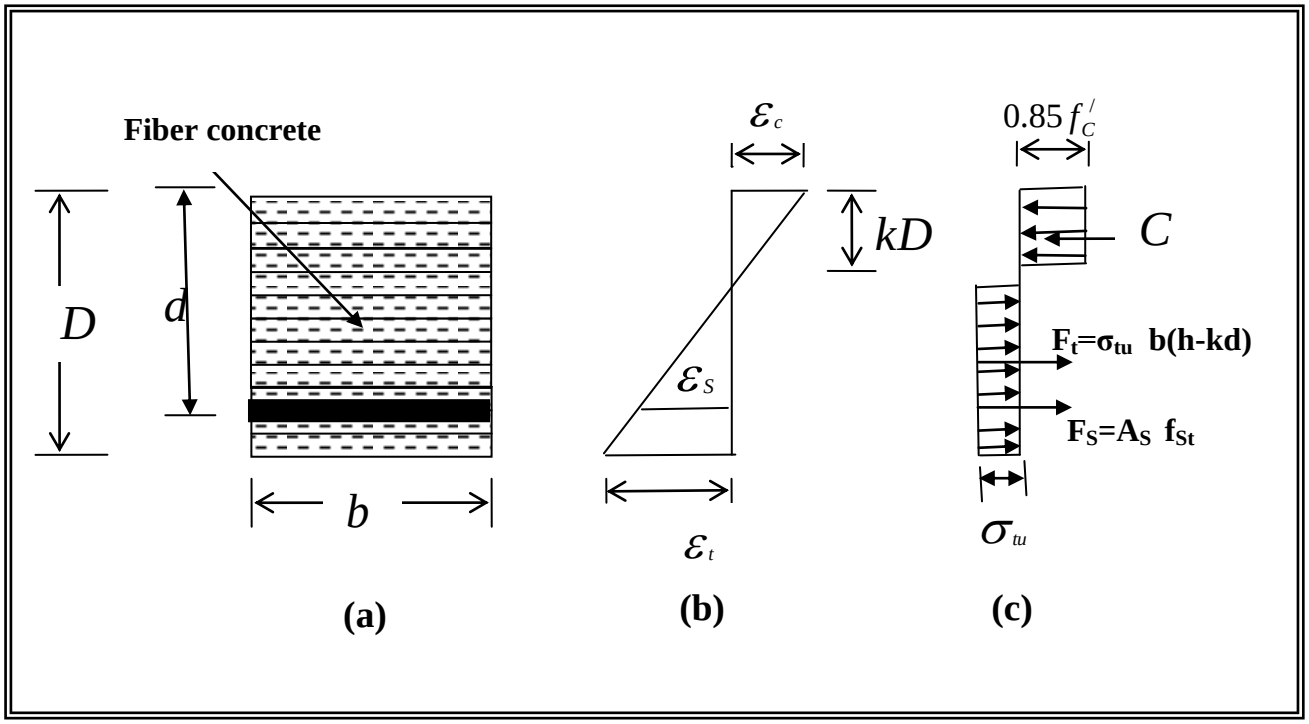

Fig. (٣.٥)(a) Cross-sectional details for full-depth fiber reinforced concrete members in flexure; (b) strain distribution; (c) stress distribution

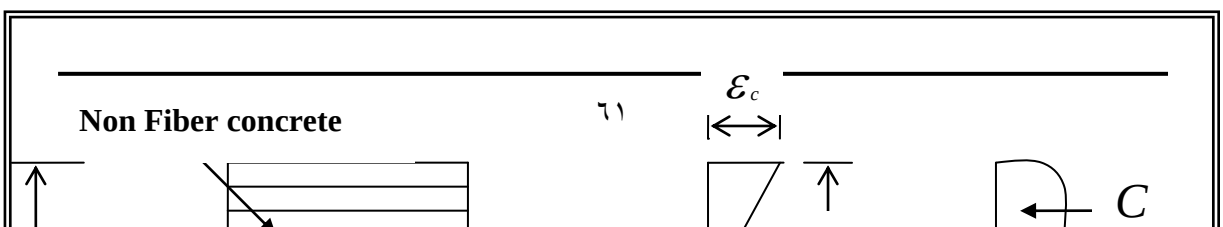

Fig. (٣.٦)(a) Cross-sectional details for half-depth fiber reinforced concrete members; (b) strain distribution; (c) stress distribution

٣.٧ Reinforcing Steel

The properties of reinforcing steel, unlike concrete, are generally not dependent on environmental conditions or time. Thus, the specification of a single stress-strain relation is sufficient to define the material properties needed in the analysis of reinforced concrete structures.

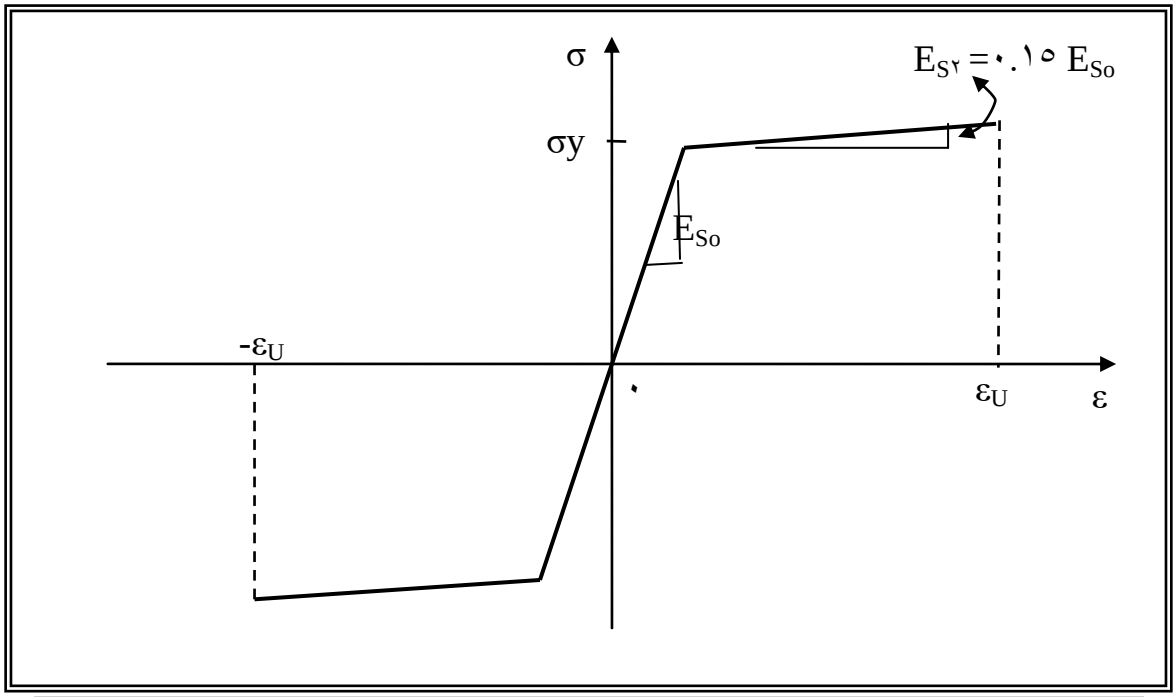

Fig. (٣.٧) Steel stress-strain relation

Typical stress-strain curves for reinforcing steel bars used in concrete construction are obtained from coupon tests of bars loaded monotonically in tension. For all practical purposes steel exhibits the same stress-strain curve in compression as in tension. The steel stress-strain relation exhibits an initial linear elastic portion, a yield plateau, a strain-hardening range in which stress again increases with strain and, finally, a range in which the stress drops off until fracture occur.

٣.٧.١ Steel Reinforcement Modeling

Compared to concrete, steel is a much simpler material to represent. Steel reinforcement is a homogenous material, exhibiting a similar stress-strain relationship in compression and tension.

In the present study, the steel reinforcement is smeared into equivalent steel layers with uniaxial properties. An elasto-plastic behavior with possible strain hardening is assumed and elastic unloading and reloading in the plastic rang are allowed to follow a path parallel to the initial elastic modulus E_{s0} as shown in Fig. (٣.٨).

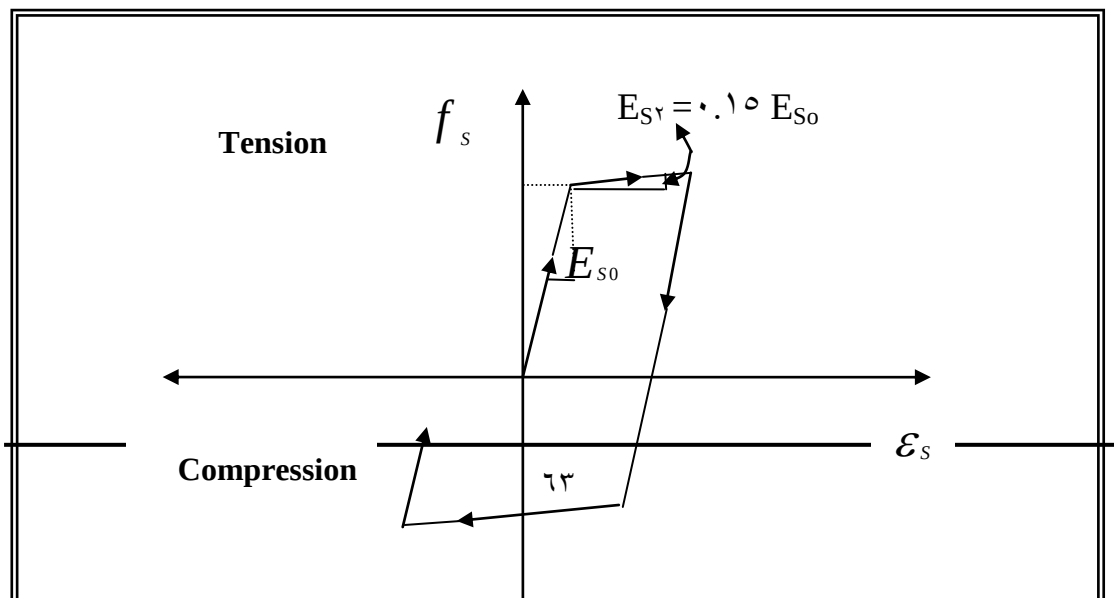

Fig. (٣.٨) Stress-strain relationship for steel bars under cyclic loads (Thompson and Park ١٩٨٠ [٧٣])

CHAPTER FOUR
FORMULATION OF THE STIFFNESS MATRIX

٤.١ Introduction

The finite element method can be defined as a general method of structural analysis in which a continuum is replaced by finite number of elements interconnected at finite number of nodal points. The shape, size and the number of elements are related to the geometry of the body, material properties and loading condition [٢٨].

٤.٢ Concrete Stress-Strain Relationship

In a layered finite element the analysis of plain or fibrous concrete is initially considered to be as isotropic material. For convenience, the frame element is assumed to be loaded in the **xz**-plane and thus for an isotropic elastic material the relevant elastic stress-strain relationships are [٥٥]:

$$\begin{bmatrix}\sigma_X\\ \sigma_Z\\ \tau_{XZ}\end{bmatrix} = \frac{E_{cf}}{\left(1-\nu^2\right)}\begin{bmatrix}1 & \nu & 0\\ \nu & 1 & 0\\ 0 & 0 & \frac{1-\nu}{2}\end{bmatrix}\begin{bmatrix}\varepsilon_X\\ \varepsilon_Z\\ \gamma_{XZ}\end{bmatrix} \qquad (٤\text{-}١)$$

where: E_{cf} is the Young`s modulus of elasticity and ν is the Poisson's ratio.

For the condition of σ_Z is equal to zero, the lateral strain ε_Z will be:

$$\varepsilon_Z = -\nu\,\varepsilon_X \qquad (٤\text{-}٢)$$

By eliminating ε_z from equations (٤-١) and (٤-٢). It is possible to write the following elastic stress-strain relationship.

$$\begin{bmatrix}\sigma_X\\ \tau_{XZ}\end{bmatrix} = [D_C]\ \begin{bmatrix}\varepsilon_X\\ \gamma_{XZ}\end{bmatrix} \qquad (٤\text{-}٣)$$

where:

$[D_C]$ = is the concrete elastic matrix, which takes the following form:

$$[D_C]=\begin{bmatrix} E_{cf} & 0 \\ 0 & G_{cf} \end{bmatrix} \qquad (٤-٤)$$

here:

G_{cf} is the shear modulus of elasticity and for an isotropic material within elastic range is equal to:

$$G_{cf}=\frac{E_{cf}}{2(1+\nu)} \qquad (٤-٥)$$

The matrix $[D_c]$ has the prescribed form shown in equation (٣-٤) within the elastic range. For the plastic range, $[D_c]$ will be calculated according to the flow rule.

٤.٣ Steel Stress–Strain Relationship

The steel layer deformation in the direction of the bar has strength and stiffness characteristics in such direction only. The dowel action of the reinforcing steel is neglected and the bond between steel and concrete is assumed to remain perfect. The elastic stress–strain relationship can be written as [٥٥]:

$$\begin{bmatrix} \sigma_{SX} \\ \tau_{SXZ} \end{bmatrix}=[D_S]\begin{bmatrix} \varepsilon_{SX} \\ \gamma_{SXZ} \end{bmatrix} \qquad (٤-٦)$$

where:

$[D_S]$ is the steel elasticity matrix which takes the following form:

$$[D_S]=\begin{bmatrix} E_S & 0 \\ 0 & 0 \end{bmatrix} \qquad (٤-٧)$$

In the elastic range, E_s will be equal to E_{so} during loading, unloading and reloading stages. In the plastic range, E_s will be equal to $E_{s٢}$ (on the

envelop) in loading stages. (Refer to Fig. (٣.٨)). While the unloading and reloading stages E_s is assumed to be equal to E_{so}.

٤.٤ Theoretical Consideration

In the present study the researcher consider solutions for the Euler-Bernoulli and Timoshenko theories of beams in which material behavior may be elastic or inelastic. These theories are well established and widely used in the analysis of beams. In this study the inclusion of axial, bending and shear effects is considered. This permits consideration in a direct manner of elastic and inelastic behavior with or without shear deformation.

The following assumptions are made for the analysis:

١. The hypothesis of plane sections of member bending and the resulting linear distribution of strain within the depth of the member section is adopted Fig. (٤.١).

٢. The fiber reinforced concrete and the longitudinal reinforcement are assumed to be perfectly bonded, i.e. there is no slip between the concrete and the reinforcement.

٣. The constitutive model is based on the smeared crack approach.

٤. The element is divided into two zones through the longitudinal direction and divided into the number of fibrous concrete and steel layers along the depth as shown in Fig. (٤.٢) and (٤.٣).

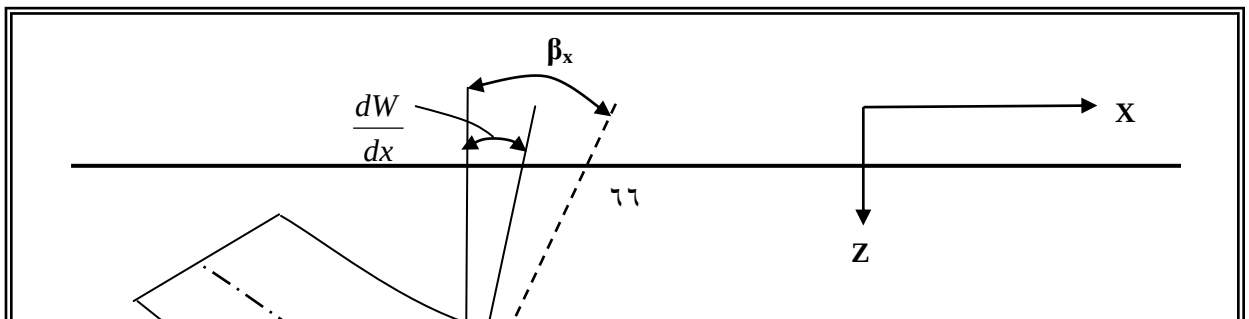

Fig.(٤.١) Assumed Deformation of Timoshenko beam theory

٤.٤.١ Nonlinear Layered Finite Element Model for Fiber Reinforced Concrete

In the layered finite element, strain compatibility is assumed and each cross-section of a member is divided into N layers, some of which may represent the reinforcing bars, adopted in Lee et al. [٣٥].

In this study, fibrous concrete is represented by layered modeling and the tapered element is rectangular in cross section with constant width and two-node for each element with three degrees of freedom at each node. In the layered modeling, Fig. (٤.٣), concrete is divided into a set of layers, while the reinforcing steel is smeared into a layer between concrete layers Fig.(٤.٣). $F=(N_١,W_١,M_١,N_٢,W_٢,M_٢)^T$ and $d=(u_١,w_١,\beta_١,u_٢,w_٢,\beta_٢)^T$, respectively, where subscript T denotes transpose of a corresponding vector and subscript ١ and ٢ represent the adjacent cross-section at the ends of element as shown in Fig.(٤.٢).

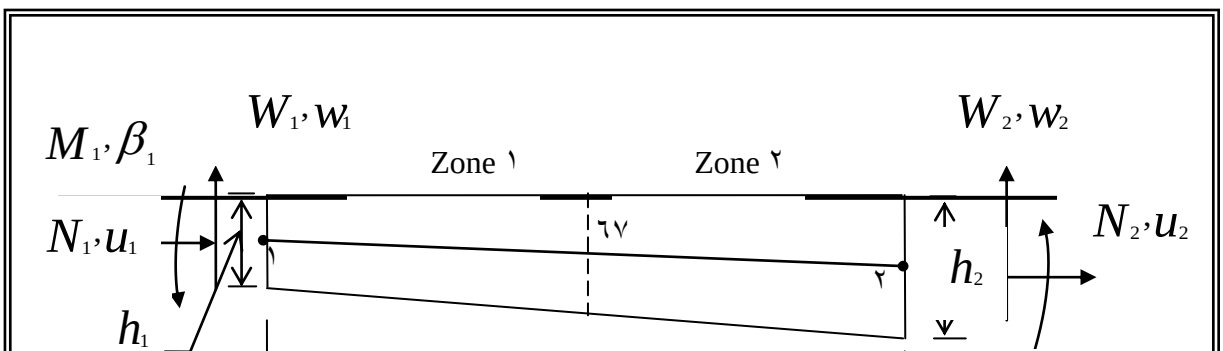

Fig. (٤.٢) Degree of freedom and sign convention

٤.٤.٢ Displacement Field

Based on the Timoshenko-beam theory, the assumed displacement field for a beam which includes the primary effect of shear deformation is given by:

$$u(x,z) = u_o(x) - z\beta(x) \qquad (٤\text{-}٨)$$

$$w(x,z) = w_o(x) \qquad (٤\text{-}٩)$$

where:

$\beta(x)$ is the rotation of a cross-section .

In this case we have two strain components at each point in the element which is given by:

$$\varepsilon_x = \frac{\partial u(x,z)}{\partial x} \qquad (٤\text{-}١٠)$$

or

$$\varepsilon_X = \frac{du_o(x)}{dx} - z\,\frac{d\beta(x)}{dx} \qquad (٤\text{-}١١)$$

The transverse shear strain is constant through the thickness of element and can be expressed as follows (Assuming the shear rigidity across the thickness is very large):

$$\gamma_{xz} = \frac{\partial w(x,z)}{\partial x} - \beta(x) \qquad (٤\text{-}١٢)$$

$$= \frac{dw(x)}{dx} - \beta(x) \qquad (٤\text{-}١٣)$$

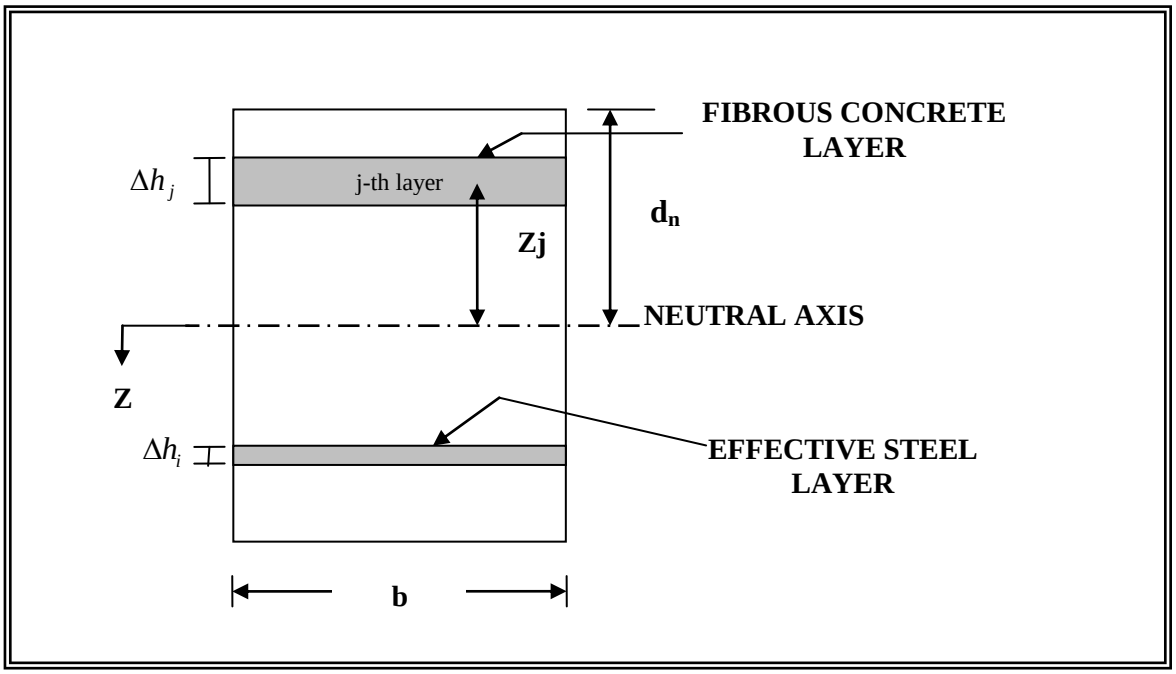

Fig. (٤.٣) Layer Section

٤.٤.٣ Formulation of Shape Function

The finite element analysis of a continuum starts with the subdivision of the physical system into an assemblage of discrete elements. Following the assumptions of the Timoshenko beam theory, the resulting stresses are assumed to be constant through the thickness of each element and stresses σy, $\tau_{xy}$and τ_{yz} are ignored. The displacement field is described by u(x,z) and w(x,z), which represent the node displacements in the x and z-direction, respectively, and are in general functions of *x* and z.

considering a ٢-node element in which the displacement degree of freedom at each node is:

$$\begin{Bmatrix} u \\ w \\ \beta \end{Bmatrix} = \sum_{i=1}^{n} \begin{bmatrix} N_{ui} & 0 & 0 \\ 0 & N_{wi} & 0 \\ 0 & 0 & N_{\beta i} \end{bmatrix} \begin{Bmatrix} u \\ w \\ \beta \end{Bmatrix}_i \qquad (٤\text{-}١٤)$$

In the finite element format, axial displacement $u_o(x)$, lateral displacement $w_o(x)$ and bending rotation $\beta(x)$ may be related to the nodal displacement {d} by linear shape functions, adopted in Taylor[٧٤]:

$$u_o(x) = [N_u]\{d\}; \qquad (٤\text{-}١٥)$$

$$w_o(x) = [N_w]\{d\}; \qquad (٤\text{-}١٦)$$

and

$$\beta(x) = [N_\beta]\{d\} \qquad (٤\text{-}١٧)$$

where

$$[N_{u,\alpha}] = \begin{bmatrix} \frac{L-x}{L} & 0 & 0 & \frac{x}{L} & 0 & 0 \end{bmatrix}; \qquad (٤\text{-}١٨)$$

$$[N_{w,\alpha}] = \begin{bmatrix} 0 & \frac{L-x}{L} & 0 & 0 & \frac{x}{L} & 0 \end{bmatrix}; \qquad (٤\text{-}١٩)$$

and

$$[N_{\beta,\alpha}] = \begin{bmatrix} 0 & 0 & \frac{L-x}{L} & 0 & 0 & \frac{x}{L} \end{bmatrix} \qquad (٤\text{-}٢٠)$$

where: $\alpha = 1,2$

The shapes functions $N_{\lambda 1}$ and $N_{\lambda 2}$ take the following forms:

$$N_{\lambda 1} = \frac{L - x}{L} = 1 - m \quad , \quad \frac{dN_{\lambda 1}}{dx} = -\frac{1}{L} \qquad (٤\text{-}٢١)$$

$$N_{\lambda 2} = \frac{x}{L} = m \quad , \quad \frac{dN_{\lambda 2}}{dx} = \frac{1}{L} \tag{٤-٢٢}$$

where: $\lambda = u, w, \beta$

By Substituting Equations (٤-١٥), (٤-١٦) and (٤-١٧) into Equation (٤-١١):

$$\frac{\partial u(x,z)}{\partial x} = \frac{dN_{u1}}{dx}u_1 + \frac{dN_{u2}}{dx}u_2 - z\left[\frac{dN_{\beta 1}}{dx}\beta_1 + \frac{dN_{\beta 2}}{dx}\beta_2\right]$$

$$= \frac{dN_{u1}}{dx}u_1 - z\,\frac{dN_{\beta 1}}{dx}\beta_1 + \frac{dN_{u2}}{dx}u_2 - z\,\frac{dN_{\beta 2}}{dx}\beta_2 \tag{٤-٢٣}$$

$$\varepsilon_X = \begin{bmatrix} \frac{dN_{u1}}{dx} & 0 & -z\,\frac{dN_{\beta 1}}{dx} & \frac{dN_{u2}}{dx} & 0 & -z\,\frac{dN_{\beta 2}}{dx} \end{bmatrix} \begin{bmatrix} u_1 \\ w_1 \\ \beta_1 \\ u_2 \\ w_2 \\ \beta_2 \end{bmatrix} \tag{٤-٢٤}$$

By substituting Equations (٤-١٥), (٤-١٦) and (٤-١٨) into Equation (٤-١٣):

$$\gamma_{XZ} = \frac{dN_{w1}}{dx}w_1 + \frac{dN_{w2}}{dx}w_2 - N_{\beta 1}\beta_1 - N_{\beta 2}\beta_2$$

$$= \frac{dN_{w1}}{dx}w_1 - N_{\beta 1}\beta_1 + \frac{dN_{w2}}{dx}w_2 - N_{\beta 2}\beta_2$$

$$\gamma_{XZ} = \begin{bmatrix} 0 & \frac{dN_{w1}}{dx} & -N_{\beta 1} & 0 & \frac{dN_{w2}}{dx} & -N_{\beta 2} \end{bmatrix} \begin{bmatrix} u_1 \\ w_1 \\ \beta_1 \\ u_2 \\ w_2 \\ \beta_2 \end{bmatrix} \tag{٤-٢٥}$$

Then, the relation between strains and displacements becomes:

$$\begin{Bmatrix} \varepsilon_x \\ \gamma_{xz} \end{Bmatrix} = \begin{bmatrix} \frac{dN_{u1}}{dx} & 0 & -z\frac{dN_{\beta 1}}{dx} & \frac{dN_{u2}}{dx} & 0 & -z\frac{dN_{\beta 2}}{dx} \\ 0 & \frac{dN_{w1}}{dx} & -N_{\beta 1} & 0 & \frac{dN_{w2}}{dx} & -N_{\beta 2} \end{bmatrix} \begin{Bmatrix} u_1 \\ w_1 \\ \beta_1 \\ u_2 \\ w_2 \\ \beta_2 \end{Bmatrix} \quad (٤\text{-}٢٦)$$

This strain matrix can be expressed in symbolic form:

$$\{\varepsilon\} = [B]\{d\} \quad (٤\text{-}٢٧)$$

$$[B] = \begin{bmatrix} \frac{dN_{u1}}{dx} & 0 & -z\cdot\frac{dN_{\beta 1}}{dx} & \frac{dN_{u2}}{dx} & 0 & -z\frac{dN_{\beta 2}}{dx} \\ 0 & \frac{dN_{w1}}{dx} & -N_{\beta 1} & 0 & \frac{dN_{w2}}{dx} & -N_{\beta 2} \end{bmatrix} \quad (٤\text{-}٢٨)$$

Application of the virtual work principle yields [٣٥]:

$$\delta d \cdot F = \int_V \delta \varepsilon^T \cdot \sigma \, dV$$

$$= \delta d^T \cdot \int_V [B]^T \cdot \sigma \, dV \quad (٤\text{-}٢٩)$$

Since the above relation must hold for arbitrary δd^T , and obtain:

$$F = \int_V [B]^T \cdot [D][B].dV \cdot \{d\} \quad (٤\text{-}٣٠)$$

$$\{F\} = [K_e]\{d\}$$

where

V Element volume

[D] Elasticity material matrix

[Ke] Element stiffness matrix

The integration through the depth of the member, which is placed in parentheses in Equation (٤.٣٠) is performed by subdividing the member into imaginary steel and concrete layers. Each layer can have different material properties, which are, however, assumed to be constant through the thickness of the layer. In the layered finite element method, [K_e] is constructed by integrating analytically and assuming its results over all layers:

$$[K_e]=\int_0^L \sum_{i=1}^{Nl}[B]^T\cdot[D]\cdot[B]\cdot b\cdot\Delta h_i\cdot dx \qquad (٤\text{-}٣١)$$

where:

Δh_i Thickness for each layer.

L Length of element.

For the element varying linearly with the length, the thickness for each concrete layer at any section at a distance (x) from the first end of the element can be determined as:

$$\Delta h_j(x)=\Delta h_{j,1}+\frac{\Delta h_{j,2}-\Delta h_{j,1}}{L\ \Delta h_{j,1}}x \qquad (٤\text{-}٣٢)$$

$$\Delta h_j(x)=\Delta h_{j,1}(1+C_j x) \qquad (٤\text{-}٣٣)$$

٤.٥ Stiffness Matrix Evaluation

The stiffness matrix of the composite reinforced concrete finite element is arrived at by superposition of the concrete and reinforcing steel.

$$[K]=[K]_C+[K]_S \qquad (٤\text{-}٣٤)$$

The concrete element stiffness $[K]_C$ is determined from

$$[K]_C=b\sum_{n=1}^{2}\int_{m_n}^{m_{n+1}}\sum_{j=1}^{NC}[B]_j^T\cdot[D]_{C,j}\cdot[B]_j\cdot\Delta h_{j,C}\,dm \qquad (٤\text{-}٣٥)$$

where:

$[D]_{C,j}$ is the concrete elasticity matrix for each concrete layer, which can be written as:

$$[D]_{C,j} = \begin{bmatrix} E_{cf,j} & 0 \\ 0 & G_{cf,j} \end{bmatrix} \qquad (٣\text{-}٣٦)$$

and the matrix $[B]_j$ is the strain displacement matrix for each concrete layer, which can be written as

$$[B]_j = \begin{bmatrix} \frac{-1}{L} & 0 & \frac{-z_j}{L} & \frac{1}{L} & 0 & \frac{z_j}{L} \\ 0 & \frac{-1}{L} & -(1-m) & 0 & \frac{1}{L} & -m \end{bmatrix} \qquad (٣\text{-}٣٧)$$

By substituting equations (٤-٢٨) and (٤-٣٦) into equation (٤-٣٥)

$$[K]_C = b \sum_{n=1}^{2} \int_{m_n}^{m_{n+1}} \sum_{j=1}^{NC} \Delta h_{j,C} \begin{bmatrix} k_{C,1} & k_{C,2} & k_{C,3} & -k_{C,1} & k_{C,2} & -k_{C,3} \\ & k_{C,4} & k_{C,5} & k_{C,2} & -k_{C,4} & k_{C,6} \\ & & k_{C,7} & -k_{C,3} & k_{C,5} & k_{C,8} \\ & & & k_{C,1} & k_{C,2} & k_{C,3} \\ & & & & k_{C,4} & -k_{C,6} \\ & & & & & k_{C,9} \end{bmatrix} dm \qquad (٤\text{-}٣٨)$$

Symmetric

$$k_{c,1} = \frac{E_{Cf}}{L^2} \qquad (٤\text{-}٣٩)$$

$$k_{c,2} = 0 \qquad (٤\text{-}٤٠)$$

$$k_{c,3} = -z_j \frac{E_{Cf}}{L^2} \qquad (٤\text{-}٤١)$$

$$k_{c,4} = \frac{G_{Cf}}{L^2} \qquad (٤\text{-}٤٢)$$

$$k_{c,5} = (1-m) \frac{G_{Cf}}{L} \qquad (٤\text{-}٤٣)$$

$$k_{c,6} = m\frac{G_{Cf}}{L} \qquad (٤-٤٤)$$

$$k_{c,7} = z_j^2\frac{E_{Cf}}{L^2} + (1-m)^2 G_{Cf} \qquad (٤-٤٥)$$

$$k_{c,8} = -z_j^2\frac{E_{Cf}}{L^2} + m(1-m)G_{Cf} \qquad (٤-٤٦)$$

$$k_{c,9} = -z_j^2\frac{E_{Cf}}{L^2} + m^2 G_{Cf} \qquad (٤-٤٧)$$

The steel reinforcement element stiffness $[K]_S$ is determined from:

$$[K]_S = \sum_{n=1}^{2}\int_{m_n}^{m_{n+1}}\sum_{i=1}^{NS} A_{Si}[B]_i^T\cdot[D]_{S,i}\cdot[B]_i\cdot dm \qquad (٤-٤٨)$$

where:

$[D]_{S,i}$ Is the elasticity matrix for each steel layer, which takes the following form:

$$[D_S]=\begin{bmatrix} E_S & 0 \\ 0 & 0 \end{bmatrix} \qquad (٤-٤٩)$$

$[B]_i$ Is the strain-displacement matrix for each steel layer, which can be written as:

$$[B]_i=\begin{bmatrix} -\frac{1}{L} & 0 & \frac{z_i}{L} & \frac{1}{L} & 0 & \frac{-z_i}{L} \\ 0 & -\frac{1}{L} & -(1-m) & 0 & \frac{1}{L} & -m \end{bmatrix} \qquad (٤-٥٠)$$

$$\left[K\right]_s = \sum_{n=1}^{2} \int_{m_n}^{m_{n+1}} \sum_{i=1}^{NS} A_{s,i} \begin{bmatrix} k_{s,1} & k_{s,2} & k_{s,3} & -k_{s,1} & k_{s,2} & -k_{s,3} \\ & k_{s,2} & k_{s,2} & k_{s,2} & k_{s,2} & k_{s,2} \\ & & k_{s,4} & -k_{s,3} & k_{s,2} & -k_{s,4} \\ & & & k_{s,1} & k_{s,2} & -k_{s,3} \\ & & \text{Symmetric} & & k_{s,2} & k_{s,2} \\ & & & & & k_{s,4} \end{bmatrix} dm \qquad (٤-٥١)$$

where:

$$k_{s,1} = \frac{E_s}{L^2} \qquad (٤-٥٢)$$

$$k_{s,2} = 0 \qquad (٤-٥٣)$$

$$k_{s,3} = -z_i \frac{E_s}{L^2} \qquad (٤-٥٤)$$

$$k_{s,4} = z_i^2 \frac{E_s}{L^2} \qquad (٤-٥٥)$$

Integration of Equations (٤-٣٨) and (٤-٥١) have been made by using Gaussian Quadrature method. Five points at each zone and one point Gaussian Quadradure for $\left[k\right]_s$.

٤.٦ Solution of Nonlinear Equations

In the nonlinear finite element analysis, nonlinearities occur in two different forms. The first is material or physical nonlinearity, which results from the nonlinear material behavior. The second is geometric nonlinearity which results from changes in the geometry deformation body or structure. In the analysis of fibrous reinforced concrete, the nonlinear response arises from updating the stiffness due to cracking, yielding and crushing of fibrous concrete, yielding of steel reinforcement. In the nonlinear finite element analysis, the nonlinear response of

member is achieved by dividing the load into many small increments of load.

Once the global-stiffness matrix is assembled with the incremental element stiffness matrices, the nonlinear incremental equilibrium equation has the form

$$\{F\} = [K]\{d\} \qquad (٤-٥٦)$$

where:

[K] is the assembled global nonlinear stiffness matrix;

{d} is the vector of incremental nodal displacement; and

{F} is the vector of incremental nodal forces.

A number of techniques have been used for solving the nonlinear equilibrium equation of the form of Eq. (٤-٥٦). In the present study the nonlinear incremental method is used.

٤.٦.١ Incremental Methods

The numerical implementation of the finite element model requires the solution of Eq. (٤.٥٦). This is a system of simultaneous nonlinear equations since the stiffness matrix [K], in general, depends on the displacement vector {d}. The solution of this system of nonlinear equations is typically accomplished with an iterative method. The load vector {F} is subdivided into a number of sufficiently small load increments.

At each load step a linear approximation of the stiffness matrix [K] is established and the resulting system of linear equilibrium equations is solved for the displacement increments which correspond to the applied load increments. Since the stiffness matrix [K] changes under these displacement increments, the resisting forces of the structure do not equilibrate the applied loads and unbalanced loads result. These are

corrected during the subsequent iteration until a specified tolerance is satisfied. The unbalanced nodal forces are the difference between applied and resisting or equivalent forces

$$\{F\}_{unbalanced} = \{F\}_{applied} - \{F\}_{equivalent} \qquad (٤-٥٧)$$

٤.٦.٢ Solution Algorithm

Every nonlinear analysis algorithm consists of four basic steps:

- The formation of the current stiffness matrix,
- The solution of the equilibrium equations for the displacement increments,
- The state determination of all elements in the model,
- The convergence check.

A summary of the steps of the nonlinear solution algorithm is presented below:

Step (١) For each cycle of loading, the external load increments are applied in a sequence form to the structure.

Step (٢) Transform all the sections into elastic concrete sections and find position of the central axis for each section.

Step (٣) Calculate the global stiffness matrix of the structure and solve the following equation of equilibrium. The equation (٤-٥٦) is solved by Gauss-Jordan's elimination method, and updating the nodal coordinates and accumulating displacements and forces at the end of each increment solve.

Step (٤) Calculate the accumulating strain values for each fibrous concrete and steel layer at each critical section by using equation (٤-٢٤) and (٤-٢٥) respectively.

Step (٥) For each concrete layer within the compression state, calculate the effective stress from equation (٣-٣٣). If the effective stress reaches ٣٠% of the ultimate stress $f_c^{/}$, then use hardening /

softening rule and flow rule to calculate the constitutive elasto-plastic matrix. Otherwise the material is still within elastic range.

Step (٦) For each concrete layer within the tension state, if the normal stress reaches $f'_{tf}(\sigma_{Cr})$, i.e., the layer is cracked, then the values of the constitutive matrix will be calculated according to tension stiffening rule and the rule of calculation of cracked shear modulus. Otherwise the material is still within elastic range.

Step (٧) Repeat steps (٢-٦) until the value of the constitutive matrix converge.

Step (٨) For each concrete layer within plastic range, calculate the effective strain by using equation (٣-٤٩). If the effective strain reaches equation (٣-١٣) then the crushing failure is occurred and the solution is finished.

Step (٩) Repeat steps (١-٨) until crushing failure occurs or the total cycles of loading are applied.

٤.٧ Computer Program

A computer program was developed, as a part of this study, for the analysis of a plane fiber reinforced concrete frame based on prescribed procedure. The program is written in FORTRAN ٧٧ language under PC PENTIUM III at ٦٥٠ MHz Intel Compatible computer with ١٢٨ MByte RAM. The flow chart of this program is given in Fig. (٤.٤) to outline the main steps in the program [٢٩].

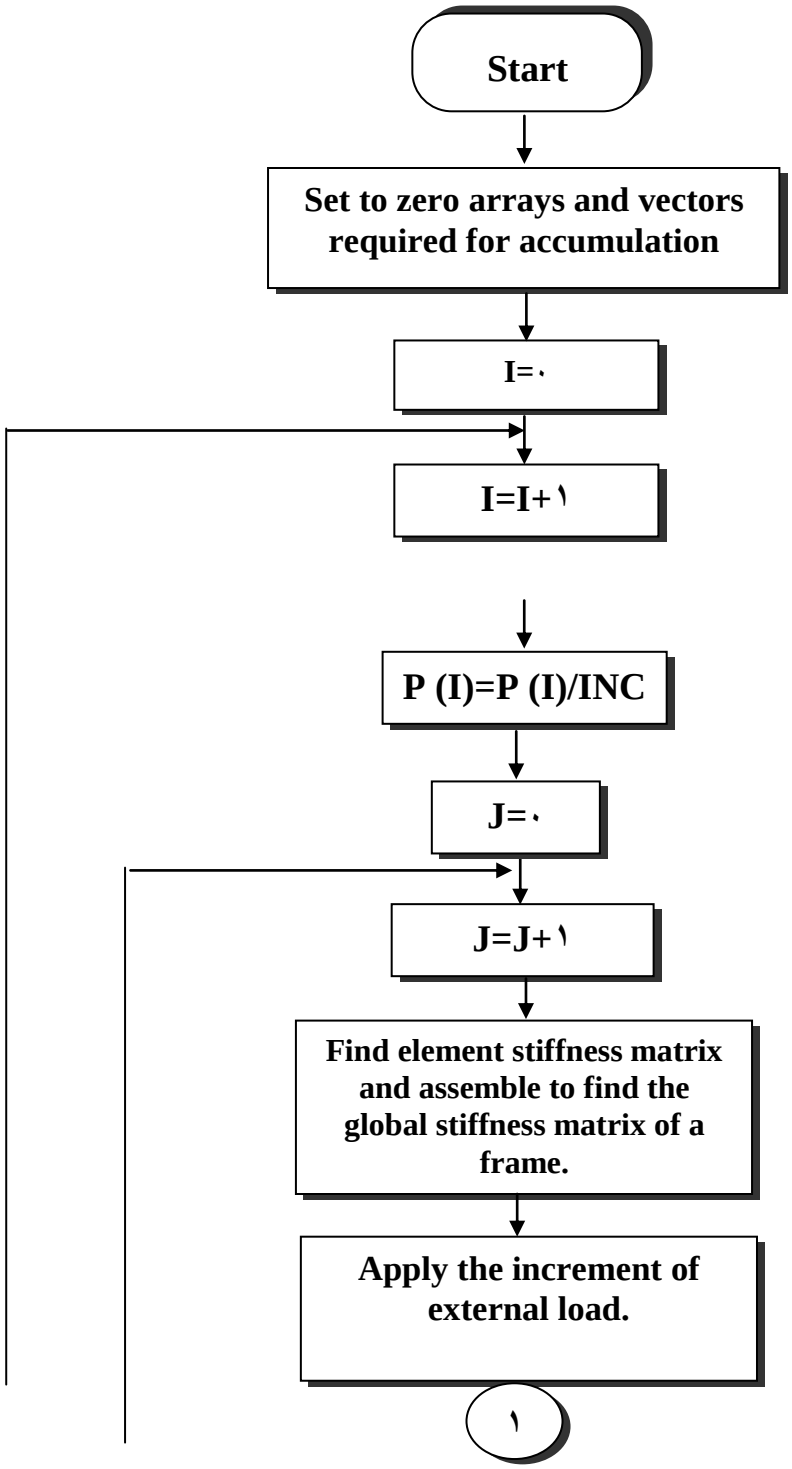
Start
Set to zero arrays and vectors required for accumulation
I=٠
I=I+١
P (I)=P (I)/INC
J=٠
J=J+١
Find element stiffness matrix and assemble to find the global stiffness matrix of a frame.
Apply the increment of external load.
١

Fig. (٤.٤) Flow Chart of the Computer

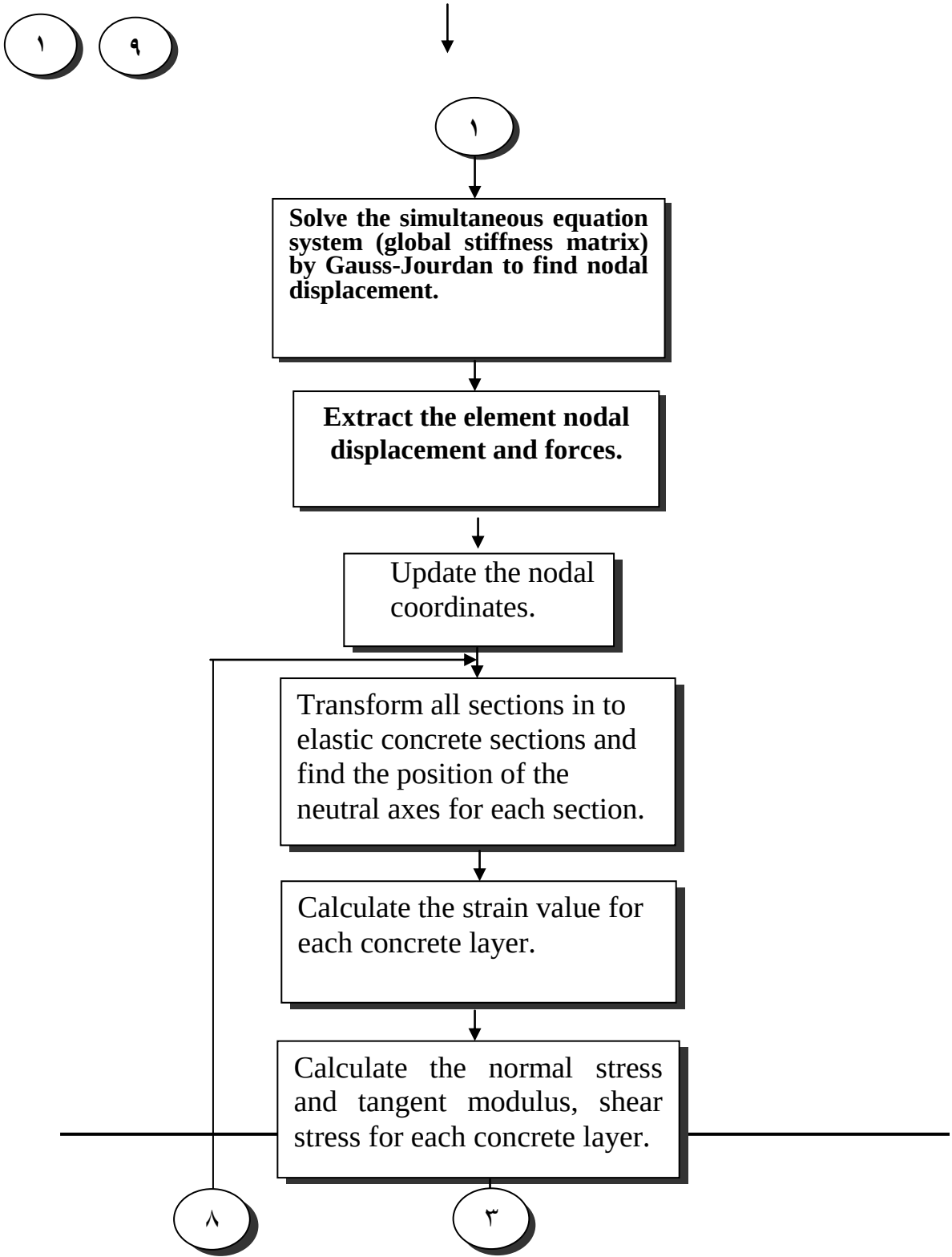

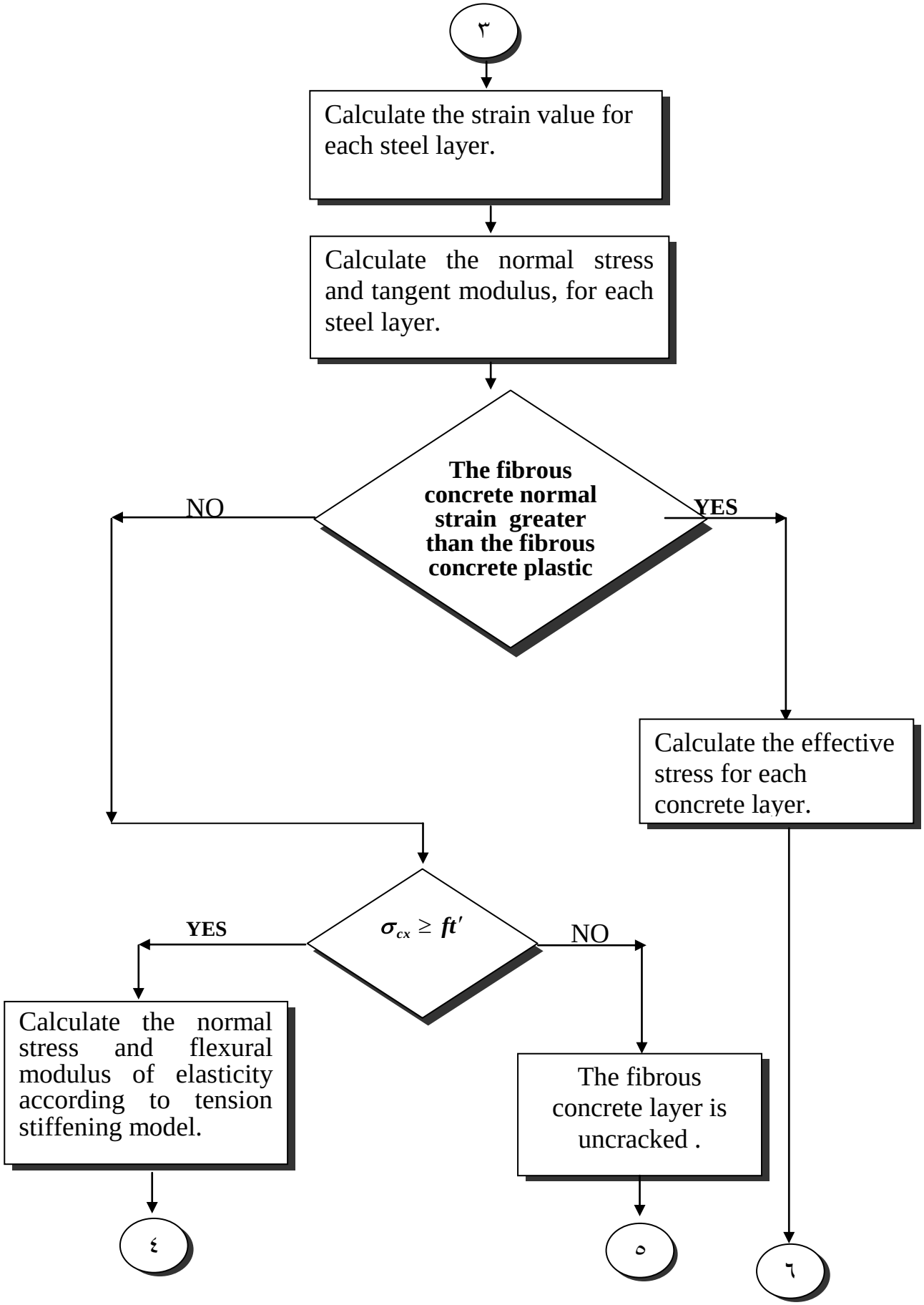

Fig. (٤.٤) continue

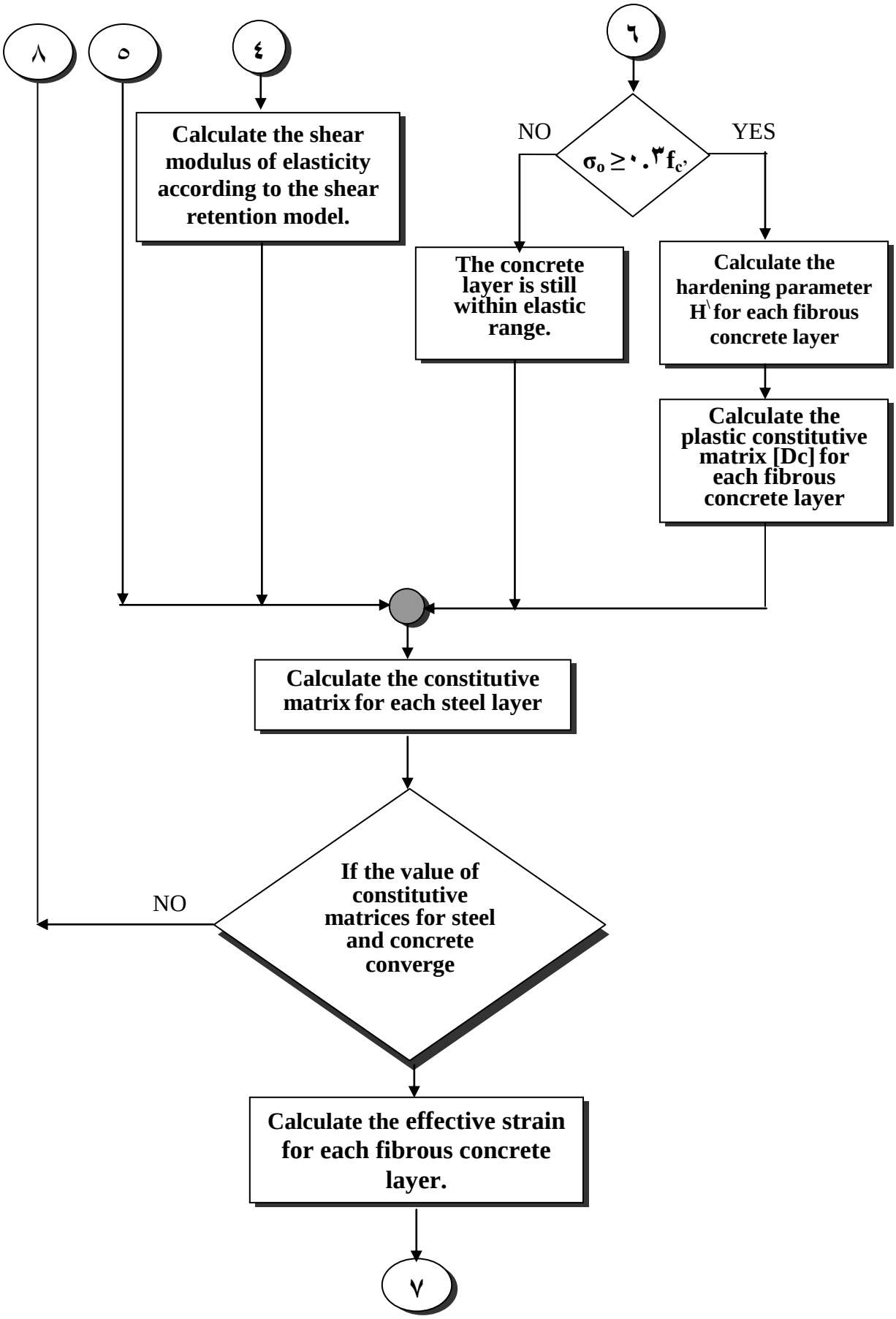

Fig. (٤.٤) continue

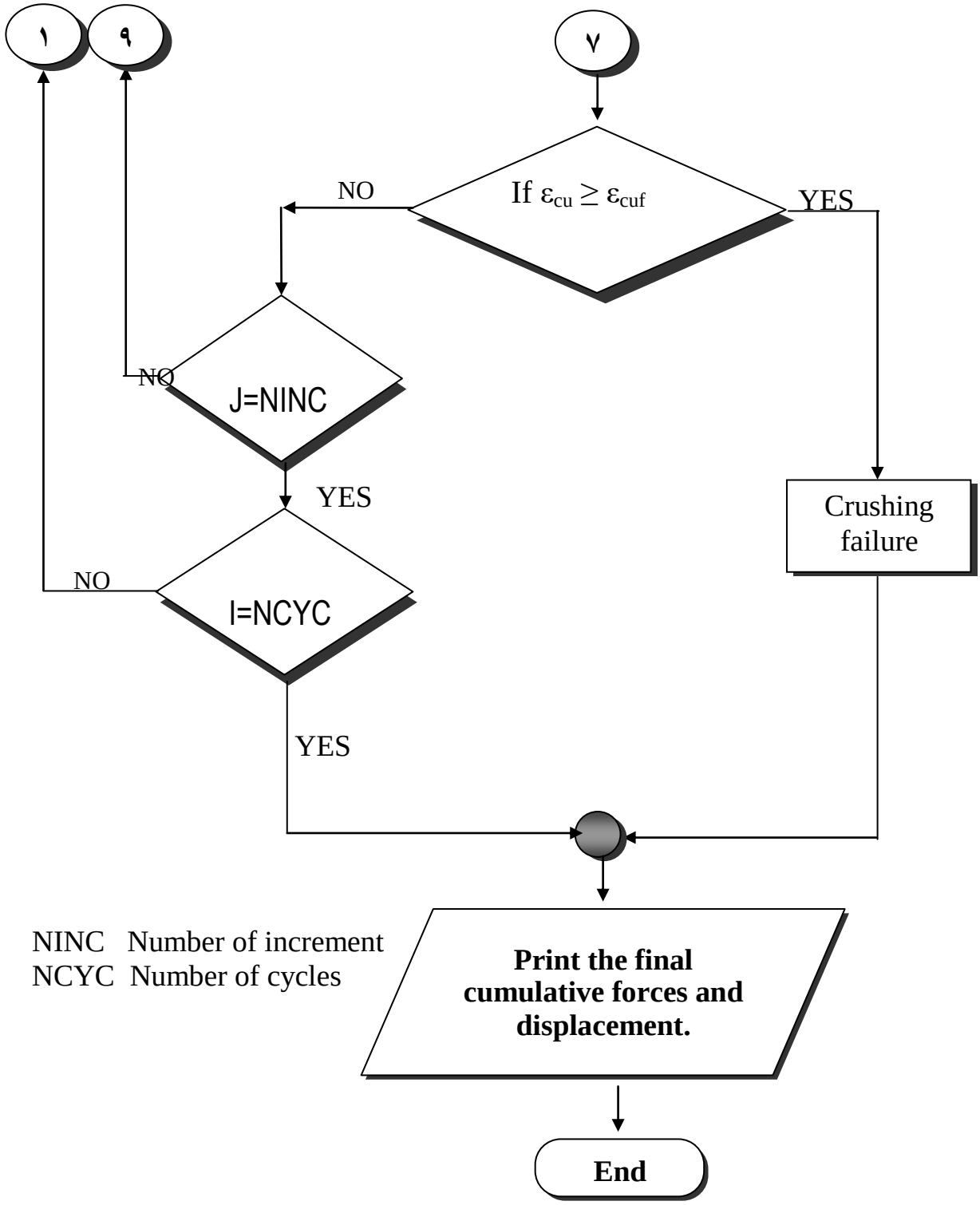
١
٩
٧
If $\varepsilon_{cu} \geq \varepsilon_{cuf}$
NO
YES
NO
J=NINC
YES
Crushing failure
NO
I=NCYC
YES
NINC Number of increment
NCYC Number of cycles
Print the final cumulative forces and displacement.
End

Fig. (٤.٤)

CHAPTER FIVE
MODEL VERIFICATION AND PARAMETRIC STUDY

٥ . ١ Introduction

In this chapter, various examples have been analyzed to prove the validity of the proposed models, and to show the accuracy and efficiency of the computational method. The main parameters studied in this investigation are;

١. The ratio of longitudinal steel reinforcement.
٢. Volume of steel fibers.
٣. Aspect ratio of steel fibers.
٤. Partial-depth of steel fibers.
٥. Element type.
٦. Loading distribution.

٥ . ٢ Reinforced Concrete Frame (F١)

The reinforced concrete frame shown in Fig. (٥.١) is analyzed under reversible cyclic loads to check the cyclic behavior models for concrete and reinforcing steel adopted in the present study for predicting the concrete and steel behavior under cyclic stresses.

Bertero and McClure [٤] presented experimental tests on a series of one-story, single-bay rigid frame subjected to cyclic loading. The testing load conditions are shown in Fig. (٥.٢).

Based on the present analysis, the frame (F١) is analyzed by divided into six elements with fourteen layer of concrete and two layers of steel for beam, and five elements with fourteen concrete layers and two steel layers for each column. Fig. (٥.٣) shows the load-horizontal displacements curves

obtained by the present study and the experimental work during the loading processes of the first two cycles. The horizontal displacement for each loading case is listed in Table (٥-١). Good agreement is observed between the results of the present study and the experimental work.

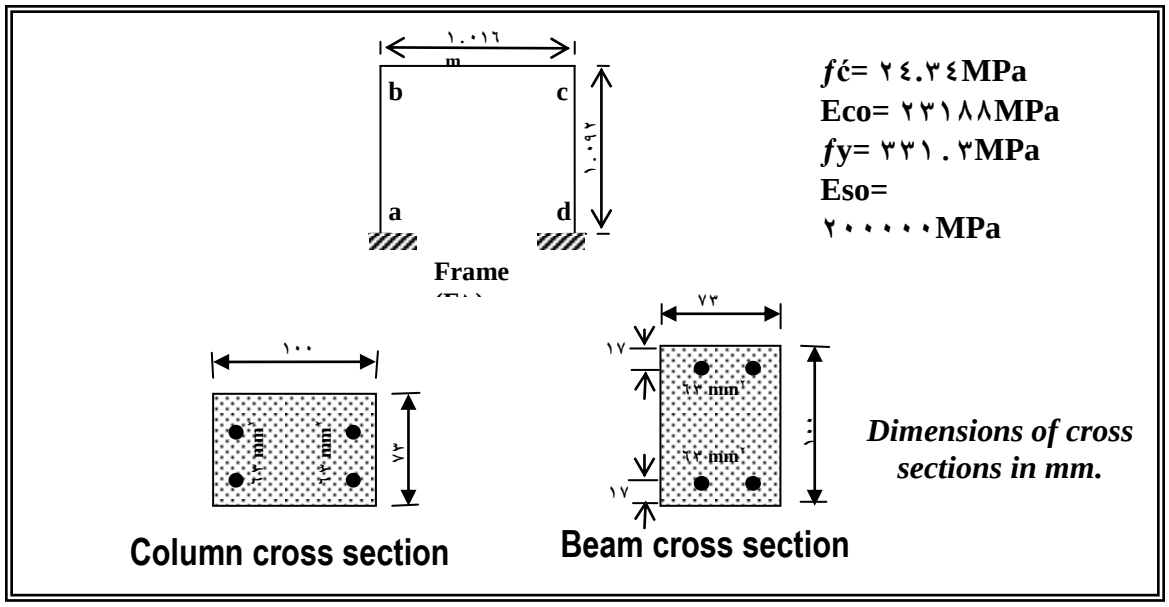

Fig. (٥ . ١) Details of frame (F١)

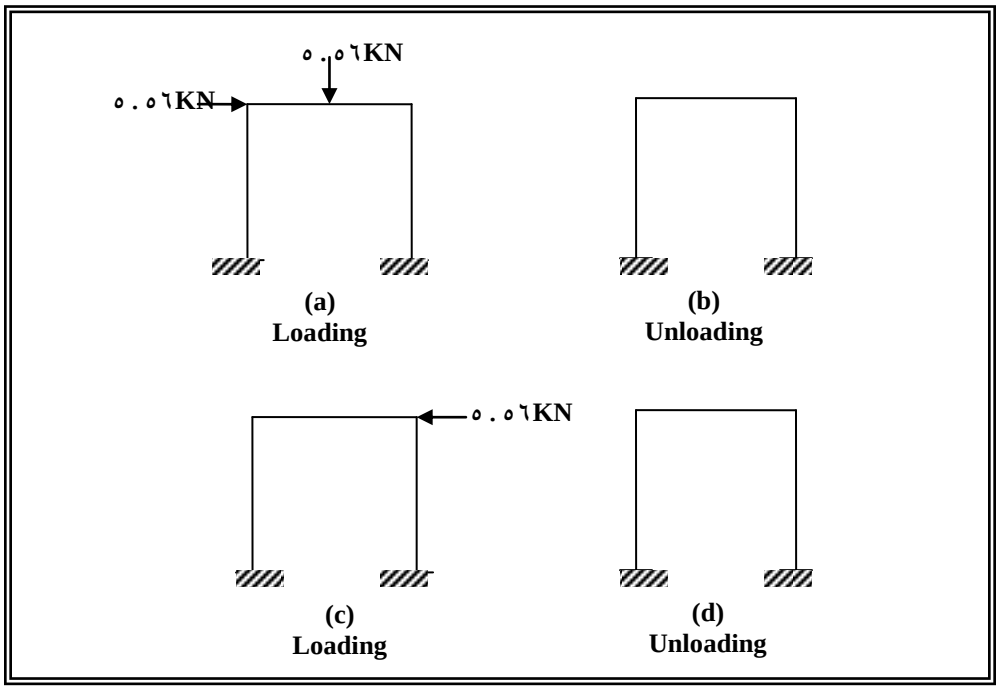

Fig. (٥.٢) Tested load conditions for frame (F١)**.**

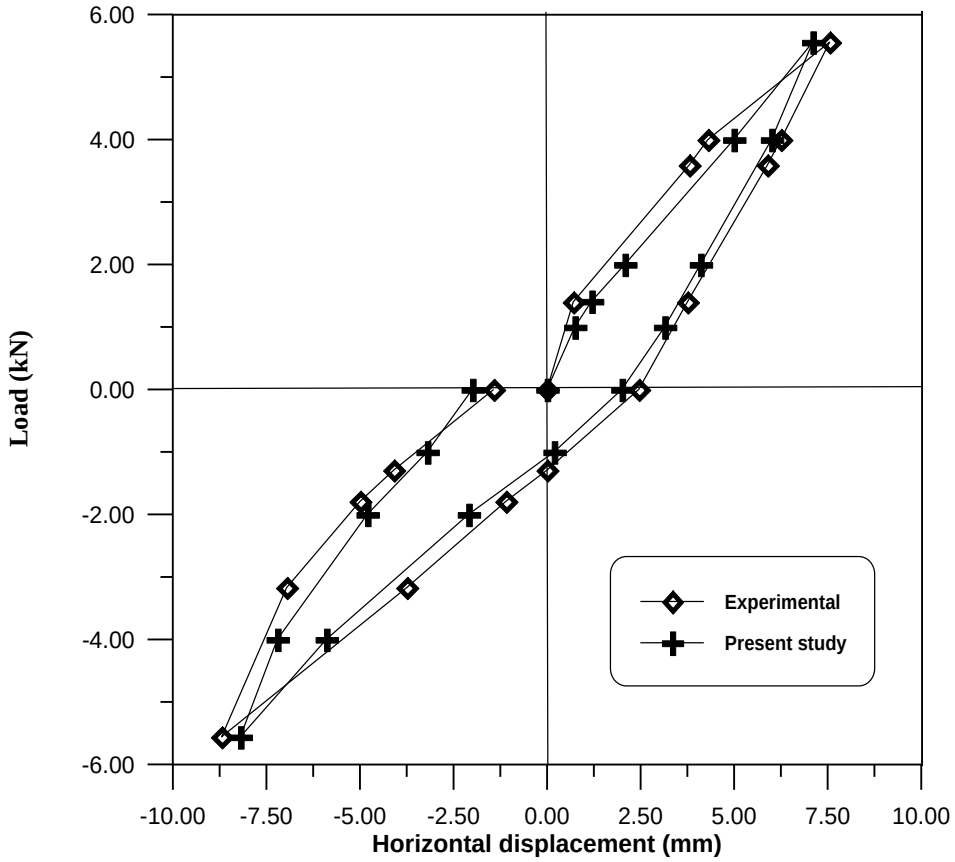

Fig. (٥ . ٣) Load-horizontal displacement at point b for frame (F١)

Example No. ١

Table (٥-١) Horizontal displacement values for loading cases

Loading case	Horizontal displacement at point b (mm)	
	Experimental (Bertero)	Present study
a	٧ . ٧	٧ . ١
b	٢ . ٤٤	٢
c	-٨ . ٨	-٨ . ٢
d	-١ . ٤٥	-٢

٥ . ٣ Steel Fiber Reinforced Concrete Beam under Monotonic Load

A simply supported steel fiber reinforced concrete beam is considered here in. This beam was considered by ***Omer*** [٥٧], and experimental program for testing for this beam was given. The details of this beam are shown in Fig. (٥.٤). This example serve to check the validity and efficiency of the proposed analysis technique to analyze fiber reinforced concrete members.

Based on the proposed procedure, the beam is divided into eighteen layers for fibrous concrete and two layers for steel with six elements along the beam axis. The results of the present study are compared with those of experimental work. The available data for this example was shown in table (٥-٢). The comparison was done using the load-deflection curve, ultimate load and maximum displacement. Fig. (٥.٥) shows the load-deflection curves of the experimental work and the present study. Reasonable agreement with experimental results is achieved through the entire load-deflection range.

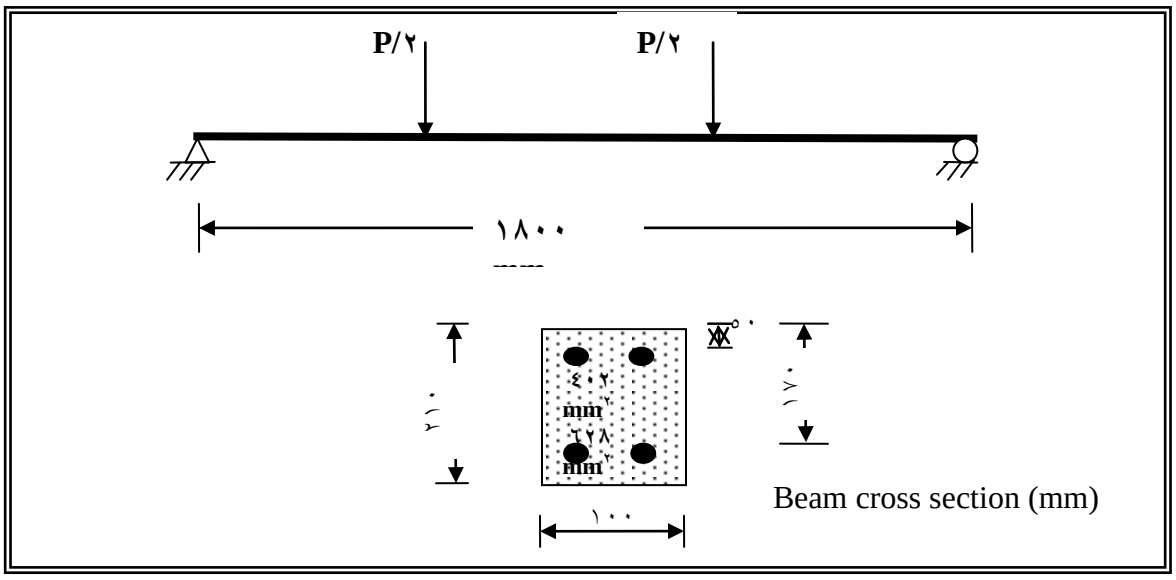

Beam cross section (mm)

Fig. (٥ . ٤) Details for Example No.٢

Table (٥ . ٢) Details and Data of Studied Beams

Example No.	f'_{cf} (MPa)	E_{cf} (MPa)	L_f (mm)	D_f (mm)	Ar	V_f %
٢	١٨.٤٨	٣٤.٢٤	٥٠	٠.٥	١٠٠	١

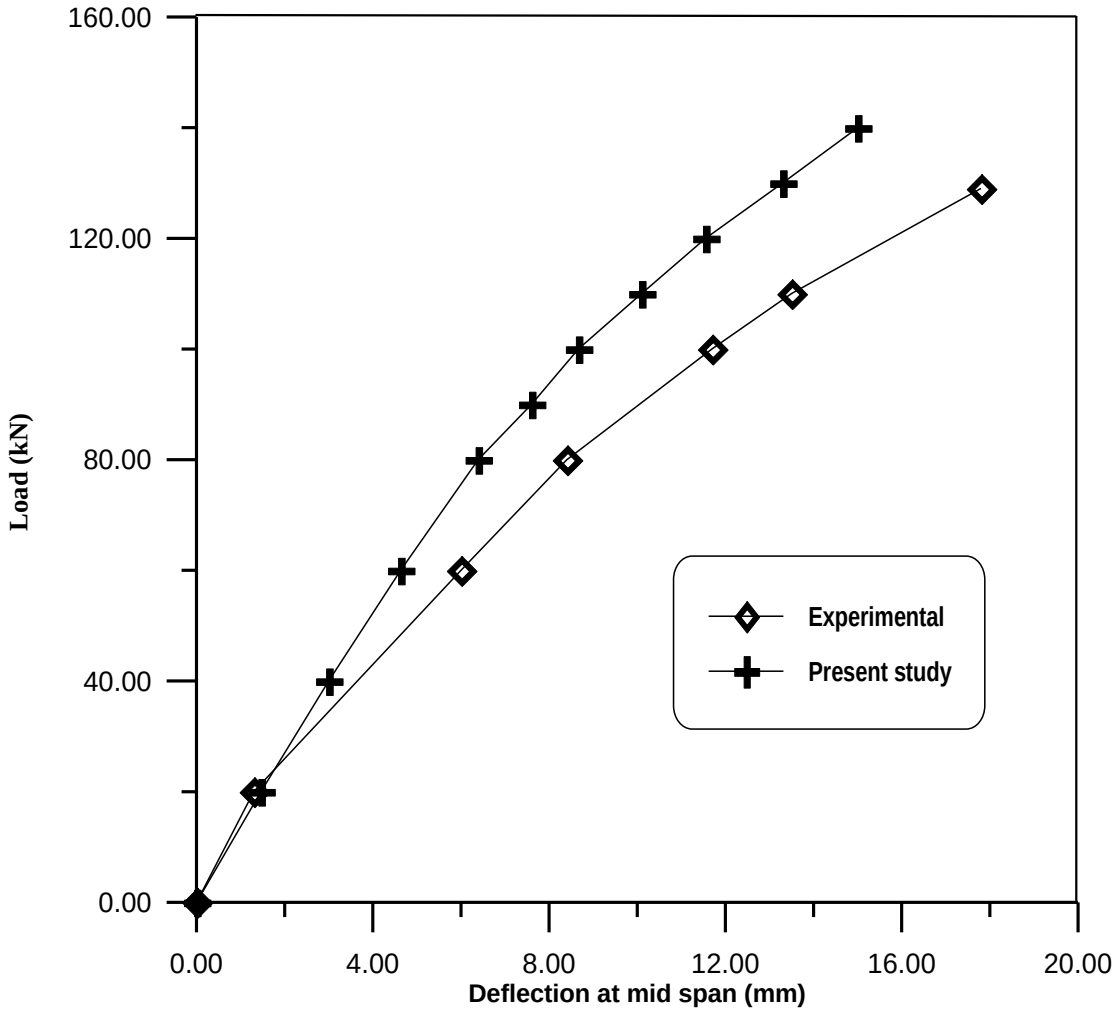

Fig. (٥.٥) Load-deflection curve for Example No.٢

٥ . ٤ Steel Fiber Reinforced Concrete Beam subjected to cyclic load

Nimnim [٥٠] presented experimental tests on simply supported fibrous concrete beams subjected to cyclic loading. According to the proposed procedure, the beams are divided into eighteen layers of fibrous concrete with six elements along the beam axis. Geometry and the test loading conditions for the beams are given in Figs. (٥.٦) and (٥.٧), respectively.

The results of the present study are compared with those of experimental work. The comparison was done using the load-deflection curve with experimental values.

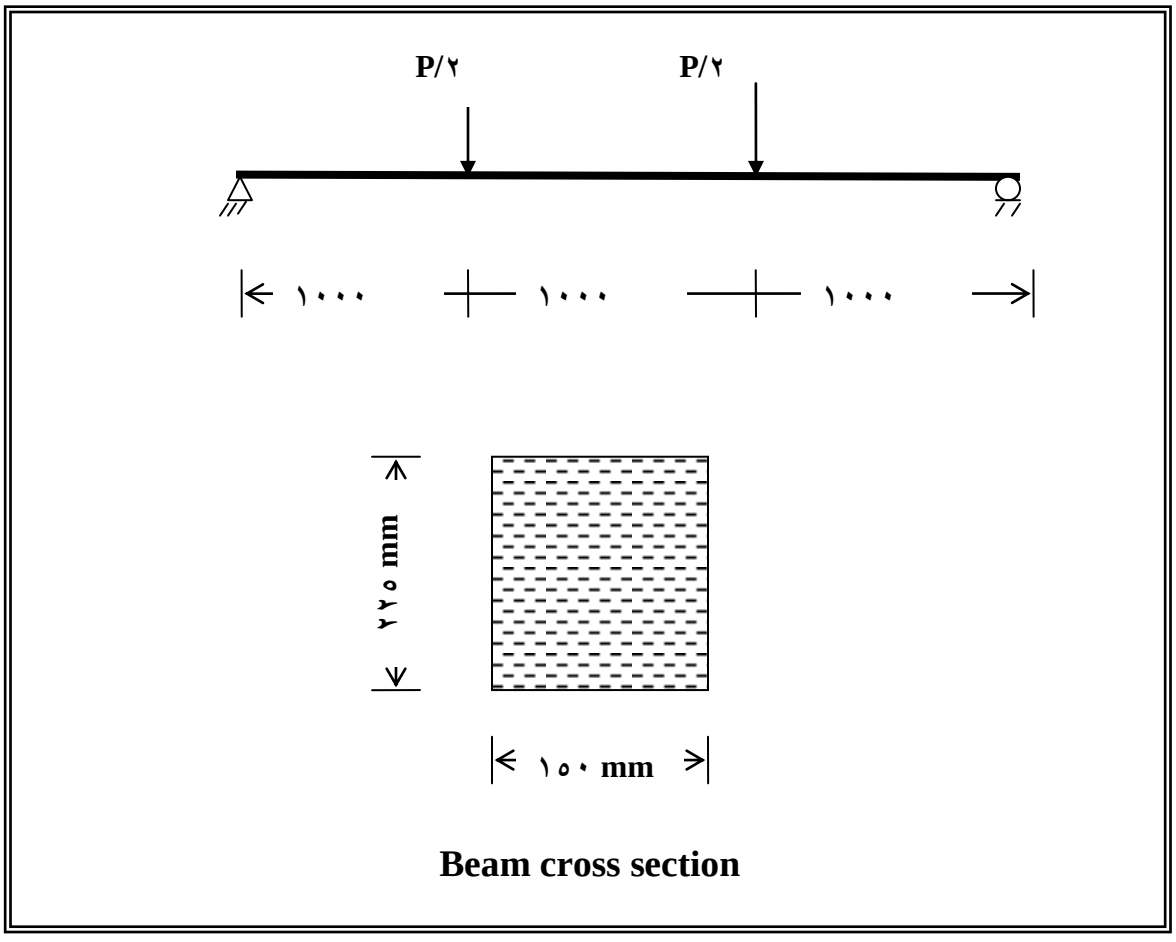

Beam cross section

Fig. (٥.٦) Examples Details

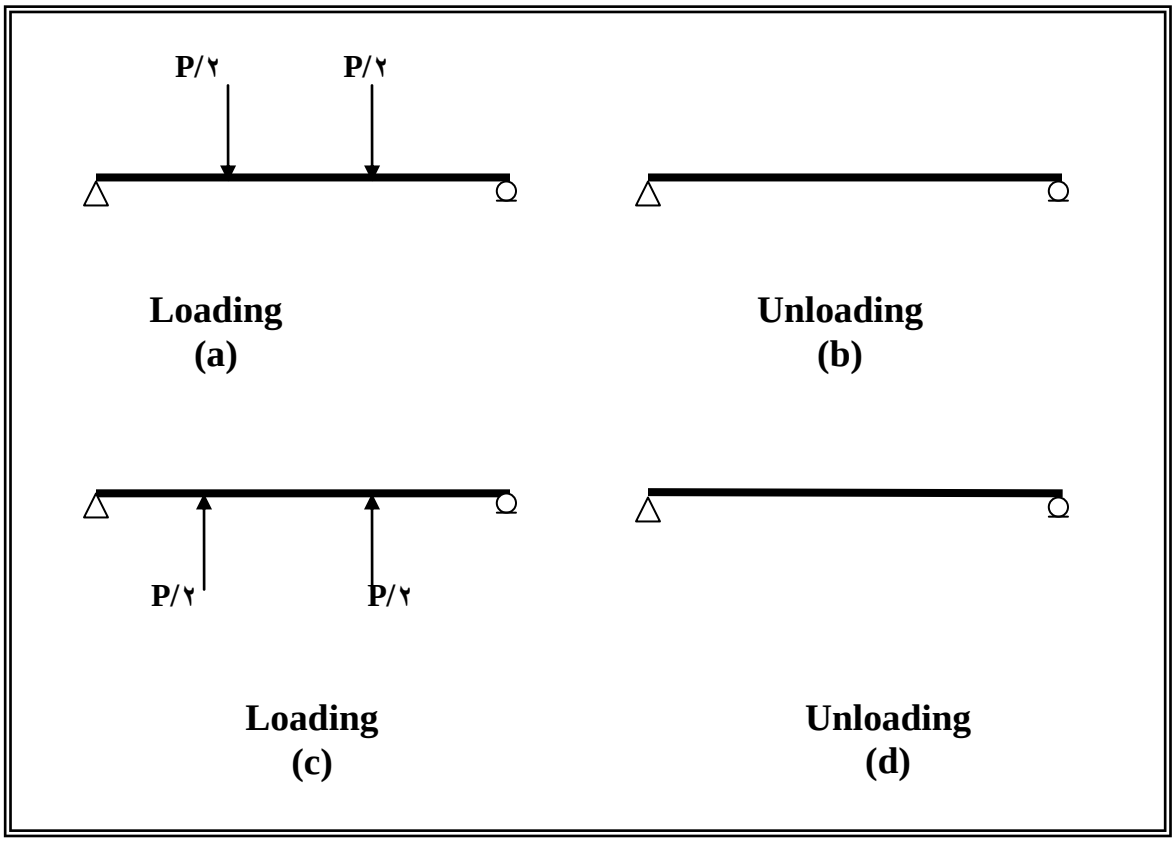

Fig. (٥.٧) Tested load conditions

٥ . ٤ . ١ Example No.٣

The beam shown in Fig. (٥ . ٧) which has a steel fiber content ١% volume fraction, with aspect ratio ١٠٠ is considered. The material properties are listed in Table (٥-٣).

Fig. (٥ . ٨) shows a comparison between the experimental values and the values obtained from the proposed method. The deflections for each load case are listed in Table (٥-٤).

Example No.	f'_{cf} (MPa)	E_{cf} (MPa)	L_f (mm)	D_f (mm)	Ar	V_f %
٣	٣٥.٢١	٣٤.٢٤	٥٠	٠.٥	١٠٠	١

Table (٥-٣) material properties

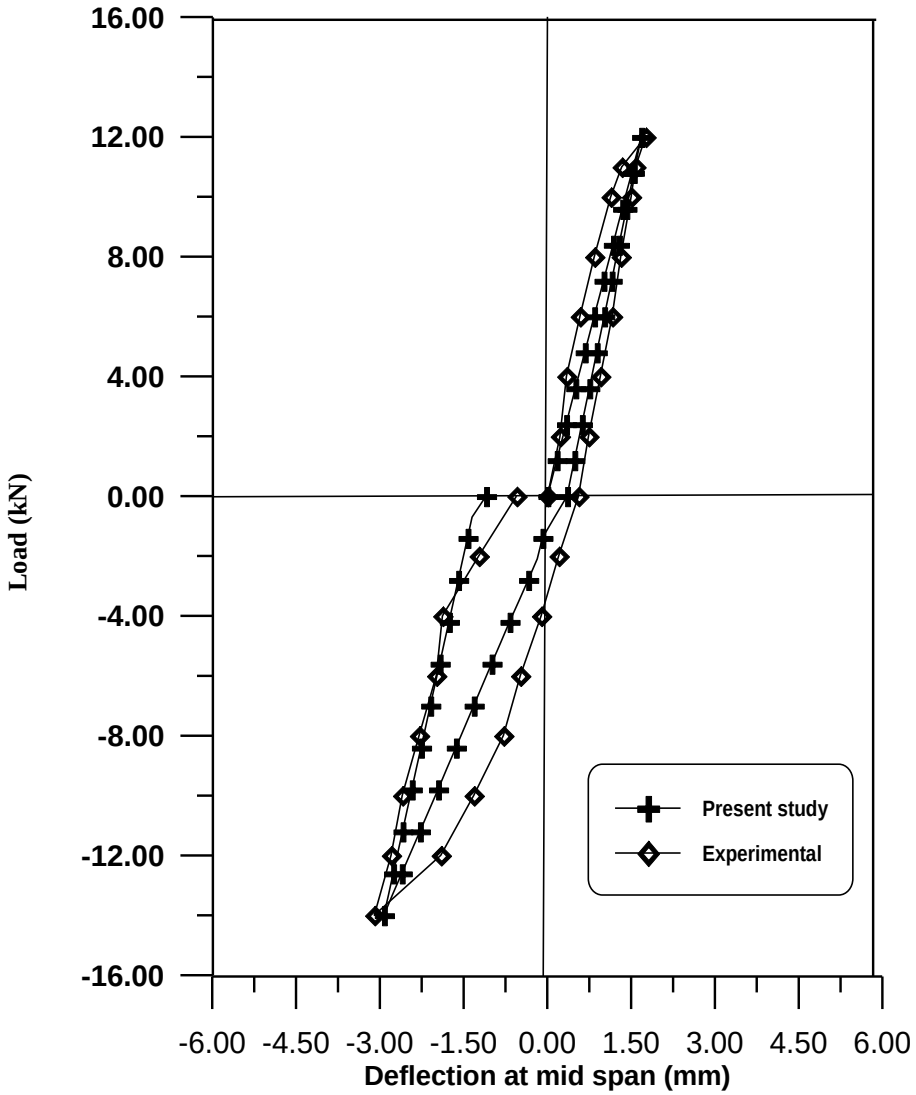

Fig. (٥ . ٨) Load-deflection curve for Example No.٣

Table (٥-٤) Deflection values for loading

Loading case	(mm)	
	Experimental	**Present study**
a	١.٧٦	١.٦٨٢٢
b	٠.٥	٠.٣٥
c	-٣.٠٤	-٢.٩
d	-٠.٥٥	-١.١

٥.٤.٢ Example No.٤

This example used steel fibers contain ٠.٥% by volume fraction, with aspect ratio ١٠٠. The materials properties are listed in Table (٥-٥).

Fig. (٥.٩) shows a comparison between analytical and experimental results. The deflections for each load cases are listed in Table (٥.٦).

Table (٥-٥) material properties

Example No.	f'_{cf} (MPa)	E_{cf} (MPa)	L_f (mm)	D_f (mm)	Ar	V_f %
٤	٣٣.٢٦	٣٣.٢٣	٥٠	٠.٥	١٠٠	٠.٥

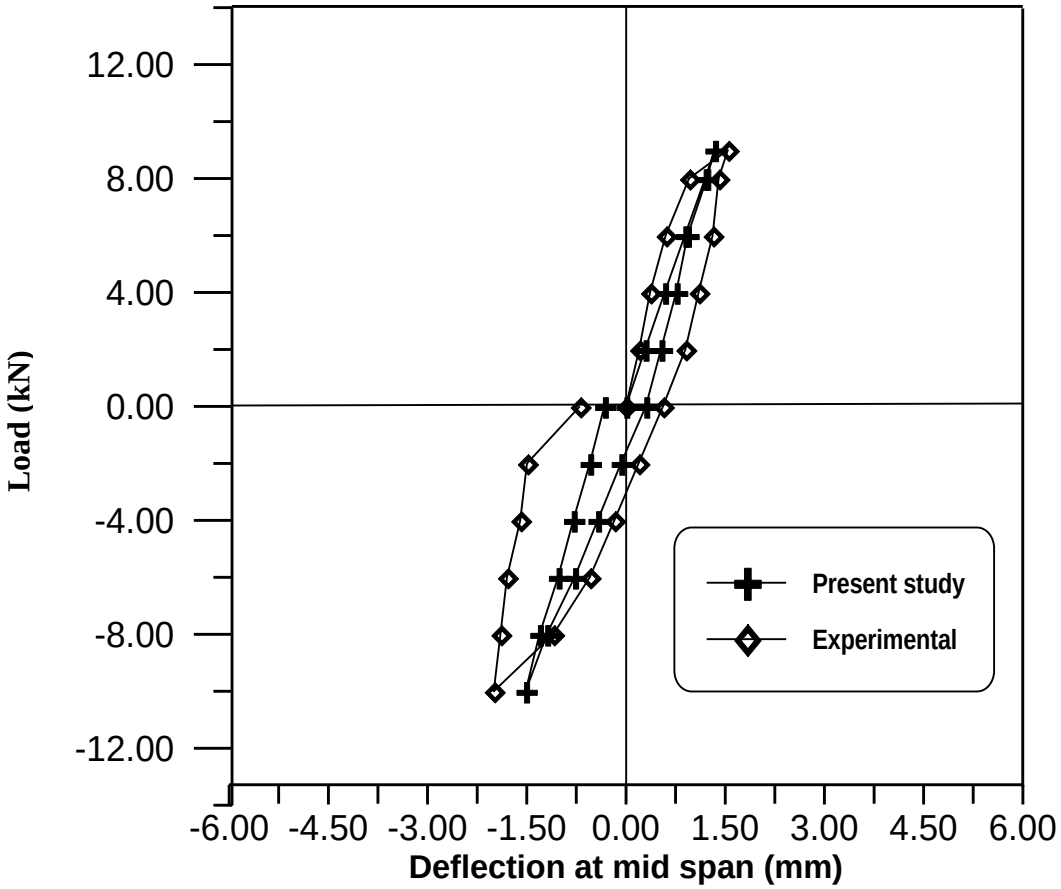

Fig.(٥ . ٩) Load-deflection for Example No.٤

Table (٥-٦) Deflection values for loading cases

Loading case	Midpoint deflection (mm)	
	Experimental	Present study
a	١ . ٥ ٤	١ . ٣ ٤
b	٠ . ٥ ٦	٠ . ٣
c	-٢	-١ . ٥ ٢

d	-٠.٧	-٠.٣٣

٥.٤.٣ Example No.٥

In the fifth example the steel fibers contain ١.٥% by volume fraction and ١٠٠ of aspect ratio. Table (٥-٧) shows the materials properties for this example.

The comparison between the results obtained by experimental test and the results obtained from the proposed method is shown in Fig.(٥.١٠); the deflection for each load cases is listed in Table (٥-٨).

Table (٥-٧) material properties

Example No.	f'_{Cf} **(MPa)**	E_{Cf} **(MPa)**	L_f **(mm)**	D_f **(mm)**	**Ar**	$\mathbf{V_f}$ **%**
٥	٣٤.١٣	٣٥.٦٣	٥٠	٠.٥	١٠٠	١.٥

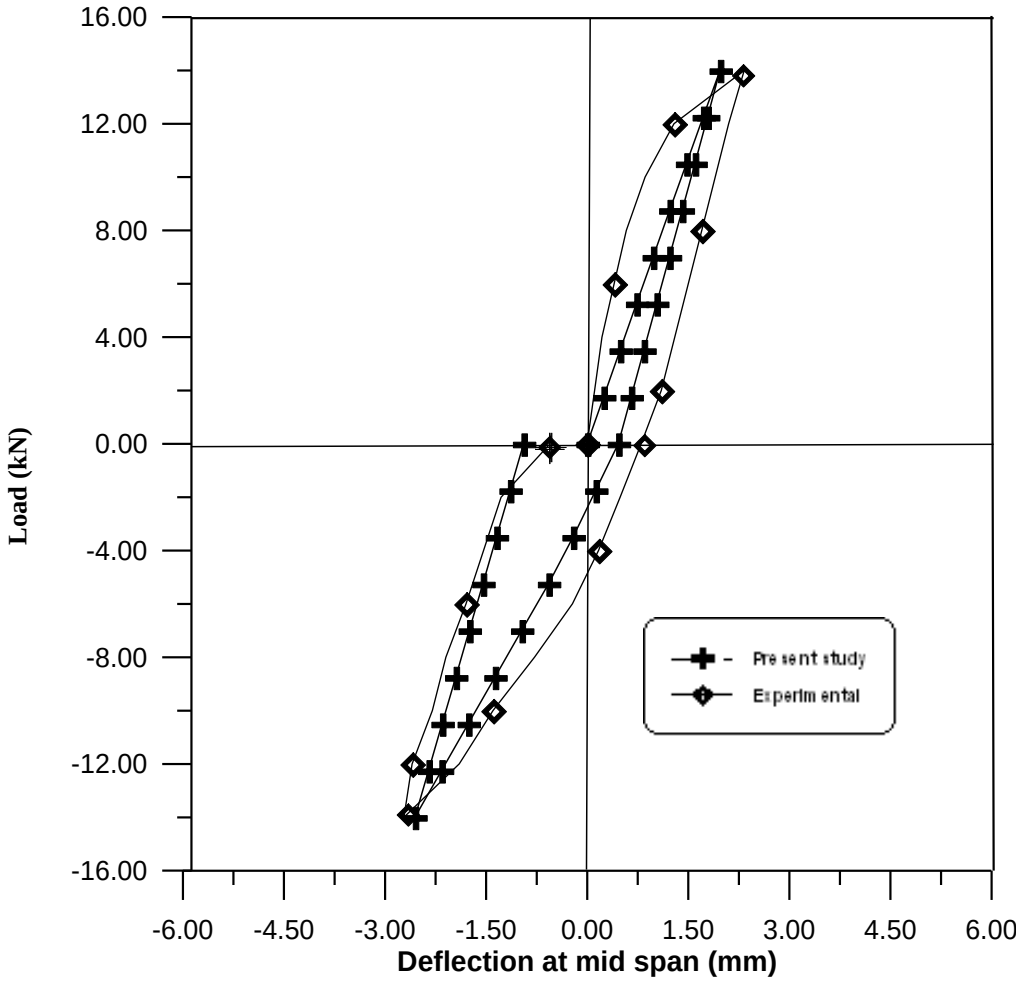

Fig.(٥ . ١٠) Load-deflection for Example No.٥

Table (٥-٨) Deflection values for loading cases

Loading case	Midpoint deflection (mm)	
	Experimental	Present study

a	٢.٣٣	١.٩٧
b	٠.٨	٠.٤٦٢
c	-٢.٧٢٢	-٢.٥٥٨
d	-٠.٥	-٠.٩

٥.٥ Parametric Study on SFRC Member

The effects of the main parameters on flexural behavior of steel fiber reinforced concrete members are investigated: the main reinforcing ratio (ρ), the fiber content (volume fraction), the aspect ratio of fibers, partial- depth of steel fibers, element type and loading distribution.

٥.٥.١ The Effect of Reinforcement Ratio

The effect of longitudinal steel reinforcement was studied through three different reinforcement ratios: ρ = ٠.٠٠٧٩, ٠.٠١٣٤ and ٠.٠٢. The beam used for parametric study is shown in Fig. (٥.١١), the steel fibers content was ١% volume fraction with aspect ratio ٧٥. The beam having cross sectional dimensions of ١٥٠ × ٢٢٥ × ٢٠٠٠ mm is subjected to two-point load.

According to the proposed procedure, the beams were divided into fourteen fibrous concrete layers and one steel layer with four elements along the beam axis. Fig. (٥.١٢) represents central deflection versus load for the beams with different steel reinforcement ratios.

From the load deflection curve, Fig. (٥.١٢), it was conducted that an increasing in the ratio of longitudinal steel reinforcement led to a decrease in deflection values, when the ratio of the longitudinal steel reinforcement was increased from ٠.٠٠٧٩ to ٠.٠٢ a decrease in deflection about ٣٠٪.

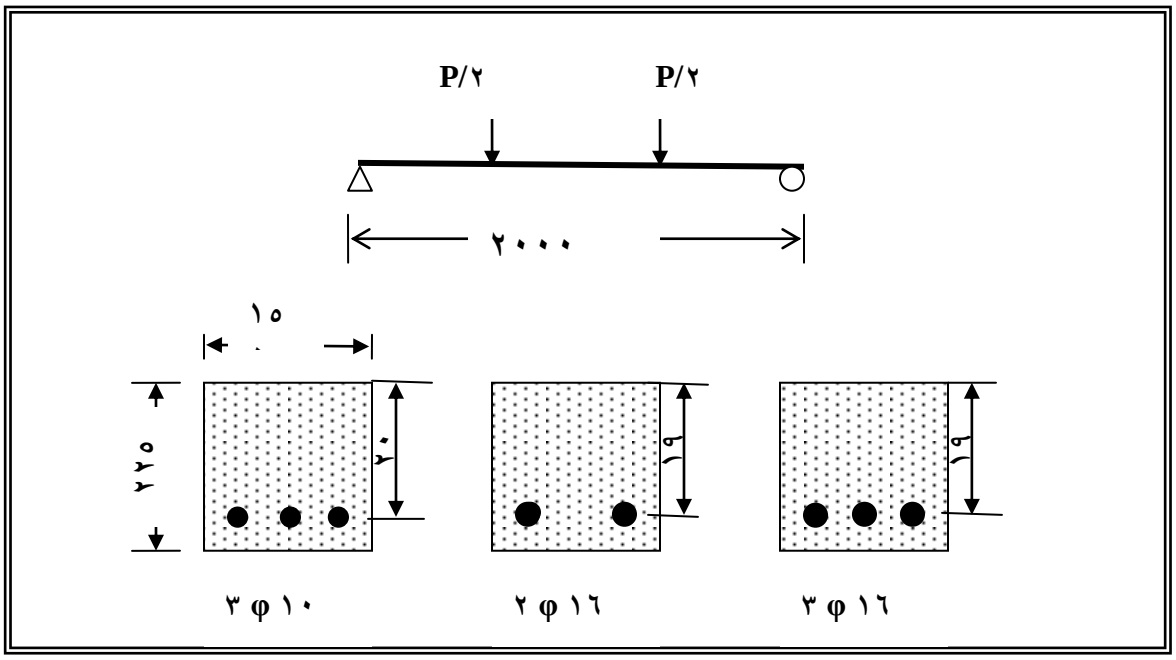

Fig. (٥ . ١١) Details for beams

Table (٥-٩) Materials properties

Beam No.	f'_c (MPa)	E_C (MPa)	f_y (MPa)	E_{So} (GPa)	V_f %	Ar	ρ %
١	٢٥	٢٣٦٥٠	٣٥٠	٢٠٠	١	٧٥	٠.٧٩
٢	٢٥	٢٣٦٥٠	٣٥٠	٢٠٠	١	٧٥	١.٣٤
٣	٢٥	٢٣٦٥٠	٣٥٠	٢٠٠	١	٧٥	٢

Previous study showed that with increasing ١% volume content of steel fibers could replace about ρ = ٠.١٥% of flexural steel reinforcement [٦٢]. In the present study verification of this case was used ρ = ٠.٧٩٪ with ١% volume content of steel fibers and then used the same beam with longitudinal steel reinforcement ratio ρ = ٠.٩٤٪ without using steel fibers as shown in Fig. (٥.١٣). The cracking patterns appear in Figs. (٥.١٥) to (٥.١٨).

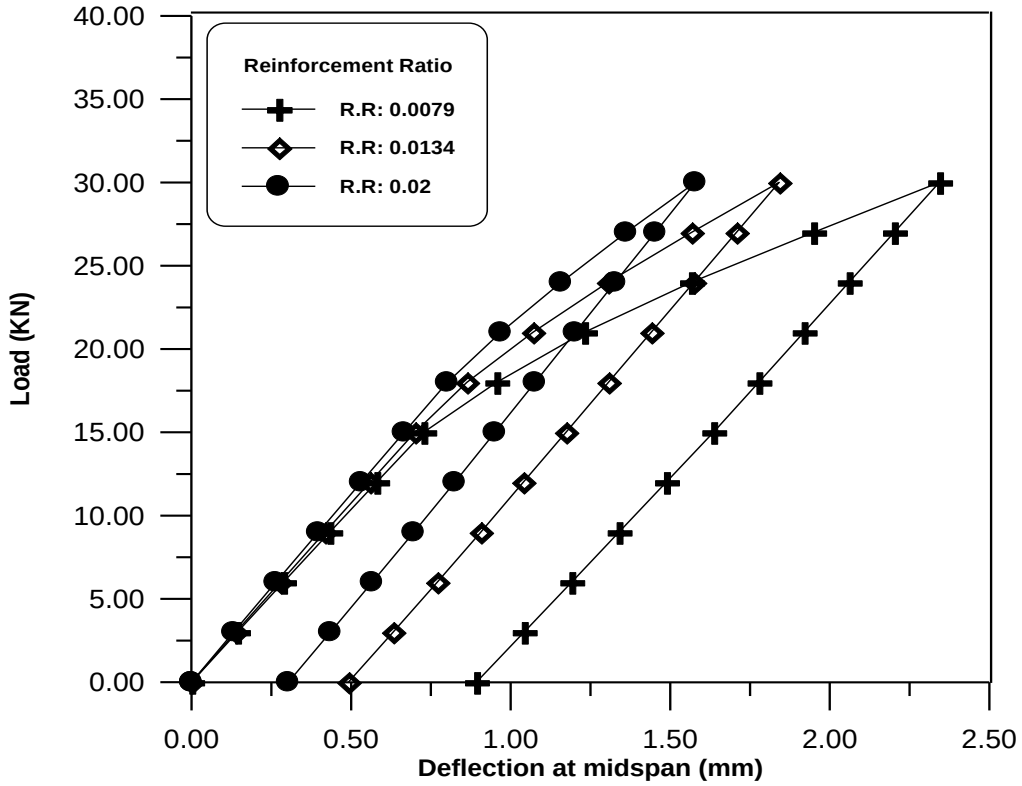

Fig. (٥.١٢) Reinforcement Ratio Effect (V_f = ١٪)

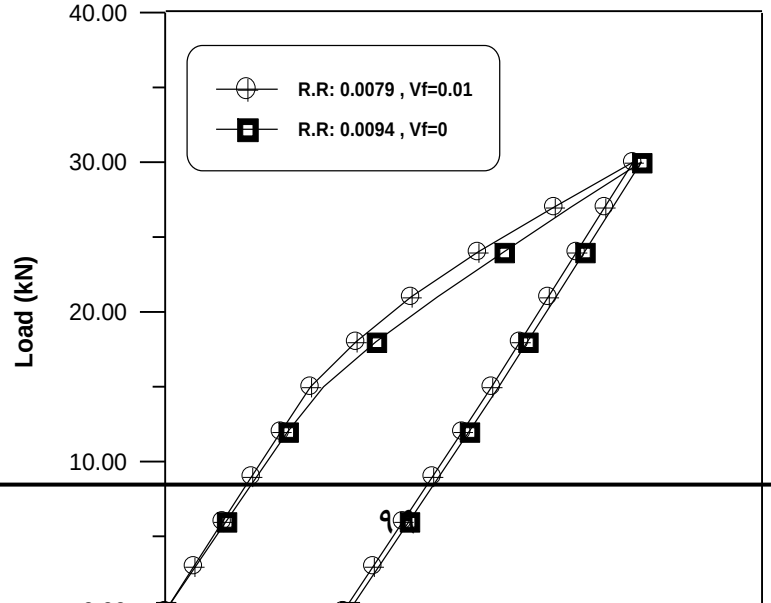

Fig. (٥ . ١٣) Comparative load-deflection curves for ρ =٠ . ٧٩%, Vf= ١% and ρ =٠ . ٩٤%, Vf= ٠

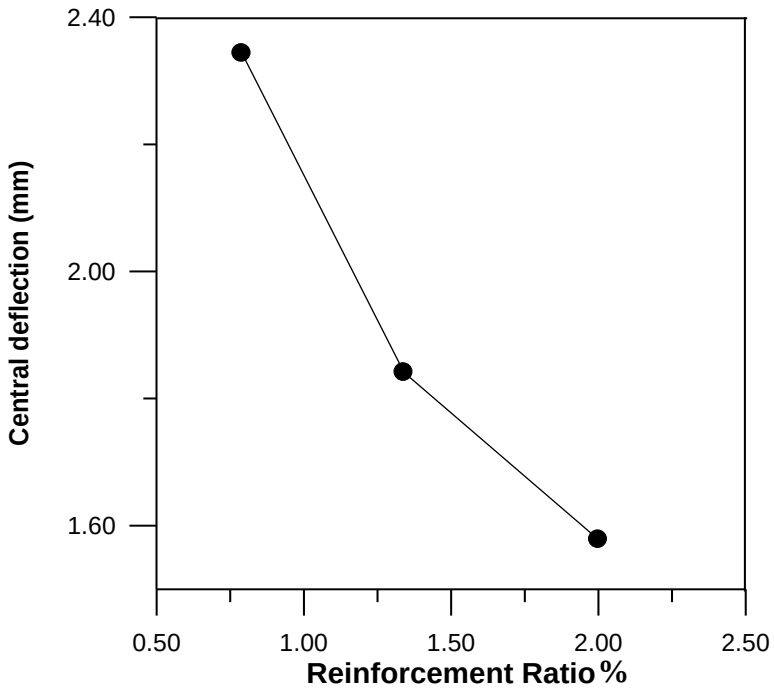

Fig. (٥ . ١٤) Relationship between ρ% and deflection (at ٣٠ KN)

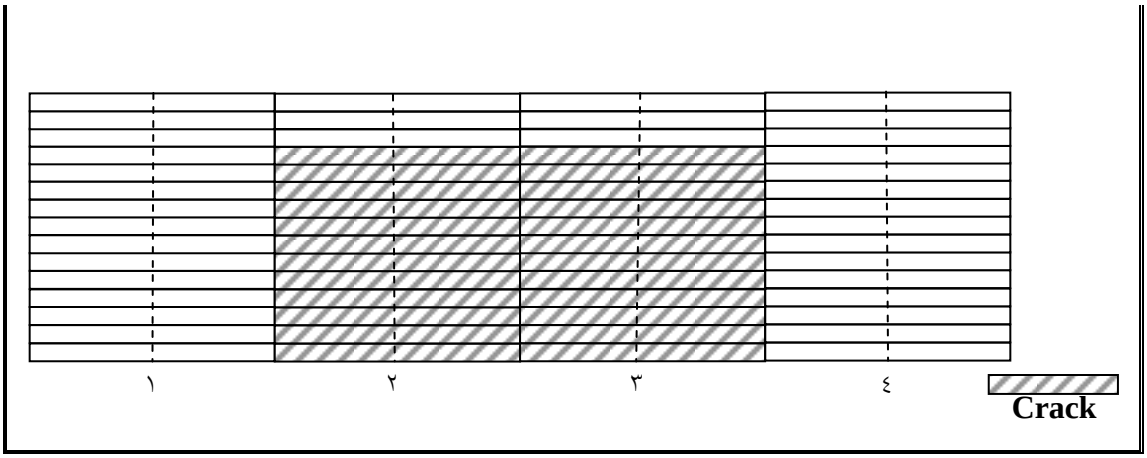

Fig. (٥.١٥) Cracking pattern of beam (ρ = ٠.٧٩ %), at load equal ٣٠KN

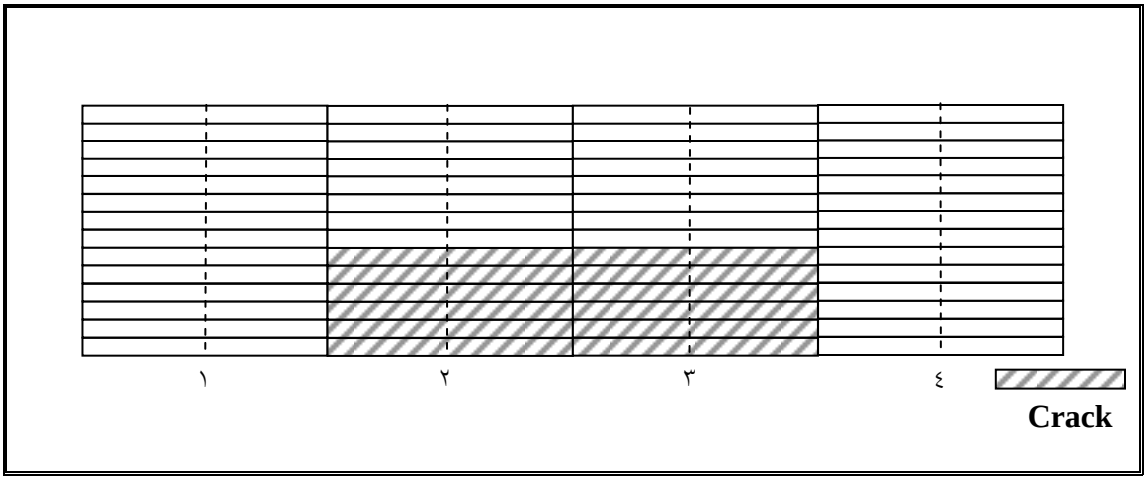

Fig. (٥.١٦) Cracking pattern beam (ρ = ١ . ٣٤ %), at load equal ٣٠ KN

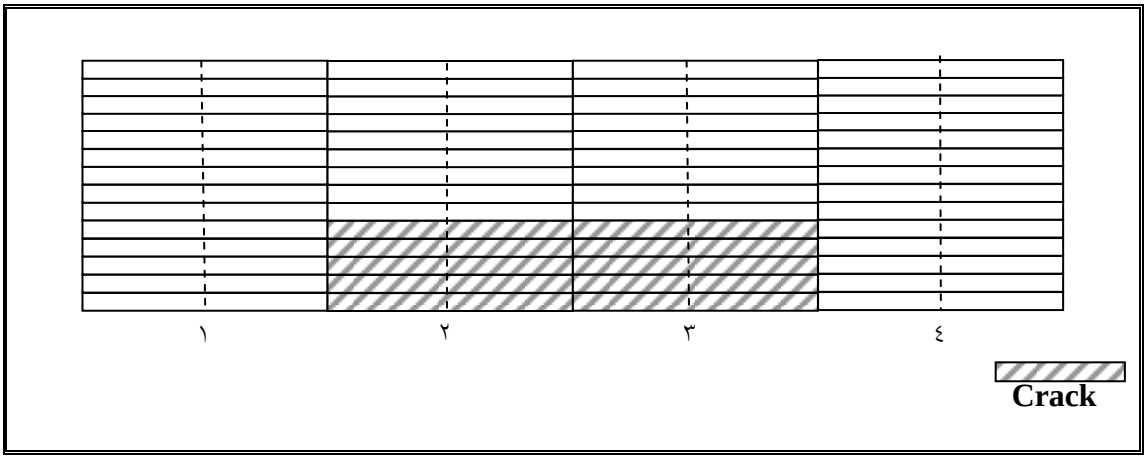

Fig. (٥.١٧) Cracking pattern beam (ρ = ٢ %), at load equal ٣٠ KN

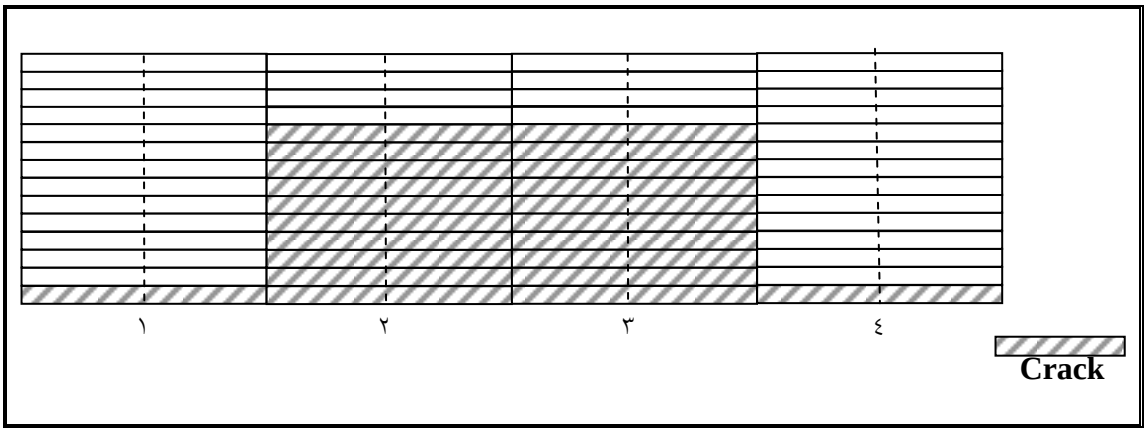

Fig. (٥.١٨) Cracking pattern beam (ρ = ٠.٩٤ %, V_f = ٠ %), at load equal ٣٠ KN

٥ . ٥ . ٢ Fiber Content

Volume fraction can be defined as the ratio of fibers volume to total volume of fibers and matrix and it is expressed as a percentage of total volume of composite material.

% Fiber by volume=volume of fibers /(volume of matrix + volume of fibers)

In the present parameter the effect of fibers content is studied through four different volume fractions ٠.٥%, ١٪, ١.٥٪ and ٢%, with constant aspect ratio ٧٥. The portal [٢٩] frame (F٢) member selected to investigate by the development computer program. The geometry, loading and reinforcement details are shown in Fig. (٥.١٩), the material properties are shown in Table (٥.١٠).

According to the proposed procedure, the beam divided into four elements with eighteen fibrous concrete layers and two steel layers for, and three elements with eighteen fibrous concrete layers and three steel layers for each column. Also cracking patterns appear in Figs. (٥.٢١) to (٥.٢٥).

The present study revealed that when the fiber content increased from ٠.٥٪ to ٢٪ Fig. (٥.٢٠), the deflection is a decreased about ٤٠٪. The

increased fiber content led to increasing at the bond strength in the cracked section. As result, the tensile strength of composite material will be increased.

Table (٥-١٠) Materials properties frame (F٢)

Materials properties (MPa)	Beam	Columns
fć	٣٥	٣٠
Eco	٢٧٨٠٠	٢٥٧٤٠
fy	٤٠٠	٤٠٠
Eso	٢٠٠٠٠٠	٢٠٠٠٠٠

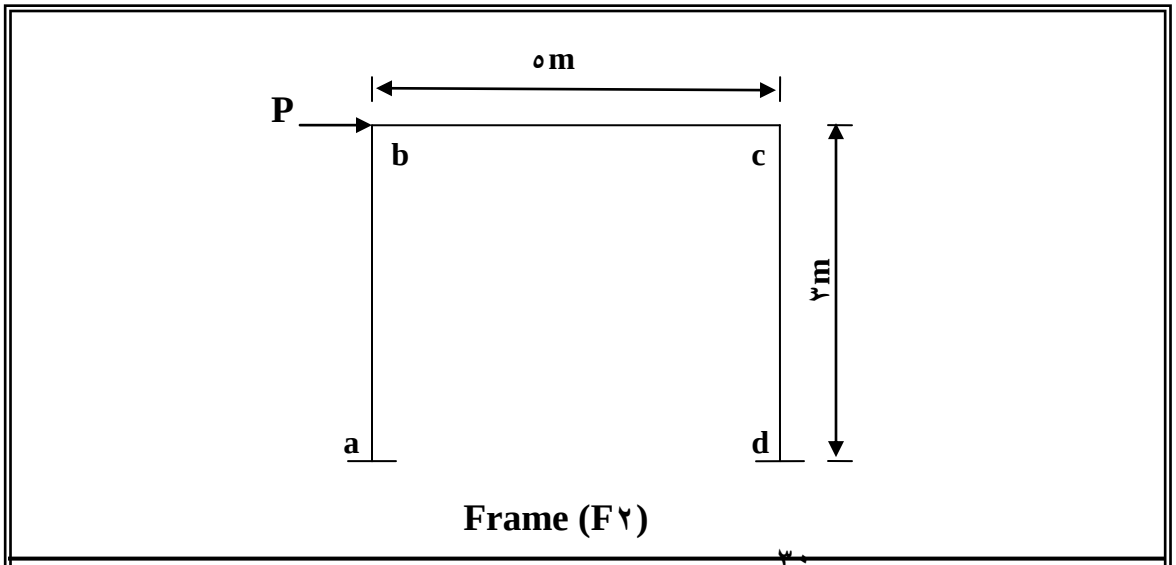

Frame (F٢)

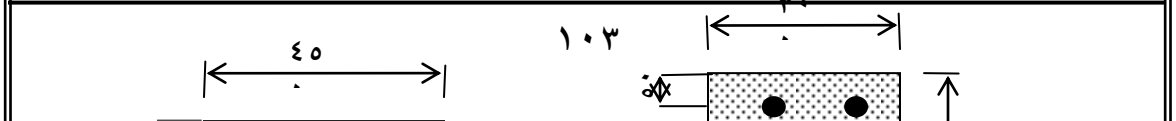

Fig. (٥.١٩) Details for frame (F٢)

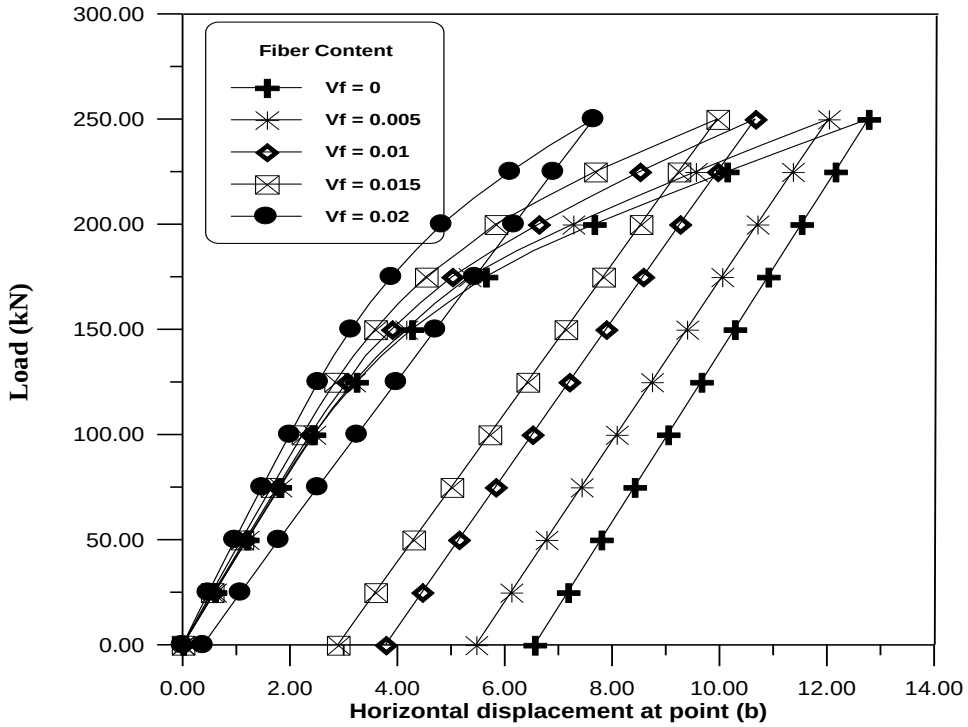

Fig. (٥.٢٠) Effect of Fiber Content (Frame ٢)

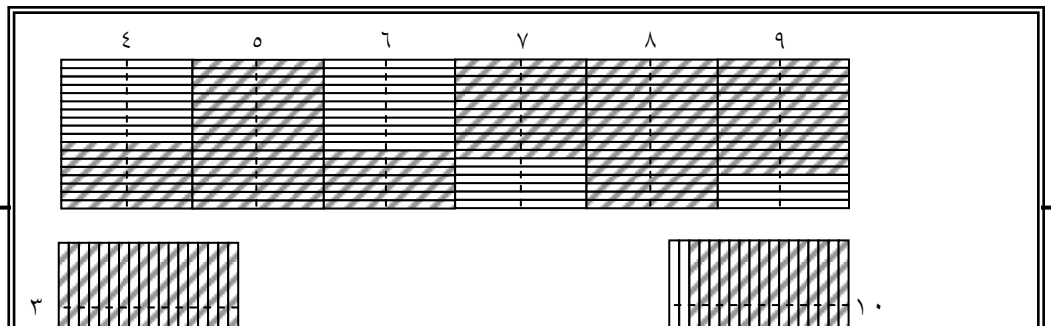

Fig. (٥.٢١) Cracked pattern frame (F٢), with volume friction ٠ %, at load equal ٢٥٠ KN

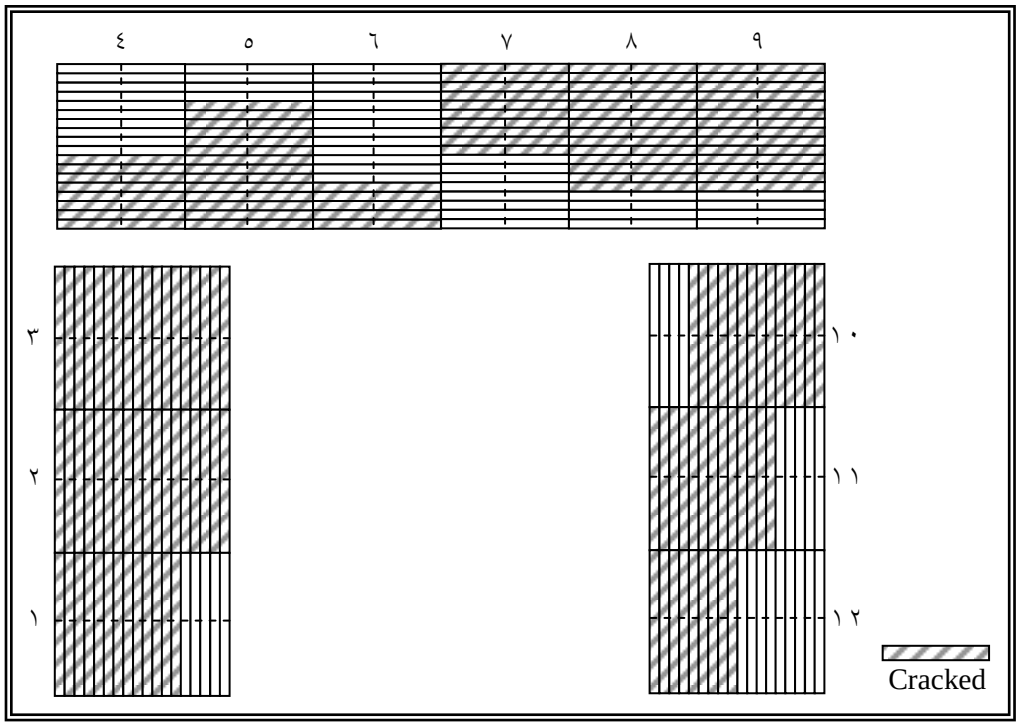

Fig. (٥.٢٢) Cracked pattern frame (F٢), with volume friction ٠.٥ %, at load equal ٢٥٠ KN

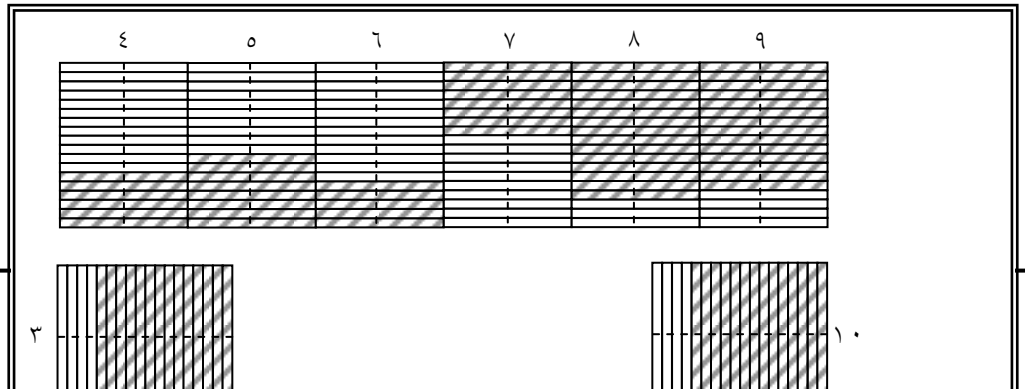

Fig. (٥.٢٣) Cracked pattern frame (F٢), with volume friction ١ %, at load equal ٢٥٠ KN

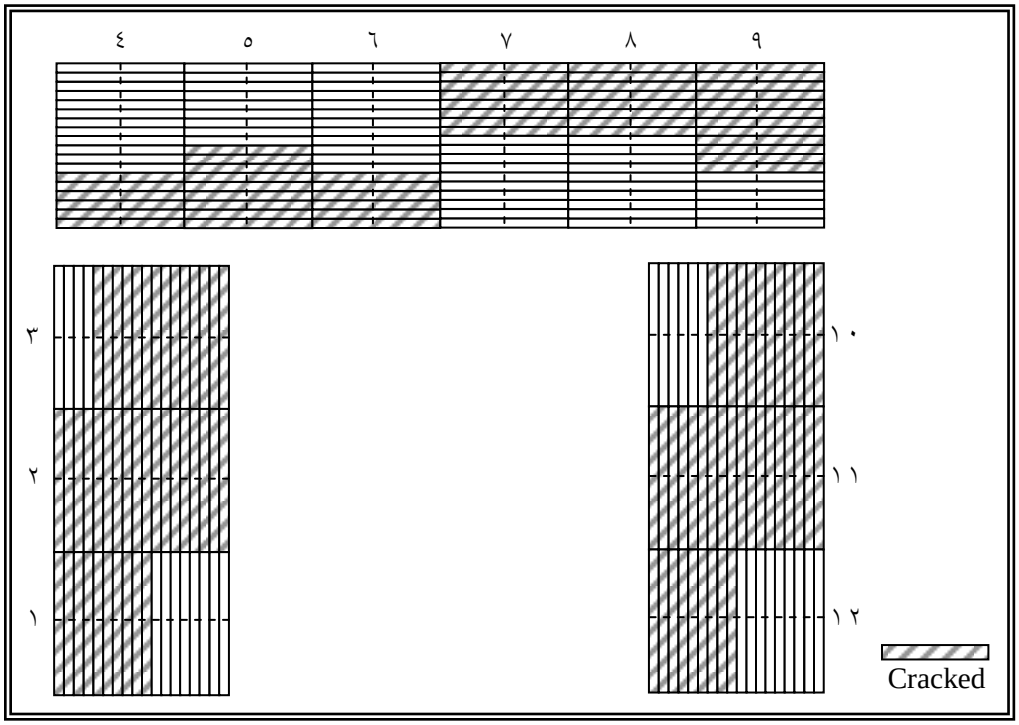

Fig. (٥.٢٤) Cracked pattern frame (F٢), with volume friction ١ . ٥ %, at load equal ٢٥٠ KN

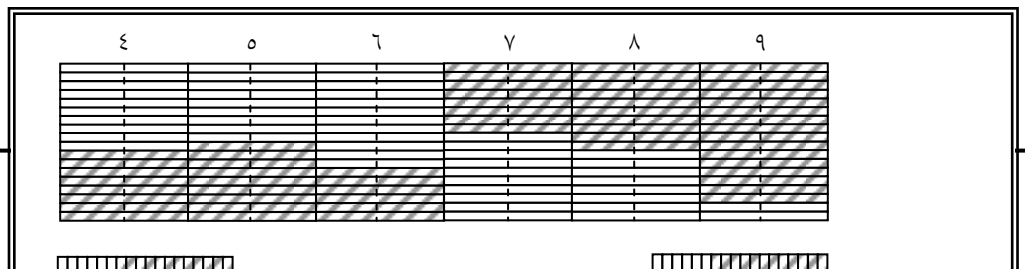

Fig. (٥.٢٥) Cracked pattern frame (F٢), with volume friction ٢ %, at load equal ٢٥٠ KN

٥.٥.٣ Aspect Ratio

Three different aspect ratios effect of fiber geometry (length and diameter) is investigated ٦٠, ٧٥ and ١٠٠, with constant steel fiber volume fraction ١%.

The frame (F٣) [٢٩] is divided into four elements with eighteen fibrous concrete layers and two steel layers for beam, and three elements with eighteen fibrous concrete layers and three steel layers for each column. The detail of this frame is shown in Fig. (٥ . ٢٦), and the materials properties are listed in Table (٥-٧). The load-deflection curves show the aspect ratio effect shown in Fig. (٥ . ٢٧), the cracking pattern is shown in Figs. (٥ . ٢٨) to (٥ . ٣٠).

As shown in the Fig. (٥ . ٢٧), when the aspect ratio an increased from ٦٠ to ١٠٠, the deflection is a decreased about ١٨٪. If the length of steel fiber increased and the fiber diameter and content are fixed, the effective length of steel fibers will increased and hence the pull out resistance

increased, then cause an improvement in the mechanical properties of the matrix. But when the diameter of steel fiber decrease with fixing the fiber length and content, that led to increase in effective number of steel fibers (increase the surface area for steel fibers) in the crack section. As result, the interfacial bonds will be increased.

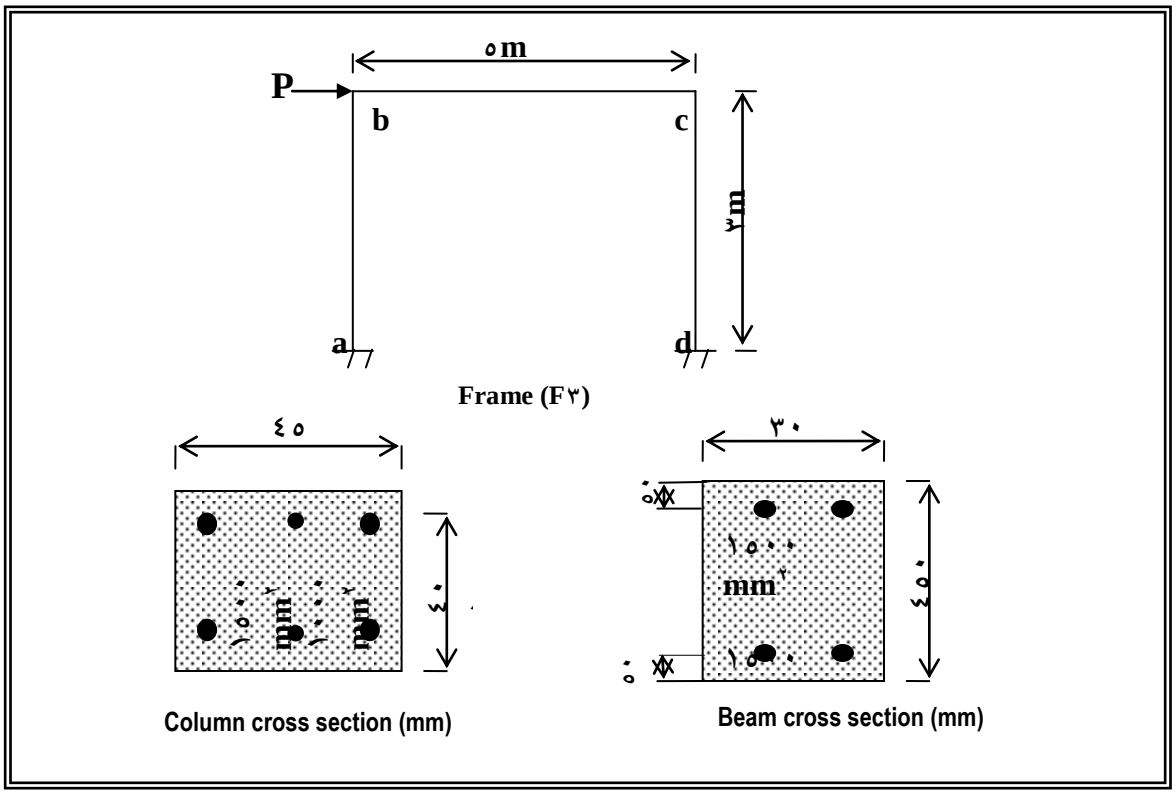

Fig. (٥ . ٢٦) Details for frame (F٣)

Table (٥-١١) Materials properties frame (F٣)

Materials properties (Mpa)	Beam	Columns
Fć	٣٥	٣٠
Eco	٢٧٨٠٠	٢٥٧٤٠
Fy	٤٠٠	٤٠٠
Eso	٢٠٠٠٠٠	٢٠٠٠٠٠

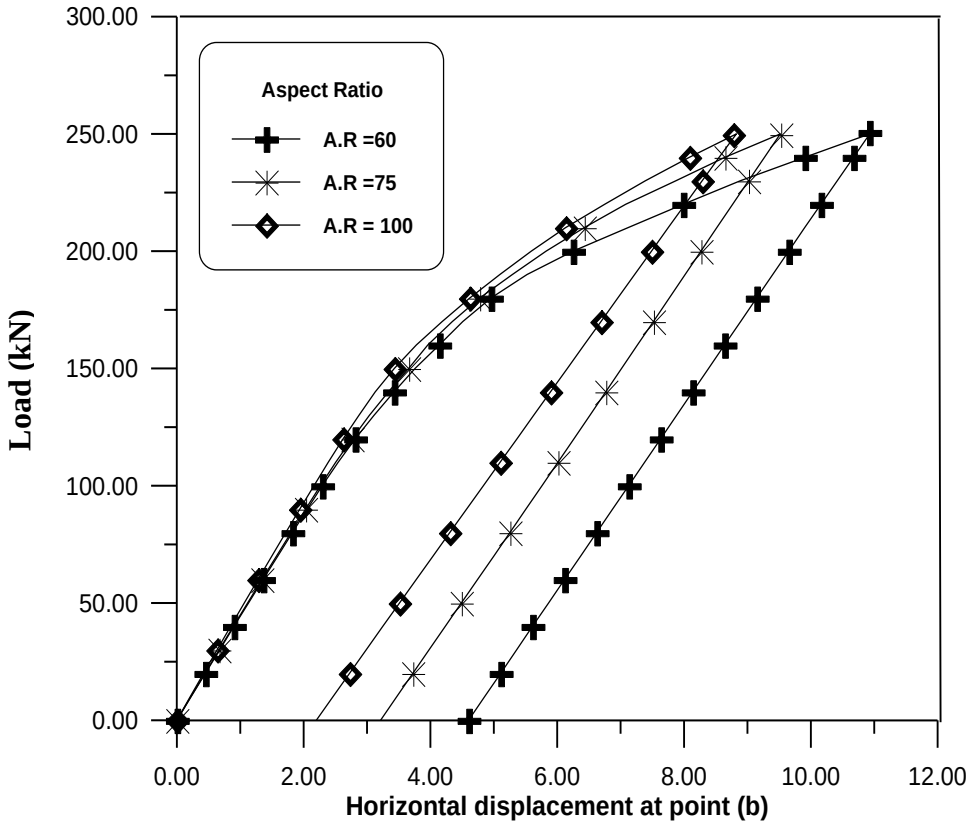

Fig. (٥.٢٧) Aspect Ratio Effect Frame (F٣)

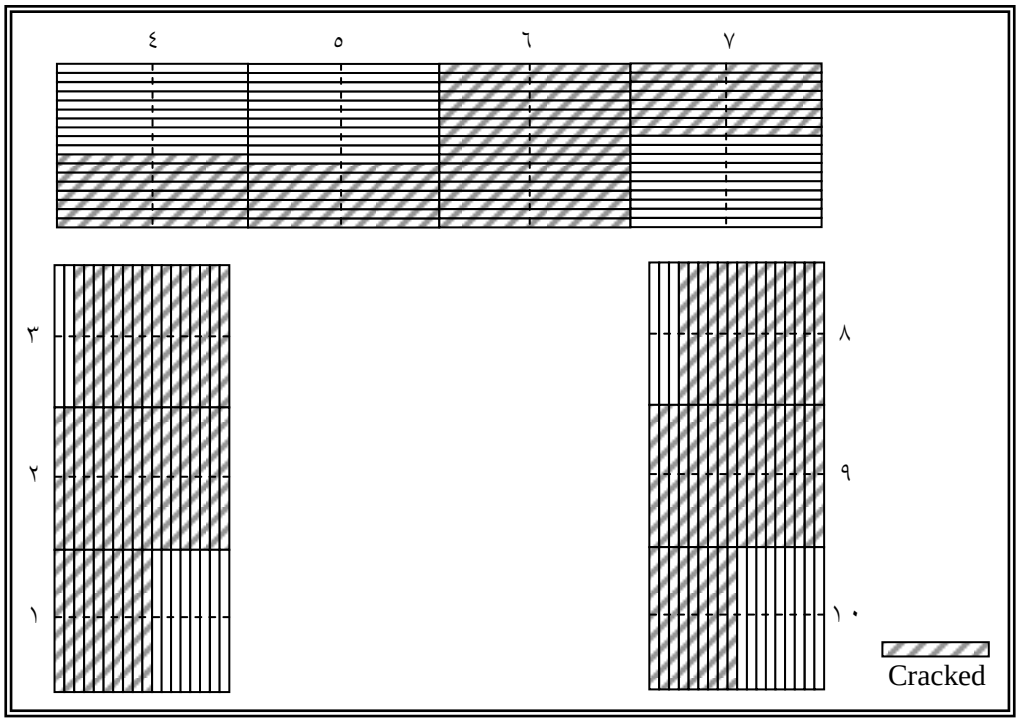

Fig. (٥.٢٨) Cracked pattern frame (F٣), with aspect ratio (L_f / D_f = ٦٠), at load equal ٢٥٠ KN

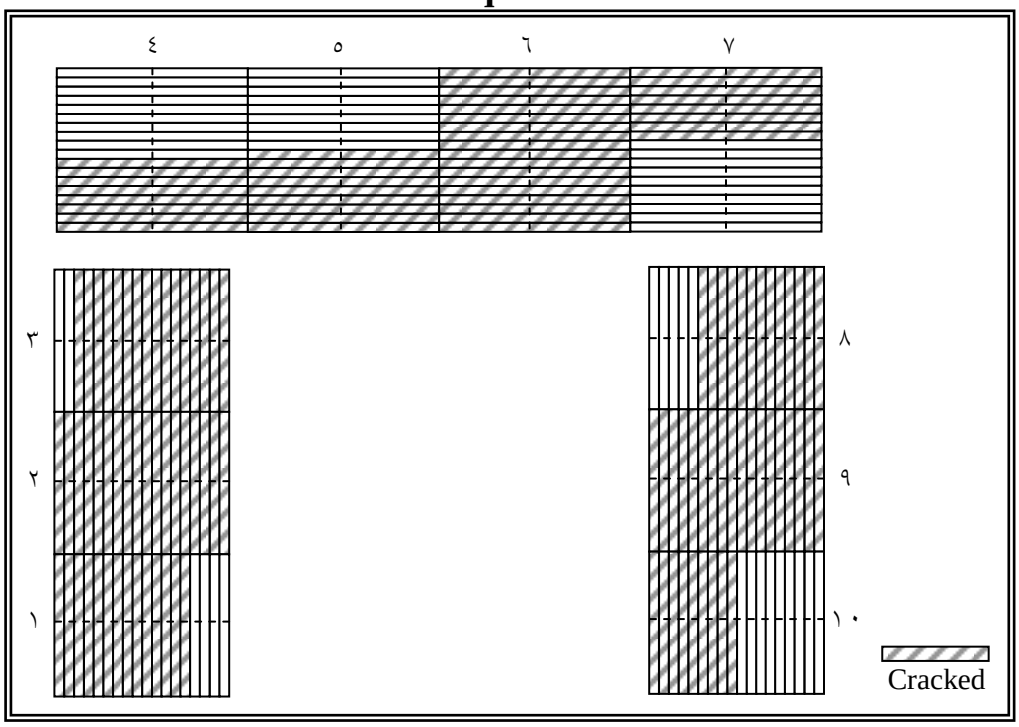

Fig. (٥.٢٩) Cracked pattern frame (F٣), with aspect ratio (L_f / D_f = ٧٥), at load equal ٢٥٠ KN

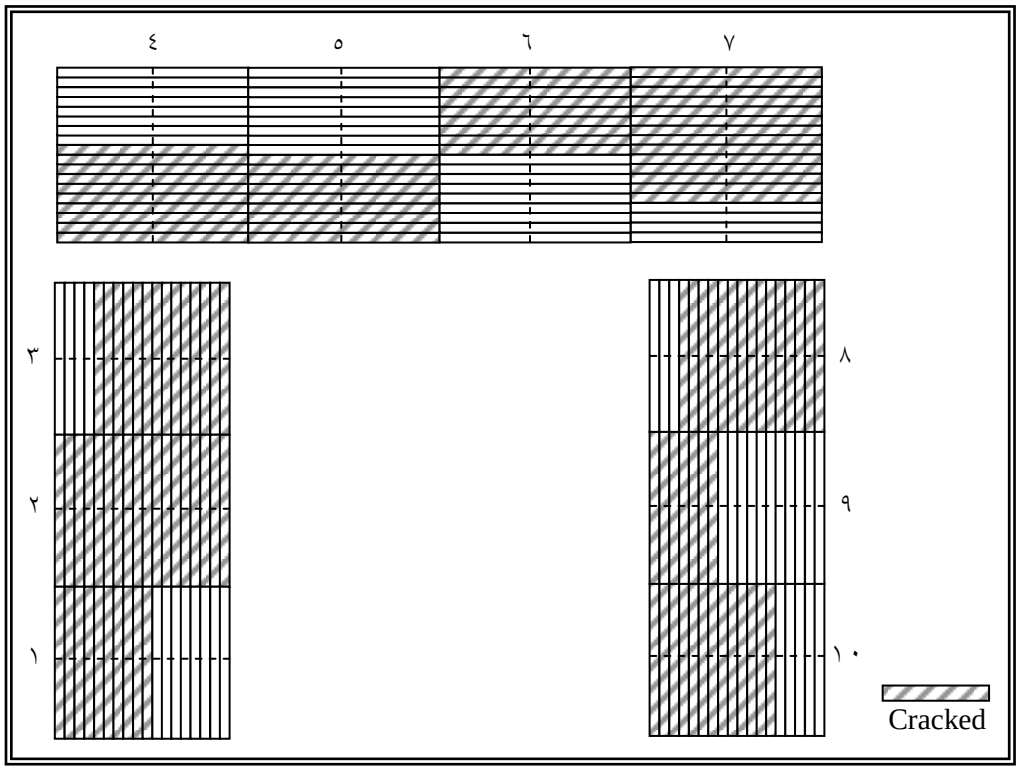

Fig. (٥.٣٠) Cracked pattern frame (F٣), with aspect ratio (L_f / D_f = ١٠٠), at load equal ٢٥٠ KN

٥ . ٥ . ٤ Partial-Depth of Steel Fibers

The behavior of partial depth of steel fiber reinforced concrete members subjected to cyclic load were investigated through three different volume fractions ٠ . ٥%, ١% and ١.٥٪ , with constant aspect ratio ٧٥.

Two examples are used, the first is frame (F٢) which is reanalyzed by adopting partial depth steel fiber. Fig. (٥.٣١) shows the load deflection curves with various steel fiber content for frame (F٢).

The second example is simply supported beam which was investigated under two points loading with different fibers content. Fig. (٥.٣٢) shows the geometry, material properties and loading conditions. Figs. (٥.٣٣) to (٥.٣٥) represent load-deflection curves for partial-depth steel fiber with different volume fraction (٠.٥-١.٥) %.

According to the proposed analysis, the beam is divided into six elements with twenty fibrous concrete layers.

To study the various depth section which contain steel fibers (٠.٢٥, ٠.٥ and ١) with keeping the volume of steel fibers constant with all various depth as shown in Fig. (٥.٣٧).

Fig. (٥.٣٨) shows the load-deflection curves for various depth of section with constant steel fibers content (٠.٥٪). The theoretical study indicated that members with partial-depth steel fibers having a flexural strength more than members with full-depth randomly oriented steel fibers. This is because that the decrease of thickness which containing steel fibers would be able to support the load after initial crack. In addition, the orientation of fibers has a big effect after that the number of steel fibers increased per unit area of the matrix cross section. For these reasons, the effective fiber is an increased in the partial-depth of steel fibers members.

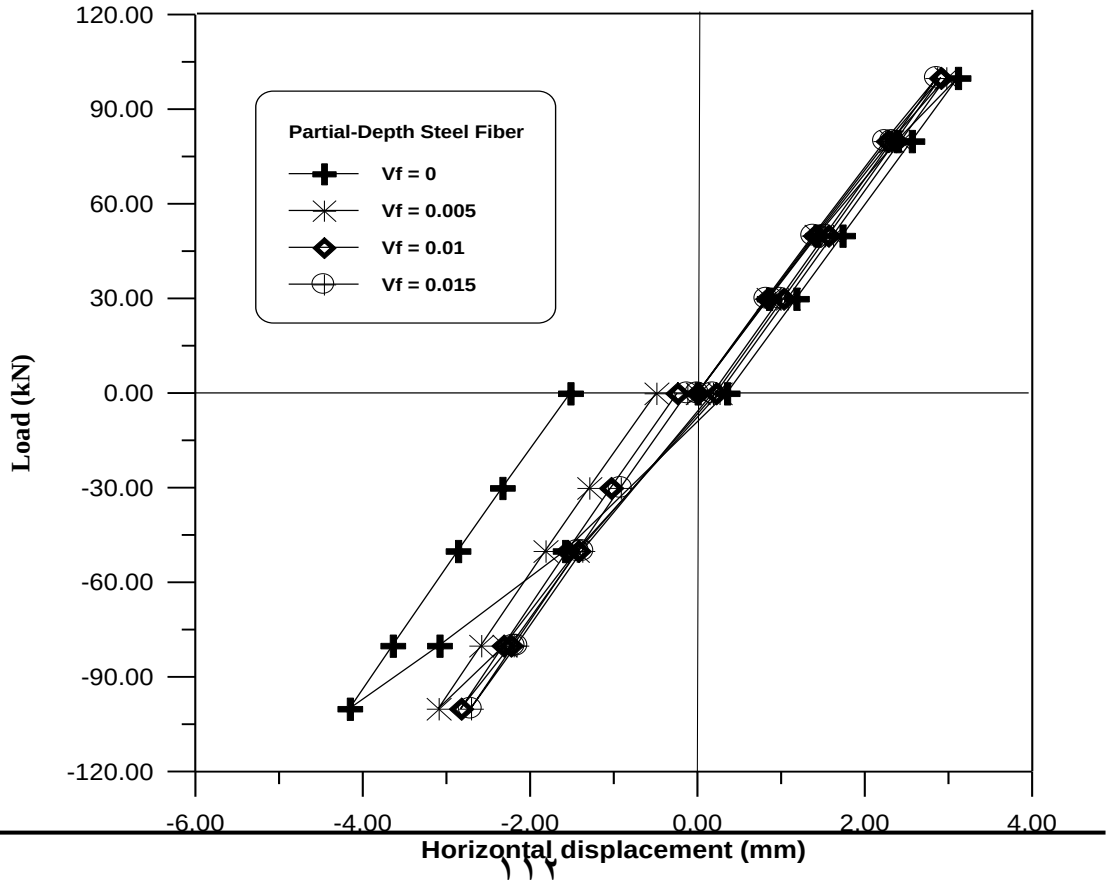

Fig. (٥ . ٣١) Load-deflection curves for partial-depth fiber reinforced concrete frame (F٢) with: V_f = ٠٪, ٠ . ٥%, ١٪ and ١.٥٪

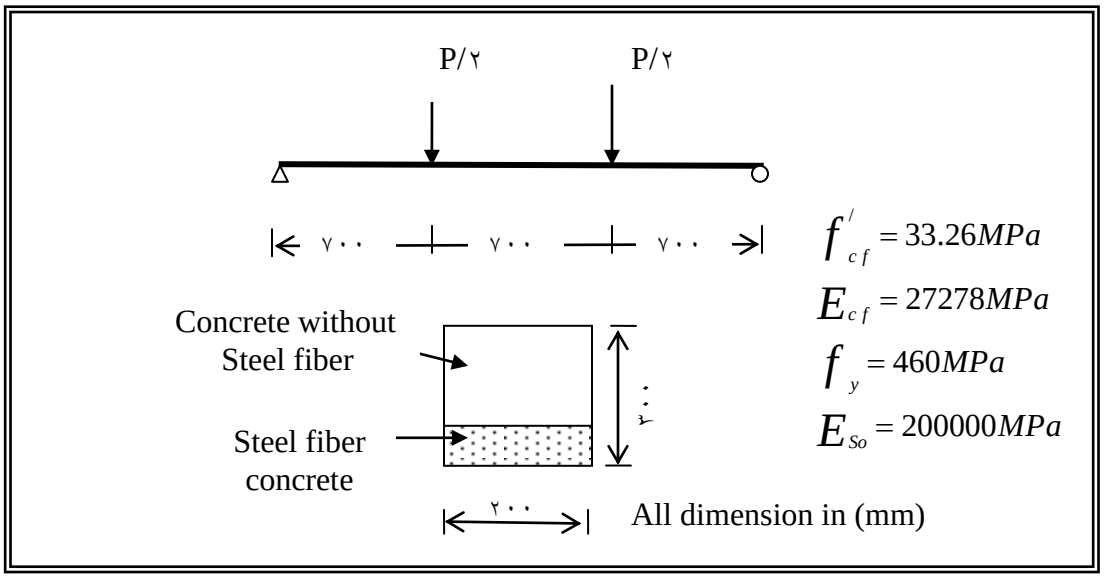

Fig. (٥ . ٣٢) Details for partial-depth steel fiber reinforced concrete beam

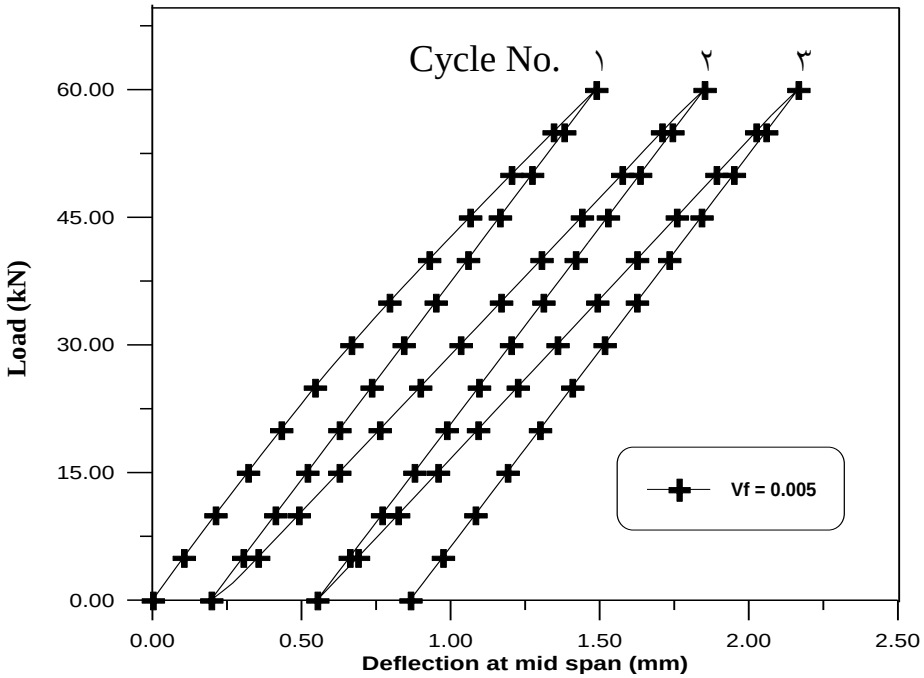

Fig. (٥ . ٣٣) Load-deflection curve for partial-depth fiber reinforced concrete beam (V_f = ٠ . ٥%)

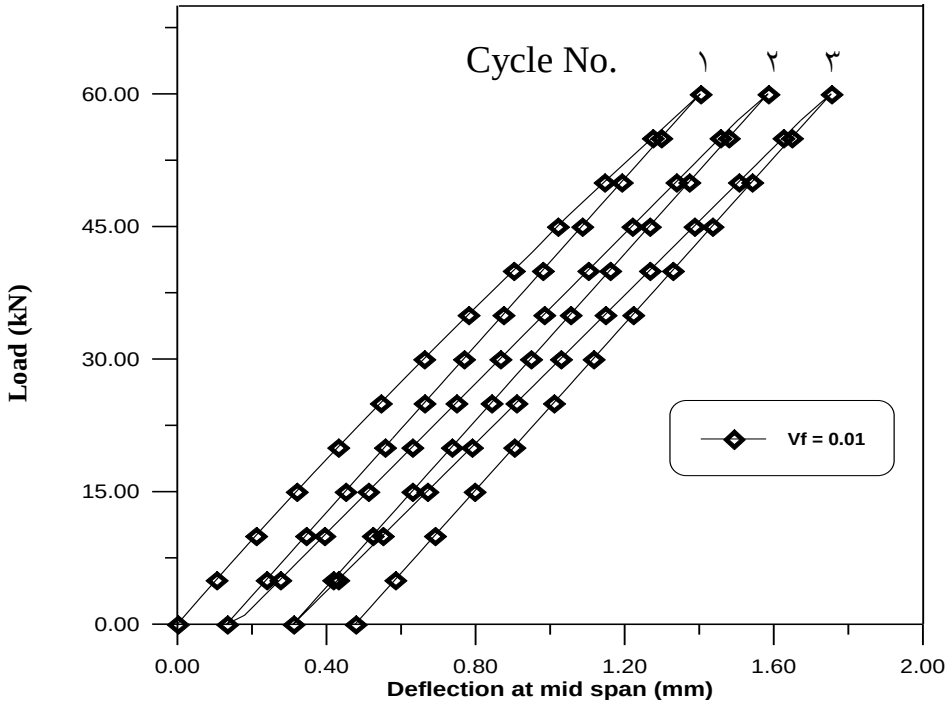

Fig. (٥ . ٣٤) Load-deflection curve for partial-depth fiber reinforced concrete beam (V_f = ١%)

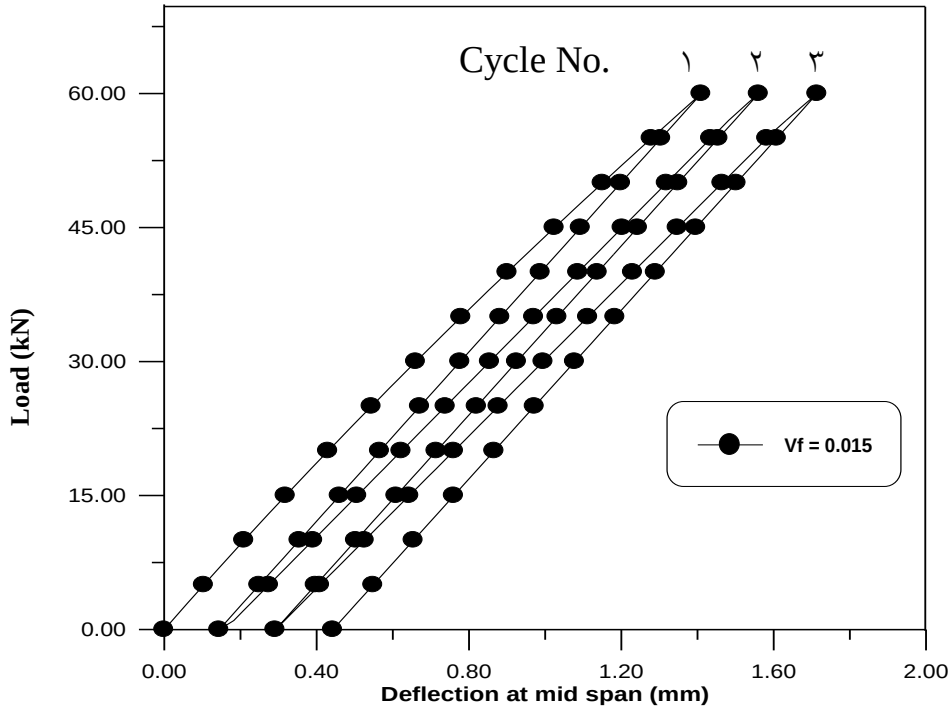

Fig. (٥ . ٣٥) Load-deflection curve for partial-depth fiber reinforced concrete beam (V_f = ١ . ٥%)

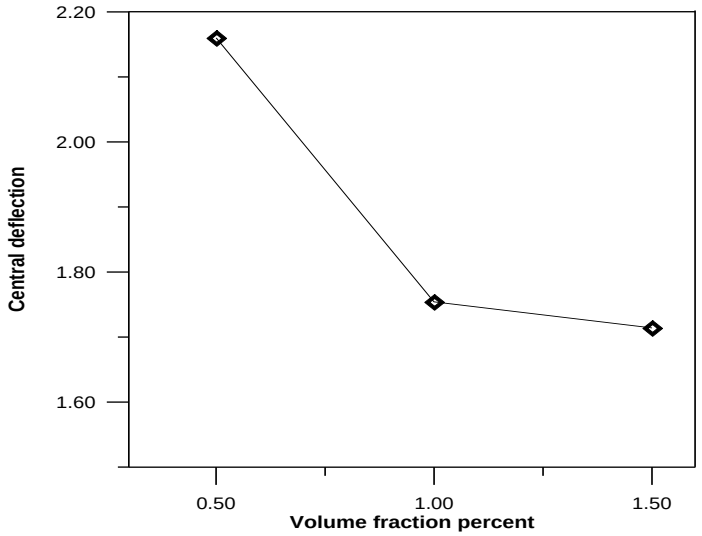

Fig. (٥ . ٣٦) Effect of fiber content for partial-depth steel fiber Reinforced concrete beams at third cycle (٦٠ KN)

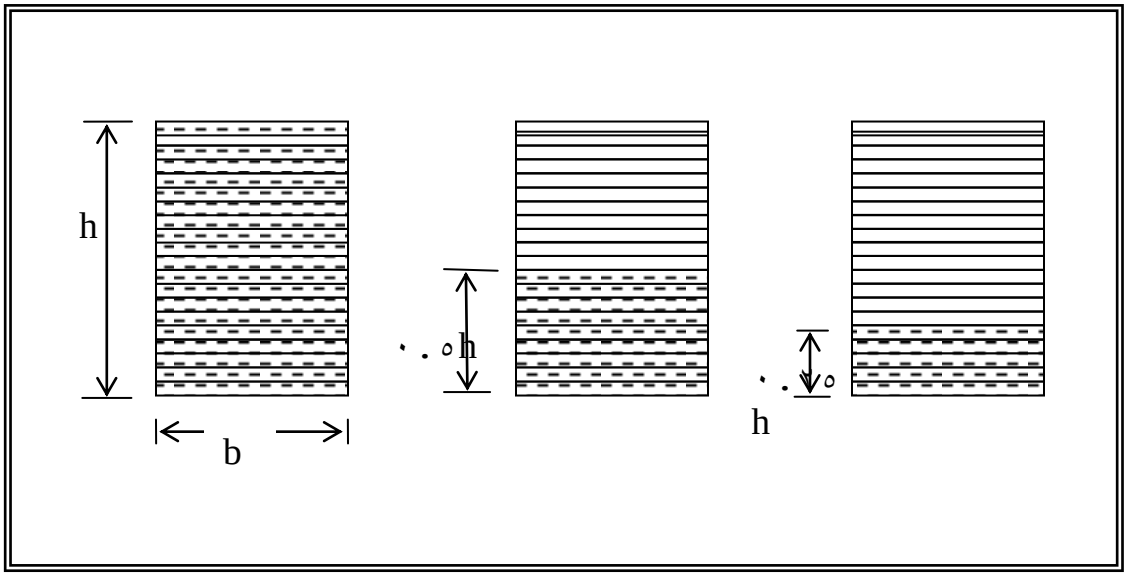

Fig. (٥. ٣٧) various depth of section with constant steel fibers (٠ . ٥٪)

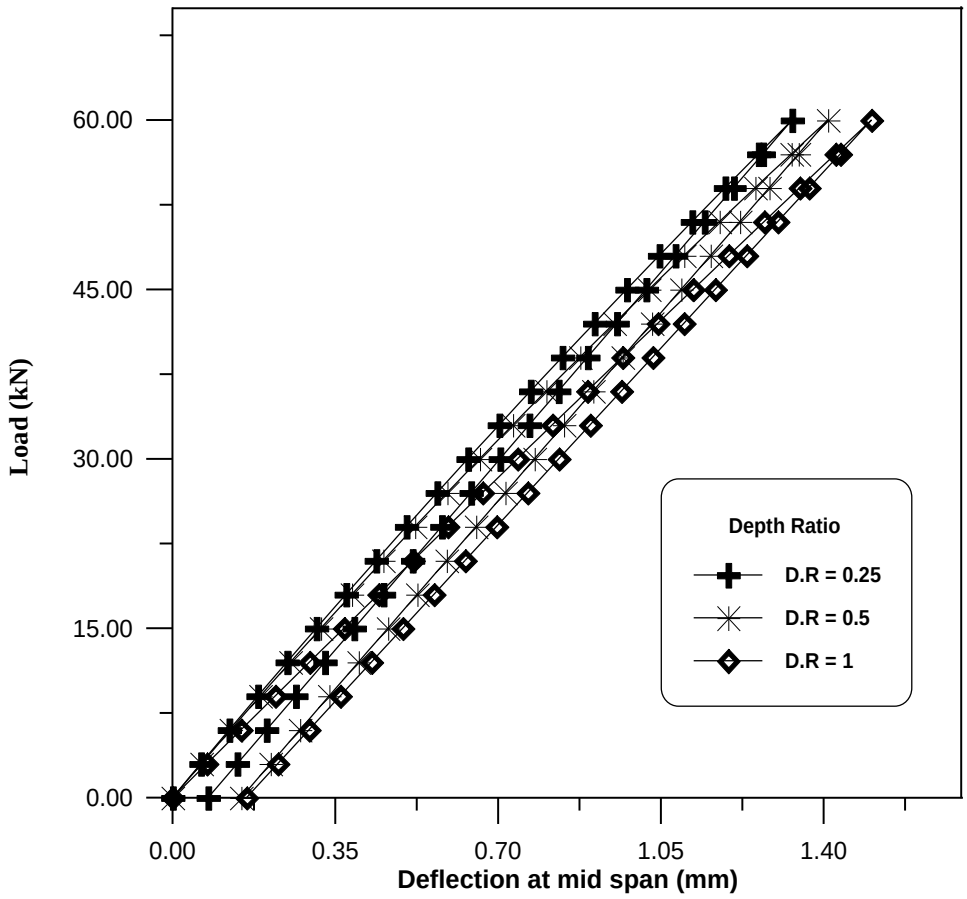

Fig. (٥.٣٨) Load-deflection curves with various depth ratio and constant volume fraction (٠.٥٪)

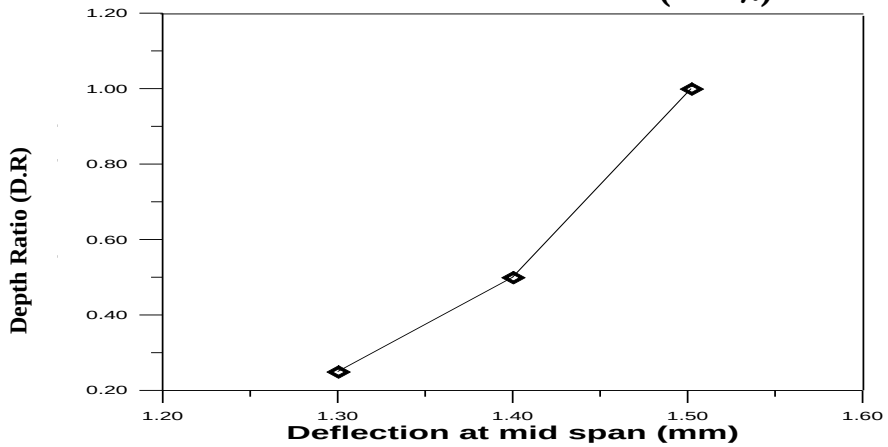

Fig. (٥.٣٩) Relationship between deflection-depth ratio

٥.٥.٥ Elements Type

In the present study, two different elements of geometry, prismatic and non prismatic are investigated, with different ratios of h_1/h_2 (١, ١.٤ and ١.٦)

with volume of steel fibers ١% and aspect ratio ٧٥ for all examples. The geometry, load condition and materials properties are shown in Fig. (٥ . ٤٠).

According to the proposed procedure, the beams were divided into twenty fibrous concrete layers and one steel layer with six elements along the beam axis. Fig. (٥ . ٤١) represents central deflection versus load for the beams with different ratio ($h_١/h_٢$) element geometry.

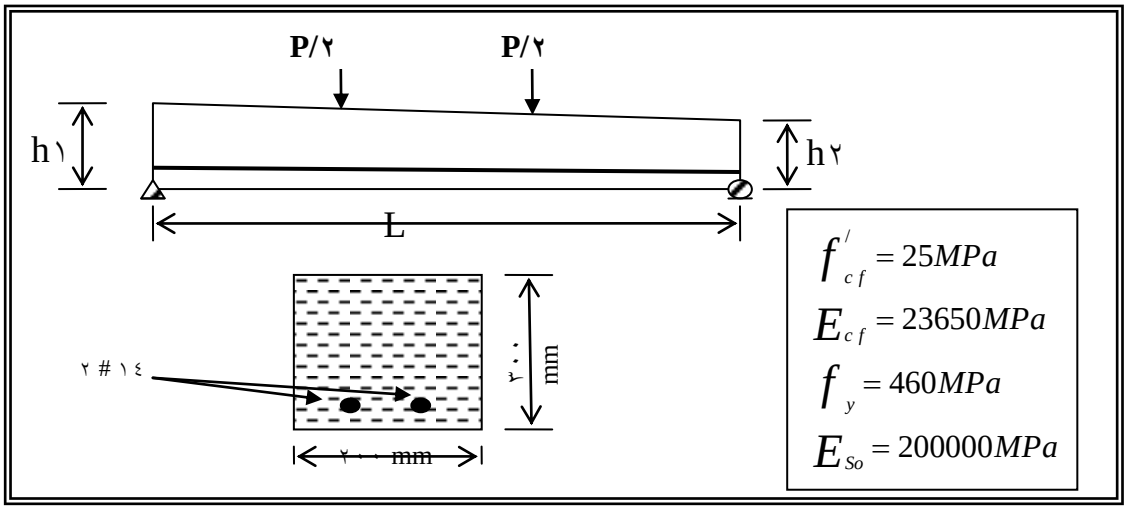

Fig. (٥.٤٠) Details of nonprismatic beam in consideration (uniform taper element)

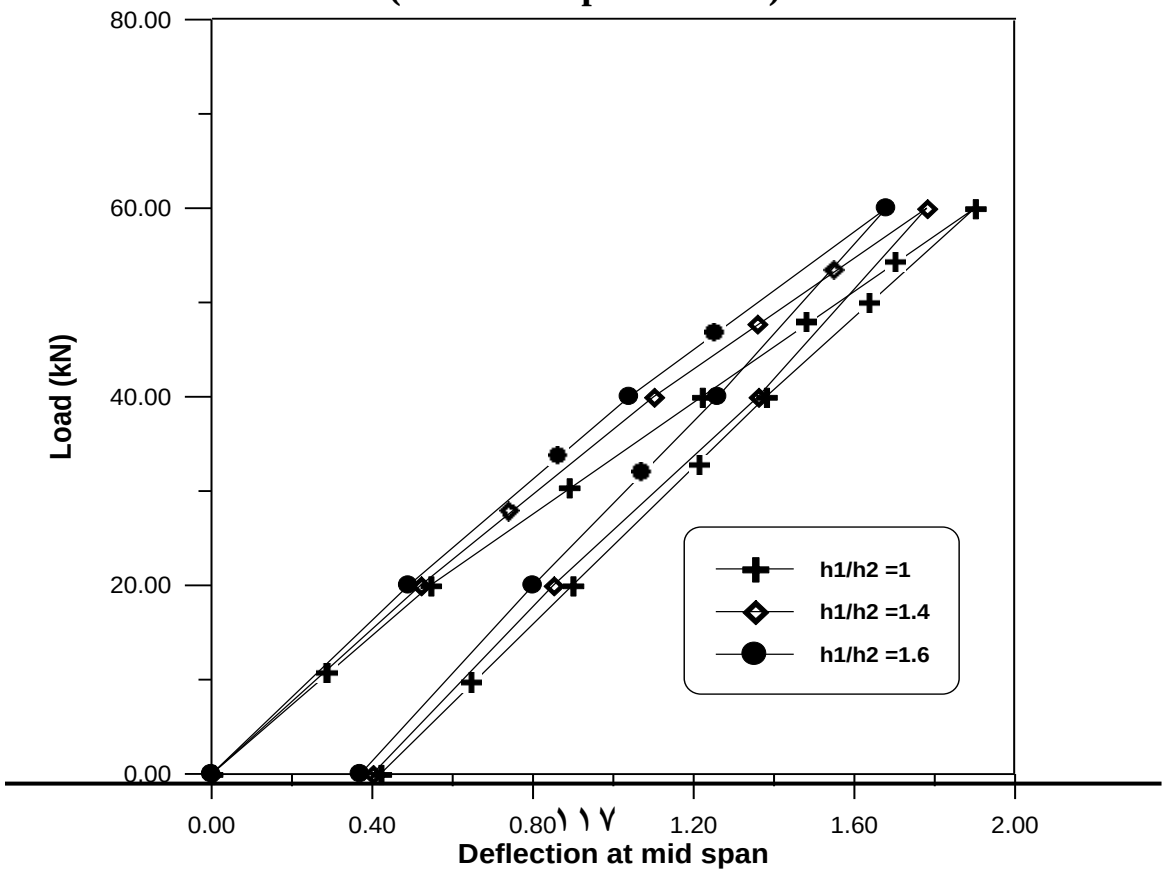

Fig. (٥.٤١) Load-deflection with various h_1/h_2 ratio

٥.٥.٦ Loading Distributions

The effect of this parameter was studied by using the reinforced concrete portal frame (F٢). The geometry of this frame is shown in Fig.(٥.٢٨). In this parameter, the steel fibers contain ١% by volume fraction and aspect ratio of steel fiber ٧٥.

The frame is divided into six elements with eighteen fibrous concrete layers and two steel layers for beam, and three elements with eighteen fibrous concrete layers and three steel layers for each column.

Two types of applied load conditions are used: the firs type is one point applied load (L.D (١)) and the second is two point applied load (L.D (٢)) as shown in Fig. (٥.٤٢). Also Fig. (٥.٤٣) represents the load-deflection curves for frame (F٢) with two types of load distribution.Figs. (٥.٤٤) to (٥.٤٥) show the cracking pattern for frame (F٢) under the effect of loading distribution.

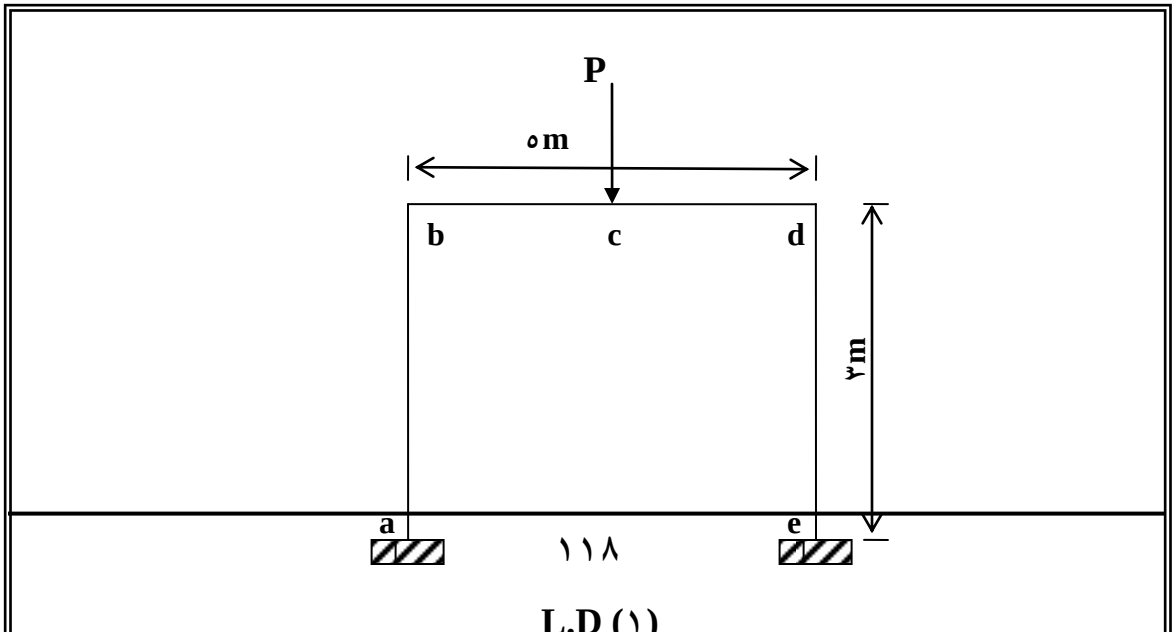

Fig. (٥ . ٤٢) Load distribution conditions for frame (F٢)

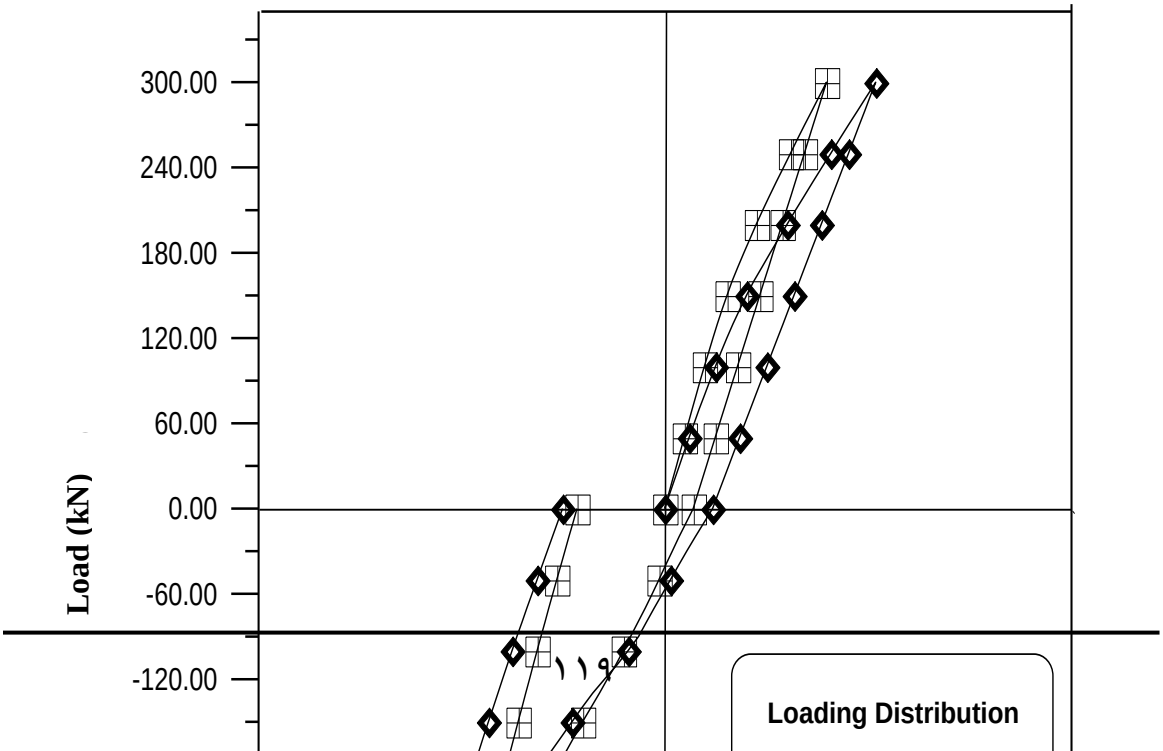

Fig. (٥.٤٣) Load-deflection curves with various load distribution frame (F٢)

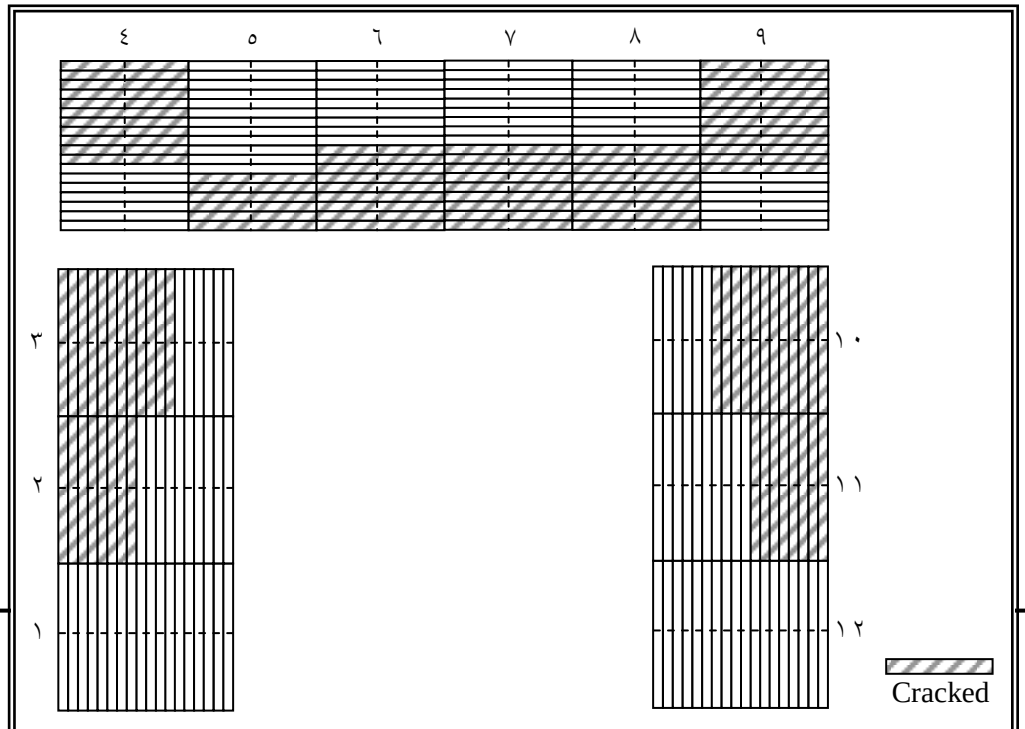

(b)
Unloading

Fig. (٥.٤٤) Cracked pattern frame ٢ (L.D = ٢), at load equal ٢٥٠ KN

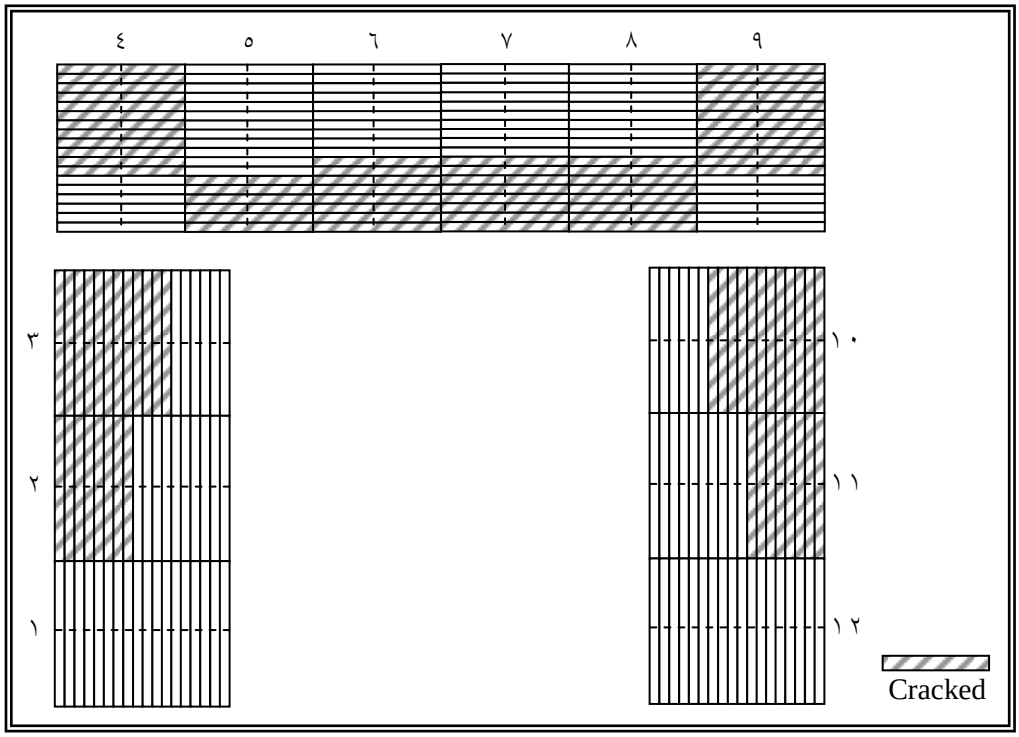

Fig. (٥.٤٥) Cracked pattern frame ٢ (L.D = ١), at load equal ٢٥٠ KN

CHAPTER SIX
CONCLUSIONS AND RECOMMENDATIONS

٦.١ Conclusions

From the numerical results presented in this study, the following conclusions can be drawn:

١. The proposed analytical model to predict the response of steel fiber reinforced concrete members appears to be satisfactory and provides useful tool for the nonlinear analysis of SFRC members when subjected to monotonic and cyclic loads.

٢. The study of the effect of steel reinforcement ratio, at ١ % volume content of steel fibers could replace about ٠.١٥ % of the flexural steel reinforcement.

٣. As it is known, theoretically, the addition of steel fibers to reinforced concrete members, when the fiber content increased from ٠.٥٪ to ٢٪ the deflection is decreased about ٤٠٪, But in practical this conclusion is districted.

٤. The steel fibers length has been found to play a significant role in increasing flexural strength members, where the deflection is decreased about ١٨٪ , when the aspect ratio increase from ٦٠ to ١٠٠.

٥. For partial-depth steel fibers members the flexural strength increased with limited decrease for depth ratio of section about (h, ٠.٥h, and ٠.٢٥h) with constant steel fibers content.

٦. The addition of steel fibers reduces the number of cracks and slow crack propagation during incremental loading.

٧. The full-depth steel fiber subjected to reversible cyclic load and continuous members is more acceptable than the partial-depth steel fibers members.

٦.٢ Recommendations for further studies

١. Extension of the constitution materials relationships to include long terms effects such as creep and shrinkage.

٢. Modifying the present model to incorporate bond-slip model.

٣. Since fibers concrete be used for refractory applications; the behavior of this material must be investigated when subjected to high temperatures.

٤. Analytical approaches are required to study the flexural behavior of steel fiber reinforced concrete with T-cross section members under the effect of cyclic loads.

٥. Research into the practicality of using more than ٢.٥ % fiber content.

٦. An experimental study on the behavior of partial – depth of steel fibers member subjected to repeated cyclic loads.

٧. Investigated the stability of solution for slender fibers (long length fibers with small diameter), which may be effected on the ultimate strength of beam.

CERTIFICATION

We certify that this thesis titled "**Non Linear Analysis of Steel Fiber Reinforced Concrete Member Under Cyclic Loading"**, was prepared by "**Ayoub A. Ibrahim**" under our supervision at Babylon University in partial fulfillment of the requirements for the degree of Master of Science in Civil Engineering.

Signature:

Name: Asst. Prof. Dr. Mustafa B. Dawood

(Supervisor)

Date:

Signature:

Name: Asst. Prof. Dr. Haitham AL-daamy

(Supervisor)

Date:

REFRENCES

١. Al Ta'an, S. A. (١٩٩٢). "***Flexural Analysis of Reinforced Fibrous Concrete Beams***" Journal of Engineering and Technology, Vol. ١١, No. ٣, pp. ٧-١٩.

٢. ACI Committee (٣١٨-٣١٨) "***Building Code Requirements for Reinforced Concrete***", (ACI-٣١٨-٨٣), American Concrete Institute, Detroit, ١٩٨٤, ١١١ pgs.

٣. Ahmad, H. I. (١٩٩٨). "***Nonlinear Finite Element Analysis of Plan Stress Fiber Reinforced ConcreteMembers***" M.Sc. Thesis, Collage of Engineering University of Mousal.

٤. Bertero, V. V., and McClure, G. (١٩٦٤). "***Behavior of Reinforced Concrete Frames Subjected to Repeated Reversible Loads***" ACI Journal, Vol. ٦١, No. ١٠, pp. ١٣٠٥-١٣٢٩.

٥. Bahn, B. Y., and Hsu, C. T. (١٩٩٨). "***Stress-Strain Behavior of Concrete under cyclic loading***", ACI Materials Journal, Vol. ٩٥, No. ٢, pp. ١٧٨-١٩٣.

٦. Chen, W. F. (١٩٨٢). "***Plasticity in Reinforced Concrete***" McGrawHill Book Co., New York.

٧. Craig, R.J., (١٩٨٤). "***Structural Applications of Reinforced Fibrous Concrete***", Concrete International: Design & Construction, Vol. ٦, No: ١٢, pp. ٢٨-٣٢.

٨. Chern, J. C., Yang, H. J., and Chen, H. W. (١٩٩٢). "***Behavior of Steel Fiber Reinforced Concrete in Multiaxial Loading***", ACI Materials Journal, Vol. ٨٩, No. ١, pp.٣٢-٤٠.

٩. Delvasto,S.,Naaman, A. E., and Throne, J. L. (١٩٨٦). "***Effect of Pressure after Casting on High Strength Fiber Reinforced Mortar***", The International Journal of Cement Composites and Lightweight Concrete, Vol. ٨, No. ٣, pp. ١٨١-١٩٠.

١٠. D'Ambrisi, A., and Filippou, F. C. (١٩٩٩). "***Modeling of Cyclic Shear Behavior in RC Members***", Journal of Structural Engineering, ASCE, Vol. ١٢٥, No. ١٠, pp. ١١٤٣-١١٤٩.

١١. Ezeldin, A. S., and Lowe, S. R. (١٩٩١). "***Mechanical Properties of Steel Fiber Reinforced Rapid-Set Materials***", ACI Materials Journal, Vol. ٨٨, No. ٤, pp. ٣٨٤-٣٨٩.

١٢. Ezeldin, A. S., and Balaguru, P. N. (١٩٩٢). "***Normal and High Strength Fiber-Reinforced Concrete Under Compression***", Journal of Materials in Civil Engineering, Nov, Vol. ٤, No. ٤, pp. ٤١٥-٤٢٩.

١٣. Farhang, A. A., and Silfwerbrand, J. "***Plain and Steel Fiber Reinforced Concrete Beams Subjected to Combined Mechanical and Thermal Loading***", Royal Institute of Technology, Stocholm, Sweden.

١٤. Galli, G., Grimaldi A., and Rinaldi, Z. (٢٠٠٣). "***Optimal Design of FRC Structural Elements***", Laboratoirede Mècanique des Solides Ecole Polytechnique Palaiseau France November ٢٦-٢٨.

١٥. Gustafsson, J., and Noghabai K. "***Steel Fibers as Shear Reinforcement in High Strength Concrete Beams***", Luleå University of Tech., Div. of Struct. Eng., Sweden.

١٦. Gençoglu, M., and Eren, İ. (٢٠٠٢). "***An Experimental Study on the Effect of Steel Fiber Reinforced Concrete on the Behavior of the Exterior Beam-Column Joints Subjected to Reversal Cyclic Loading***", Turkish Journal Eng. Env. Sci., ٢٦, pp.٤٩٣-٥٠٢.

١٧. Gopalaratnam, V. S., and Shah, S. P. (١٩٨٦). "***Micromechanical Model for the Tensile Fracture of Steel Fiber Reinforced Concrete***", University of Sheffield.

١٨. Gencoglu, M., Komur, M., and Taskin, B. (٢٠٠٢). "***Bending Behavior of Steel-Fiber Reinforced-Concrete***", Proceeding of the Fourth GAP Engineering Congress.

١٩. Gray, R. J., and Johnston, C. D. (١٩٨٧). "***The influence of Fiber-Matrix interfacial Bond strength on the Mechanical Properties of Steel Fiber Reinforced Mortars***", The International Journal of Cement Composites and Lightweight Concrete, Vol. ٩, No. ١, pp.٤٣-٥٤.

٢٠. Gebman, M. (٢٠٠١). "***Application of Steel Fiber Reinforced Concrete in Seismic Beam- column Joints***", M.Sc. Thesis, San Diego State University, USA.

٢١. Hinton, E., and Owen, D. R. J. (١٩٨٤). "***Finite Element Software for Plate and Shells***", Pinneridge Press, Swansea.

٢٢. Hughes, B. P., and Fattuhi, N. I. (١٩٧٧). "***Load-Deflection Curves for Fiber-Reinforced Concrete Beams in Flexure***", Magazine of concrete Research, Vol. ٢٩, No. ١٠١, pp. ١٩٩-٢٠٦.

٢٣. Hsu, C. T. T., He, R. L., and Ezeldin, A. S.(١٩٩٢). "***Load-Deformation Behavior of Steel Fiber Reinforced Concrete Beams***", ACI Structural Journal, Vol. ٨٩, No. ٦, pp. ٦٥٠-٦٥٧.

٢٤. Hartmann, T. (١٩٩٩). "***Steel Fiber Reinforced Concrete***", This Thesis was prepared and conducted at the Department of Structural Engineering at the Royal Institute of Technology in Stockholm.

٢٥. Harajli, M., Hamad, B., and Karam, K. (٢٠٠٢). "***Bond-slip Response of Reinforcing Bars Embedded in Plain and Fiber Concrete***", Journal of Materials in Civil Engineering, ASCE, Vol. ١٤, No. ٦, pp. ٥٠٣-٥١١.

٢٦. Johnston, C. D., and Zemp, R. W. (١٩٩١). "***Flexural Fatigue Performance of Steel Fiber Reinforced Concrete-***

Influnce of Fiber Content, Aspect Ratio,and Type", ACI Materials Journal, Vol. ٨٨, No. ٤, pp ٣٧٤-٣٨٣.

٢٧. Jassim, Z. J. (١٩٩٩). "***Nonlinear Analysis of steel Fiber Reinforced Concrete Beams***" M.Sc. Thesis, University of Technology.

٢٨. Kwak, H. G., and Flippou, F. C.(١٩٩٠). "***Finite Element Analysis of Reinforced Concrete Structures Under Monotonic Loads***", Report No.UCB/SEMM-٩٠/١٤ Structural Engineering,Mechanics and Materials Department of Civil Engineering University of California,Berkeley

٢٩. Kadim, M. J. (٢٠٠١). "***Nonlinear Analysis of Reinforced Concrete Plane Frames under Cyclic Loading***", M.Sc. Thesis, Coliage of Engineering, University of Babylon.

٣٠. Kholmyansky, M. M. (٢٠٠٢). "***Mechanical Resistance of Steel Fiber Reinforced Concrete to Axial Load***", Journal of Materials in Civil Engineering, ASCE, Vol. ١٤, No. ٤, pp. ٣١١-٣١٩.

٣١. Kormeling, H. A., Reinhard, H. W., and Shah, S. P. (١٩٨٠). "***Static and Fatigue properties, of concrete Beams Reinforced with Continuous Bars and with Fibers***", ACI journal, Vol. ٧٧, No. ١, pp.٣٦-٤٣.

٣٢. Kwak, K., Suh, J., and Hsu, C-T. T. (١٩٩١). "***Shear-Fatigue Behavior of Steel Fiber Reinforced Concrete Beams***", ACI Structural Journal, Vol. ٨٨, No. ٢, pp ١٥٥-١٦٠.

٣٣. Kovács, I., Ulm, F. J., and Balázs, G. L. (١٩٩٨). "***Modeling of Plastic Matrix-Fiber Interaction in Fiber Reinforced Concrete***", PhD Symposium in Civil Engineering Budapest.

٣٤. Kan, Y. C., Pei, K. C., and Yang, H. C. (٢٠٠٣). "***An Investigation on Toughness of Steel Fiber Reinforced Heavy***

Concrete", Transaction of the ١٧th International Conference on Structural Mechanics in Reactor Technology.

٣٥. Lee, C., Shin, Y.S., and Lee, H.J. "***Parametric studies on Flexural Behavior of RC Beams Strengthened at Different Loading Stages***".

٣٦. Lee, I., Punurai, W., and Hsu, C.T.T. (٢٠٠٢). "***Complete Stress-Strain Behavior of High Preformance Fly Ash Concrete***", ASCE Engineering Mechanics Conference June ٢ – ٥, ٢٠٠٢, Columbia University, New York, NY.

٣٧. Lim, T. Y., Paramassivam, P., and Lee, S. L. (١٩٨٧). "***Shear and Moment Capacity of Reinforced Steel-Fiber-Concrete Beams***", Magazine of Concrete Research, Vol. ٣٩, No. ١٤٠, pp. ١٤٨-١٦٠.

٣٨. Leonard, A. T., and Mansur, S. A. (١٩٩١). "***Biaxial Strength and Deformational Behavior of Plain and Steel Fibers Concrete***", ACI Material Journal, Vol. ٨٨, No. ٤, pp.٣٥٤-٣٦٢.

٣٩. Lauy, E. H. Allose, (١٩٩٦). "***Three-Dimensional Nonlinear Finite Element Analysis of Steel Fiber Reinforced Concrete Beams in Torsion***", M.SC. Thesis, University of Technology.

٤٠. Lan, S., and Guo, Z. (١٩٩٩). "***Biaxial Compression Behavior of Concrete Under Repeated Loading***", Journal of Material in Civil Engineering, ASCE, Vol. ١١, No. ٢, pp. ١٠٥-١١٤.

٤١. Löfgren, I., Betong, A. F. (٢٠٠٣). "***Analysis of Flexural Behaviour of Reinforced FRC Members***", Design Rules for Steel Fiber Reinforced Concrete Structure.

٤٢. Mindess, S. (١٩٨٠). "***Torsion Tests of Steel-Fiber Reinforced Concrete***", The International Journal of Cement Composites, Vol. ٢, No. ٢, pp. ٨٥-٨٩.

٤٣. Morris, A. D., and Garret, G. G. (١٩٨١). "***A comparative Study of the Static and Fatigue Behaviour of Plain and Steel Fiber Reinforced Mortar in Compression and Direct Tension***", The International Journal of Cement Composites and Lightweight Concrete, Vol. ٣, No. ٢, pp. ٧٣- ٩٠.

٤٤. Mikkola, M., and Sinisalo, H. (١٩٨٢). "***Nonlinear Dynamic Analysis of Reinforced Concrete Structures***", Symp. "Concrete Structures under Impact and Impulsive Loading", June ٢-٤, pp.٥٣٤-٥٤١, BAM, Berlin (West).

٤٥. Mansur, M. A. (١٩٨٢). "***Bending-Torsion Interaction for Concrete Beams Reinforced with Steel fibers***", Magazine of Concrete Research, Vol. ٣٤, No. ١٢١, pp. ١٨٢-١٩٠.

٤٦. Maalej, M. (١٩٩٩). "***Flexural Behavior of Steel Fiber Reinforced Concrete***" Journal of Material in Civil Engineering, ASCE, Vol. ١١, No. ٢, p. ١٧٩.

٤٧. Mansour, M., Lee, J. Y., and Hsu, T. T. C. (٢٠٠١). "***Cyclic Stress-Strain Curves of Concrete and Steel Bars in Membrane Elements***" ASCE, Journal of Structural Engineering, Vol. ١٢٧, No. ١٢, pp. ١٤٠٢-١٤١١.

٤٨. Morteza, A. M., and Sonmez, M. (٢٠٠١). "***Inelastic Large Deflection Modeling of Beam-Columns***", ASCE, Journal of Structural Engineering, Vol. , No. , pp. ٨٧٦-٨٨٩.

٤٩. Naaman, A. E., and Shah, S. P. (١٩٧٦). "***Pull-Out Mechanism in Steel Fiber-Reinforced Concrete***", ASCE, Vol. ١٠٢, No. ST٨, Proc., pp. ١٥٣٧-١٥٤٨.

٥٠. Nimnim, S. T. (١٩٩٢). "***Fiber Reinforced Concrete Beams Subjected to Static Cyclic Loads***", M. Sc. Thesis, University of Technology, Iraq. (In Arabic).

٥١. Naji, J. H. (١٩٩٧). "***Nonlinear Finite Element Analysis of Steel Fiber Reinforced Concrete Beams***", Proc. To the ٤th Scientific Engineering Conf., University of Baghdad, ١٨-٢٠ Nov.

٥٢. Nogabai, K. (٢٠٠٠). "***Beams of Fibrous Concrete in Shear and Bending: Experiment and Model***", Journal of Structural Engineering, ASCE, Vol. ١٢٦, No. ٢, pp.٢٤٣-٢٤٦.

٥٣. Otter, D. E., and Naaman, A. E. (١٩٨٨). "***Properties of Steel Fiber Reinforced Concrete under Cyclic Loading***" ACI Materials Journal, Vol. ٨٥, No. ٤, pp. ٢٥٤-٢٦١.

٥٤. Otter, D. E., and Naaman, A. E. (١٩٨٩). "***Model for Response of Concrete to Random Compressive Loads***" Journal of Structural Engineering, ASCE, Vol. ١١٥, No. ١١, pp. ٢٧٩٤-٢٨٠٩.

٥٥. Owen, D. R. J., and Hinton, E. (١٩٨٠). "***Finite Element in Plasticity : Theory and Practice***", Pinneridge Press, Swansea, U.K.

٥٦. Ouaar, A., Doghri, I., Thimus, and Hugĕ, F. (٢٠٠٣). "***Micromechanical Modeling of the Deformation and Damage of Inelastic Brittle Three-Phase Composite: Application to Fiber-Reinforced Concrete***".

٥٧. Omer,Q. A. (١٩٩٣). "***Flexural Behavior of Conventionally Reinforced Concrete T-Beams with Steel Fibers***", M. Sc. Thesis, University of Technology.

٥٨. Padmarajaiah, S. K., and Ramaswamy, A. (٢٠٠٢). "***Comparative Study on Flexural Response of Full and Partial Depth Fiber- Reinforced High-Strength Concrete***", Journal of Materials in Civil Engineering, Vol. ١٤, No. ٢, pp. ١٣٠-١٣٦.

٥٩. Rahimi, M. M., and Kesler, C. E. (١٩٧٩). "***Partially Steel-Fiber Reinforced Morter***", ASCE, Vol. ١٠٥, No. ST١, pp.١٠١-١٠٩.

٦٠. Ramakrishnan , V., Brandshaug, T., Coyle, W. V., and Schrader, E. K., (١٩٨٠). "***A comparative Evaluative of Concrete Reinforced with Straight Steel Fibers and Deformed End Fibers Glued together into Bundles***", ACI Journal, Vol. ٧٧, No. ٣, pp. ١٣٥-١٤٣.

٦١. Ramakrisnan , V., Coyle, W. V., Dahl, L. F., and Schrader, E. K., (١٩٨١). "***A comparative Evaluation of Fibers Shotcrete***", Design and Construction, Vol. ٣, No. ١, pp. ٥٦-٥٩.

٦٢. Rossi, P., Acker, P., and Malier, Y. (١٩٨٧). "***Effect of Steel Fibers at Two Different Stages: The Material and the Structure***", Material and Structures, pp. ٤٣٦-٤٣٩.

٦٣. Radmix ™ "***Web:http://www.radmix.com***".

٦٤. Shah, S. P., and Rangan, B. V., (١٩٧١). "***Fiber Reinforced Concrete Properties***", ACI Journal, Vol. ٦٨, No. ٢, pp. ١٢٦-١٣٥.

٦٥. Soroushian, P., and Bayasi, Z. (١٩٩١). "***Fiber-Type Effects on the Perfarmance of Steel Fiber Reinforce Concrete***", ACI Materials Journal, Vol. ٨٨, No. ٢, pp ١٢٩-١٣٤.

٦٦. Siah, K.,Mandel, J. A., and Mousa, B. R. (١٩٩٢). "***Micromechanical Finite Element Model for Fiber Reinforced Cementitious Materials***", ACI Materials Journal, Vol. ٨٨, No. ٤, pp. ٣٥٤-٣٦١.

٦٧. Şener, S., Begimgil, M. and Belgin, Ç. (٢٠٠٢). "***Size Effect on Failure of Concrete Beams with and without Steel Fibers***", Journal of Materials in Civil Engineering, Vol. ١٤, No. ٥, pp. ٤٣٦-٤٤٠.

٦٨. Soroushian, P., and Lee, C. D. (١٩٨٩). "***Constitutive Modeling of Steel Fiber Reinforced Concrete under Direct Tension and Compression***", Recent Developments in Fiber

Reinforced Cements and Concretes, Elevier Scinece Publishers Ltd., Essex, pp. ٣٦٣-٣٧٧.

٦٩. Suthiwarapirak, P., Matsumoto, T., and Horri, H.(٢٠٠١). "***Fatigue Life Analysis of Reinforced Steel-Fiber-Concrete Beams***", Proceedings of the Japan Concrete Institute, Vol. ٢٣, No. ٣, pp. ١-٦.

٧٠. Swamy, R.N., Mangat, P.S., and Rao, C.V.S.K. (١٩٧٤). "***The Mechancs of Fiber Reinforced of Cement Material***", Fiber Reinforced Concrete ACI SP-٤٤, Detroit, Michigan, pp. ١-٢٨.

٧١. Saied, S. H. (١٩٩٠). "***Moment-Curvature Relationship for Concrete Beams Reinforced with Steel Fibers***", M. SC. Thesis, University of Technology, Iraq.

٧٢. Schumacher P., Braam C.R., and Walraven J.C.(٢٠٠١). "***Steel Fiber Reinforced Concrete Cylinders Under Uniaxial Compressive Loading –Preliminary Tests***", Delft University of Technology Faculty of Civil Engineering and Geosciences Section Concrete Structures Report No. ٢٥.٥-٠١-٠٦. Mechanics, pp. ١٩٢-٢٠٢.

٧٣. Thompson, K. J., and Park, R. (١٩٨٠). "***Moment-Curvature Behavior of Cyclically Loaded Structural Concrete Members***", Proceedings Institution Civil Engineerings Part ٢, Vol.٦٩, pp. ٣١٧-٣٤١.

٧٤. Taylor, R. L., Filippou, F. C., and Auricchio, F. (٢٠٠٣). "***A mixed Finite Element Method for Beam and Frame Proplems***", Computational.

٧٥. Wang, Y., Wu, H. C., and Li, V. C. (٢٠٠٠). "***Concrete Reinforcement with Recycled Fibers***", Journal of Material in Civil Engineering.

٧٦. Wu, H. C. (٢٠٠١). "***Mechanical Properties of Steel Microfiber Reinforced Cement Pastes and Mortars***", Journal of Material in civil Engineering, ASCE, Vol. ١١, No. ٤, pp.٢٤٠

٧٧. Yankelevesky, D. Z., and Reinhardt, H. W. (١٩٨٧). "***Model for Cyclic Compressive Behavior of Concrete***", Journal of Structural Engineering, ASCE, Vol. ١١٣, No. ٢, pp. ٢٢٨-٢٤٠.

٧٨. Yin, W. S., Eric, C. M., Mansur, M., and Tomas, T. C. (١٩٩١). "***Biaxial Tests of Plain and Fiber Concrete***" ACI Material Journal, Vol. ٨٨, No. ٤, pp. ٣٥٤-٣٦٢.

٧٩. Zia, P., Ahmad, S., and Lening, M. "***High-Performance Concretes***" A stat-of-Art Report (١٩٨٩-١٩٩٤).

٨٠. Zhang, J., Stang, H. and Li, V. C. (١٩٩٩). "***Experimental Study on Crack Bridging in FRC under Uniaxial Fatigue Tension***", Journal of Materials in Civil Engineering, ASCE, Vol. ١٢, No. ١, pp. ٦٦-٧٣.

٨١. Zhang, J., Stang, H., and Li, V. C. (٢٠٠٠). "***Experimental Study on Crack Bridging in FRC under Uniaxial Fatigue Tension***", Journal of Material in Civil Engineering, ASCE, Vol.١٢, No.١, pp.٦٦-٧٣.